

การเพิ่มสภาพละลายน้ำได้ของเฮสเพอเรทินและนารินเจนินโดยการเกิดสารประกอบเชิงซ้อนกับ
ปีตาไซโคลเดกซ์ทรินและอนุพันธ์ไเดเมทิล



นางสาวรัชดา สังกะเือก

จุฬาลงกรณ์มหาวิทยาลัย

CHULALONGKORN UNIVERSITY

วิทยานิพนธ์นี้เป็นส่วนหนึ่งของการศึกษาตามหลักสูตรปริญญาวิทยาศาสตรมหาบัณฑิต

สาขาวิชาชีวเคมีและชีววิทยาโมเลกุล ภาควิชาชีวเคมี

คณะวิทยาศาสตร์ จุฬาลงกรณ์มหาวิทยาลัย

ปีการศึกษา 2556

ลิขสิทธิ์ของจุฬาลงกรณ์มหาวิทยาลัย

บทคัดย่อและแฟ้มข้อมูลฉบับเต็มของวิทยานิพนธ์ตั้งแต่ปีการศึกษา 2554 ที่ให้บริการในคลังปัญญาจุฬาฯ (CUIR)

เป็นแฟ้มข้อมูลของนิสิตเจ้าของวิทยานิพนธ์ ที่ส่งผ่านทางบัณฑิตวิทยาลัย

The abstract and full text of theses from the academic year 2011 in Chulalongkorn University Intellectual Repository (CUIR) are the thesis authors' files submitted through the University Graduate School.

ENHANCEMENT OF WATER SOLUBILITY OF HESPERETIN AND NARINGENIN BY
COMPLEXATION WITH β -CYCLODEXTRIN AND ITS DIMETHYL DERIVATIVE

Miss Waratchada Sangpheak



จุฬาลงกรณ์มหาวิทยาลัย

CHULALONGKORN UNIVERSITY

A Thesis Submitted in Partial Fulfillment of the Requirements
for the Degree of Master of Science Program in Biochemistry and Molecular
Biology

Department of Biochemistry

Faculty of Science

Chulalongkorn University

Academic Year 2013

Copyright of Chulalongkorn University

Thesis Title	ENHANCEMENT OF WATER SOLUBILITY OF HESPERETIN AND NARINGENIN BY COMPLEXATION WITH β -CYCLODEXTRIN AND ITS DIMETHYL DERIVATIVE
By	Miss Waratchada Sangpheak
Field of Study	Biochemistry and Molecular Biology
Thesis Advisor	Thanyada Rungrotmongkol, Ph.D.
Thesis Co-Advisor	Professor Piamsook Pongsawasdi, Ph.D.

Accepted by the Faculty of Science, Chulalongkorn University in Partial
Fulfillment of the Requirements for the Master's Degree

.....Dean of the Faculty of Science
(Professor Supot Hannongbua, Dr.rer.nat.)

THESIS COMMITTEE

.....Chairman
(Professor Anchalee Tassanakajon, Ph.D.)

.....Thesis Advisor
(Thanyada Rungrotmongkol, Ph.D.)

.....Thesis Co-Advisor
(Professor Piamsook Pongsawasdi, Ph.D.)

.....Examiner
(Assistant Professor Manchumas Prousoontorn, Ph.D.)

.....External Examiner
(Associate Professor luckhana Lawtrakul, Dr.rer.nat.)

วรัชดา สังกะเสน : การเพิ่มสภาพละลายน้ำได้ของเฮสเพอเรทินและนารินเจนินโดยการเกิดสารประกอบเชิงซ้อนกับบีตาไซโคลเดกซ์ทรินและอนุพันธ์ไดเมทิล. (ENHANCEMENT OF WATER SOLUBILITY OF HESPERETIN AND NARINGENIN BY COMPLEXATION WITH β -CYCLODEXTRIN AND ITS DIMETHYL DERIVATIVE) อ.ที่ปรึกษาวิทยานิพนธ์หลัก: ดร. ธัญญดา รุ่งโรจน์มงคล, อ.ที่ปรึกษาวิทยานิพนธ์ร่วม: ศ. ดร. เปี่ยมสุข พงษ์สวัสดิ์, , หน้า.

เฮสเพอเรทินและนารินเจนินจัดเป็นสารพลาโวนอนที่พบมากในผลไม้ตระกูลส้ม เป็นกลุ่มสารที่มีการนำไปประยุกต์ใช้อย่างกว้างขวางในผลิตภัณฑ์อาหาร อาหารเสริม และเภสัชภัณฑ์ เนื่องจากมีผลดีต่อสุขภาพแต่ด้วยค่าสมบัติการละลายน้ำและความเสถียรที่ต่ำจึงเป็นข้อจำกัดต่อการนำไปประยุกต์ใช้ งานวิจัยนี้ จึงมีแนวคิดในการสร้างสารประกอบเชิงซ้อนระหว่างพลาโวนอยด์กับบีตาไซโคลเดกซ์ทรินและอนุพันธ์ไดเมทิล เพื่อปรับปรุงประสิทธิภาพการละลายน้ำของเฮสเพอเรทินและนารินเจนินให้ดีขึ้น เทคนิคโม่เลคคิวลาร์ไดนามิกส์ซิมูเลชันและการคำนวณพลังงานอิสระถูกนำมาใช้ศึกษาพฤติกรรมของสารประกอบเชิงซ้อนเฮสเพอเรทิน, นารินเจนิน กับบีตาไซโคลเดกซ์ทรินและไดเมทิลบีตาไซโคลเดกซ์ทริน พบว่าเฮสเพอเรทินและนารินเจนินชอบใช้วงแหวนพินิลในการเข้าจับกับวงไซโคลเดกซ์ทรินด้วยพันธะไฮโดรเจนที่แข็งแรง สารประกอบเชิงซ้อนไดเมทิลไซโคลเดกซ์ทรินมีความเสถียรและมีสมบัติการละลายน้ำสูงกว่าสารประกอบเชิงซ้อนบีตาไซโคลเดกซ์ทริน เพื่อสนับสนุนผลข้างต้น จึงทำการทดลองเฟสการละลายของสารประกอบเชิงซ้อนทั้งสอง จากผลการทดลองได้รูปแบบการละลายของสารประกอบเชิงซ้อนแบบ A_L ซึ่งแสดงว่าการละลายของพลาโวนอนเพิ่มขึ้นเมื่อความเข้มข้นของไซโคลเดกซ์ทรินเพิ่มขึ้น โดยการละลายของสารประกอบเชิงซ้อนของอนุพันธ์ไดเมทิลสูงกว่าของบีตาไซโคลเดกซ์ทริน หลังจากนั้นได้เตรียมสารประกอบเชิงซ้อนของแข็งและตรวจสอบการเกิดสารประกอบเชิงซ้อนนี้ด้วยเทคนิค DCS และ FTIR จากผลของ DSC ไม่พบพีคของเฮสเพอเรทินและนารินเจนินในสารประกอบเชิงซ้อน 1:1 ที่เตรียมโดยวิธีการทำแห้งแบบแช่เยือกแข็ง แต่เกิดพีคเอนโดเทอร์มิกใหม่ขึ้นมาแทน ซึ่งยืนยันได้ว่าเกิดสารประกอบเชิงซ้อนจริง ในขณะที่การเตรียมโดยวิธีบดผสมแบบเปียกไม่ทำให้เกิดสารประกอบเชิงซ้อน นอกจากนี้ยังตรวจสอบการปลดปล่อยพลาโวนอนจากสารประกอบเชิงซ้อนเทียบกับสารพลาโวนอนอิสระโดยวิธีดีสโซลูชัน ดังจะเห็นได้อย่างชัดเจนว่าการเกิดสารประกอบเชิงซ้อนกับไดเมทิลบีตาไซโคลเดกซ์ทรินทำให้สารพลาโวนอนทั้งสองถูกปลดปล่อยออกมาในสารละลายน้ำได้ดีกว่าการเกิดสารประกอบเชิงซ้อนกับบีตาไซโคลเดกซ์ทริน

ภาควิชา ชีวเคมี

ลายมือชื่อนิสิต

สาขาวิชา ชีวเคมีและชีววิทยาโมเลกุล

ลายมือชื่อ อ.ที่ปรึกษาวิทยานิพนธ์หลัก

ปีการศึกษา 2556

ลายมือชื่อ อ.ที่ปรึกษาวิทยานิพนธ์ร่วม

5572102023 : MAJOR BIOCHEMISTRY AND MOLECULAR BIOLOGY

KEYWORDS: HESPERETIN / NARINGENIN / CYCLODEXTRIN / RELEASING PROCESS / MOLECULAR DYNAMIC SIMULATION / PHASE SOLUBILITY / DISSOLUTION PROFILE

WARATCHADA SANGPHEAK: ENHANCEMENT OF WATER SOLUBILITY OF HESPERETIN AND NARINGENIN BY COMPLEXATION WITH β -CYCLODEXTRIN AND ITS DIMETHYL DERIVATIVE. ADVISOR: THANYADA RUNGROTMONGKOL, Ph.D., CO-ADVISOR: PROF. PIAMSOOK PONGSAWASDI, Ph.D., pp.

Hesperetin and naringenin, the flavonoids of the class flavanones, are abundant in citrus fruits. They are widely applied in food products to enhance the health function as well as used in developing nutraceutical and pharmaceutical products. A limiting factor hampering the use of flavonoids in many applications is its low water solubility and stability. In the present study, the inclusion complex with β -cyclodextrin and dimethyl derivative to solve this problem is our aim. Molecular behaviours of inclusion complex between hesperetin or naringenin and β -CD/DM- β -CD, were theoretically investigated using the molecular dynamics simulation and free energy calculation. Both hesperetin and naringenin most likely preferred to bind with CDs cavity via the phenyl ring with a formation of strong hydrogen bonds. The system stability and solubility of the two flavanones in complex with DM- β -CD was considerably more stable and soluble than that with β -CD. To support these results, we examined the phase solubility diagram of the two flavanones inclusion complexes. The result showed the formation of soluble complex as AL type, indicating increase in flavanone stability when cyclodextrin was increased, with higher solubility of the DM- β -CD complexes. Solid complexes were prepared and DSC and FTIR were used to confirm the inclusion complex. From the DSC profile, the endothermic peak of free hesperetin and naringenin in the 1:1 inclusion complex formed by freeze-drying method disappeared, with the appearance of a new endothermic peak. This implied that the real inclusion complex was formed while the kneading method did not result in the formation of inclusion complex. Moreover, we examined the release of flavanones from the inclusion complexes compared to the free flavanones by dissolution method. It is clearly seen that the complexation with DM- β -CD made better release of both flavanones to the aqueous solution than with β -CD complexes.

Department: Biochemistry

Student's Signature

Field of Study: Biochemistry and Molecular
Biology

Advisor's Signature

Co-Advisor's Signature

Academic Year: 2013

ACKNOWLEDGEMENTS

Many people have contributed to development of this study, which I am very appreciated for their kind cooperation and their advice. First, and foremost, I would like to express my gratitude to my advisor, Dr. Thanyada Rongrotmongkol for her invaluable advice, guidance, and encouragement. Her kindness and cheerfulness are also deeply appreciated

I wish to express appreciation for her kindness to my thesis co-advisor, Professor Dr. Piamsook Pongsawasdi in addition, to the members of my thesis committee for spending their time, comments and suggestion. I also would like to thanks the members of my thesis committee, Professor Dr. Peter Wolschann, for discussion and advice.

Moreover, I would like to thank the financial support from Ratchadapiseksomphot Endowment Fund (RES560530176-FW) and IIAC Centenary Academic Development Project of Chulalongkorn University. T.R. acknowledges the TRF-CHE Research Grant for New Scholars (MRG5580223). We thank the Computer Chemistry Unit Cell, the Vienna Scientific Cluster (VSC-2) for facilities and computing resources and the support of the Starch and Cyclodextrin Research Unit of Chulalongkorn University. I would like to thank staff of the Department of manufacturing pharmacy at the Faculty of Pharmaceutical Science, Chulalongkorn University for providing facilities and great helpful support.

CONTENTS

	Page
THAI ABSTRACT	v
ENGLISH ABSTRACT	vi
ACKNOWLEDGEMENTS	vi
CONTENTS	vii
CHAPTER I	1
INTRODUCTION	1
1.1 Flavonoids	1
1.2 Cyclodextrins structure and physicochemical properties	5
1.3 Preparation methods of inclusion complex.....	11
1.4 Characterization of inclusion complex.....	14
1.6 Molecular Docking	17
1.7 Molecular dynamics (MD) simulation	18
1.8 Umbrella Sampling simulations.....	19
1.10 The objectives of this thesis.....	22
CHAPTER II.....	23
MATERIALS AND METHODS	23
2.1 Equipments	23
2.2 Chemicals	24
2.3 Computational methods.....	25
2.4 Experimental methods	30
CHAPTER III	35
RESULTS.....	35
3.1 Molecular dynamics simulations of hesperetin-CD complexes.....	35
3.1.1 Docked hesperetin-CD inclusion complex	35
3.1.2 Stability of simulated system.....	37
3.1.3 Hesperetin binding inside the CD cavity	38
3.1.4 Binding free energy.....	43

	Page
3.2 Molecular dynamics (MD) simulations of naringenin.....	45
3.2.1 Docked naringenin-CD inclusion complex.....	45
3.2.2 Stability of the simulated system	47
3.2.3 Ligand binding inside the CD cavity	47
3.2.4 Binding free energy.....	51
3.3 Potential mean force of flavanone-CD complexation.....	54
3.4 Potential energy surface (PES)	56
3.5 Analysis of flavanones	60
3.5.1 Spectrophotometric Method.....	60
3.4.2 High performance liquid chromatography Method	60
3.6 Phase solubility studies.....	66
3.7 The Van't Hoff plot.....	69
3.8 Preparation of flavanone: CD (β -CD and DM- β -CD) solid complexes.....	71
3.9 Analysis of flavanone: CD (β -CD and DM- β -CD) solid complexes	72
3.9.1 Analysis by DSC	72
3.9.2 Analysis by FTIR.....	77
3.10 Dissolution study	84
CHAPTER VI	89
DISCUSSION.....	89
4.1 Analysis of flavanones	89
4.2 Phase solubility study.....	89
4.3 Preparation of the inclusion complex.....	93
4.4 Detection of solid complex.....	94
4.4.1 Differential Scanning Calorimetry (DSC)	94
4.4.2 Fourier Transform Infrared Spectroscopy (FTIR).....	95
4.5 Dissolution study	96
CHAPTER V CONCLUSIONS.....	98

	Page
REFERENCES	100
VITA.....	109



จุฬาลงกรณ์มหาวิทยาลัย
CHULALONGKORN UNIVERSITY

LIST OF TABLES

Table	Page
1. Flavanone aglycones	2
2. Physical properties of the CDs and some derivatives	7
3. Docking information of hesperetin	36
4. Binding free energy of hesperetin complex	44
5. Docking information of naringenin	45
6. Binding free energy of naringenin complex	53
7. Stability constants of hesperetin and naringenin complex at different temperature	69
8. Thermodynamic values for complex of hesperetin and naringenin	71
9. FTIR data of hesperetin, β -CD, and hesperetin- β -CD inclusion complex	82
10. FTIR data of hesperetin, DM- β -CD, and hesperetin-DM- β -CD inclusion	82
11. FTIR data of naringenin, β -CD, and naringenin- β -CD inclusion complex	83
12. FTIR data of naringenin, DM- β -CD, and naringenin-DM- β -CD inclusion complex	83
13. Dissolution rate of hesperetin from free and complex form at different time	87
14. Dissolution rate of naringenin at different time compared method between by spectrophotometric and HPLC	88
15. Comparison of ΔG values between the theoretical and experimental studies for all complexes.	92

LIST OF FIGURES

Figure	Page
1 Chemical structures of flavanone	1
Chemical structure of a flavanone with substitute -R groups	2
3 Chemical structures of hesperetin and naringenin	4
4 Chemical structure of three types of small ring cyclodextrins	5
5 The dimensions of the three most common cyclodextrin molecules	6
6 Chemical structure of 2,6-di-O-methyl- β -CD (DM- β -CD), where -R is -CH ₃ .	8
7 Phase solubility profiles and classification of complexes	10
8 Graphical represent: Inclusion complex formation	13
9 Free energy and the contributions A_j of some of the windows	20
10 Definition of the distance used in umbrella sampling	30
11 Top views of the CD hydrophobic cavity and H-bond showing	37
12 RMSD plots of the hesperetin in complex with β -CD and DM- β -CD	40
13 Distance from the center of gravity of each hesperetin ring to center of gravity of cyclodextrin	41
14 The possible orientations of hesperetin in the hydrophobic cavity	42
15 Cutaway views of naringenin occupied in β -CD and DM- β -CD	46
16 RMSD plots of naringenin complexes with β -CD and DM- β -CD	49
17 Distance from the center of gravity of each naringenin ring to center of gravity of cyclodextrin	50
18 Cutaway views on the MD structures of naringenin- β -CD and naringenin-DM- β -CD	51
19 Potential of mean force (PMF) profiles for the hesperetin	55
20 Potential of mean force (PMF) profiles for the naringenin	56
21 H-bond between flavanones and CDs of hesperetin- β -CD complex (left) and hesperetin-DM- β -CD complex (right)	58

22	H-bond between flavanones and CDs of naringenin- β -CD complex (left) and naringenin-DM- β -CD complex (right)	58
23	Potential energy surface of β -CD (left) and DM- β -CD (right) without guest molecule	59
24	Potential energy surface of hesperetin- β -CD complex (left) and hesperetin-DM- β -CD complex (right)	59
25	Potential energy surface of naringenin- β -CD complex (left) and naringenin-DM- β -CD complex (right)	59
26	The UV spectra of hesperetin and their complexes	62
27	The UV spectra of naringenin and their complexes	62
28	HPLC chromatogram of 0.12 mM hesperetin	63
29	HPLC chromatogram of 0.12 mM naringenin	63
30	Calibration curve of hesperetin by spectrophotometric method	64
31	Calibration curve of naringenin by spectrophotometric method	64
32	Calibration curve of hesperetin by High performance liquid chromatography method	65
33	Calibration curve of naringenin by High performance liquid chromatography method	65
34	Phase solubility study of hesperetin with β -CD and DM- β -CD in water at different temperature	67
35	Phase solubility study of naringenin with β -CD and DM- β -CD in water at different temperature	68
36	Van't Hoff plot of the formation of the complex between hesperetin and β -CD or DM- β -CD	70
37	Van't Hoff plot of the formation of the complex between naringenin and β -CD or DM- β -CD	71
38	DSC thermograms of cyclodextrin, hesperetin and their complex by freeze-drying method	73
39	DSC thermograms of cyclodextrin, naringenin and their complex by freeze-drying method	74

40	DSC thermograms of cyclodextrin, hesperetin and their complex by kneading method	75
41	DSC thermograms of cyclodextrin, naringenin and their complex by kneading method	76
42	Infrared spectra of cyclodextrin, hesperetin and their complex by freeze-drying method	78
43	Infrared spectra of cyclodextrin, naringenin and their complex by freeze-drying method	79
44	Infrared spectra of cyclodextrin, hesperetin and their complex by kneading method	80
45	Infrared spectra of cyclodextrin, naringenin and their complex by kneading method	81
46	The dissolution diagram at 37 °C in water of hesperetin and their complex	85
47	The dissolution diagram at 37 °C in water of naringenin and their complex	85
48	A typical HPLC chromatogram of hesperetin- β -CD complex when dissolution time was 30 minutes	86
49	A typical HPLC chromatogram of naringenin- β -CD complex when dissolution time was 30 minutes	86

LIST OF ABBREVIATIONS

α -CD	alpha-cyclodextrin
β -CD	beta-cyclodextrin
γ -CD	gamma-cyclodextrin
DM- β -CD	2,6 dimethyl-beta-cyclodextrin
CD	cyclodextrin
K_c	stability constant
R^2	regression coefficient
$^{\circ}\text{C}$	degree Celsius
DSC	differential scanning calorimetry
FTIR	fourier transform infrared
M	Molar
nm	nanometer
ns	nanosecond
MD	molecular dynamics simulation
RMSD	root mean square displacement
ESP	electrostatic potential
RESP	restrained electrostatic potential
vdW	van der Waals
PMF	potential of mean force
MM/PBSA	Molecular Mechanic/ Poisson-Boltzmann Surface Area
MM/GBSA	Molecular Mechanic/generalised Born

CHAPTER I

INTRODUCTION

1.1 Flavonoids

Flavonoids are a group of natural products found in many vegetables and fruits. Based on the variations in their polyphenolic structure, flavonoids can be divided into the different classes of flavonols, flavones, flavanones, catechins, anthocyanidins, isoflavones, dihydroflavonols and chalcones. Their broad pharmacological profiles include anti-lipoperoxidant, anti-inflammatory properties (Abad et al., 1993) and the ability to exert anticancer and chemopreventive activities (Verma et al., 1988).

1.1.1 Flavanones

Flavanones are compounds that give many plants color, as well as affect their taste. They are subclass of flavonoids which occur almost exclusively in *Citrus fruits*. Flavanones skeleton is the same as that for flavonoid, composed of the chromones rings (commonly designated as A and C), which are connected with a phenyl ring (B), as shown in Fig 1.

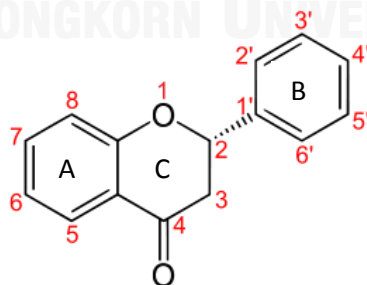


Figure 1. Chemical structure of a flavanone

Flavonoids are mainly present in *Citrus* fruits as their glycosyl derivatives. Aglycones (the forms lacking the sugar moieties) occur less frequently in juices, owing to their lipophilic nature and hence their low solubility in water (Fig. 2 and also Table 1). The presence of a relatively large number of flavonoids in *Citrus* juices is a result of the many different combinations that are possible between polyhydroxylated aglycones and a limited number of mono- and disaccharides. The most common sugar moieties include D-glucose and L-rhamnose. The glycosides are usually *O*-glycosides, with the sugar moiety bound generally to the aglycone hydroxyl group at C-7, or at the C-3 in some cases. In addition to these, C-glycosides have also been detected in various *Citrus* fruits or juices [1].

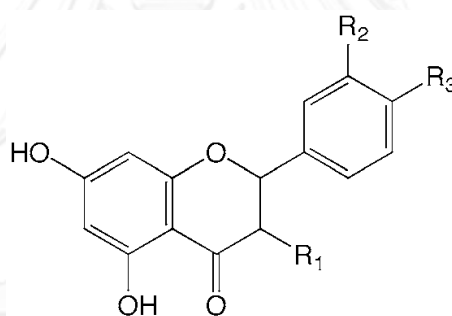


Figure 2. Chemical structure of a flavanone with substitute -R groups

Table 1. Flavanone aglycones

Compound name	R ₁	R ₂	R ₃
Hesperetin	H	OH	OMe
Naringenin	H	H	OH
Taxifolin	OH	OH	OH
Isosakuranetin	H	H	OMe
Eriodictyol	H	OH	OH

1.1.2 Hesperetin and Naringenin

In this study, we are interested in hesperetin (2S)-5,7-dihydroxy-2-(3-hydroxy-4-methoxyphenyl)-2,3-dihydrochromen-4-one in Fig. 3A) and naringenin (5,7,4-trihydroxyflavanone or 5,7-dihydroxy-2-(4-hydroxyphenyl) chroman-4-one in Fig. 3B), which belong to the flavanones class of flavonoids. They are abundant in citrus fruits, such as grapefruit (*Citrus paradise*) and orange (*Citrus sinensis*). They have many pharmacological effects [2, 3] including inhibition of chemically induced mammary [4], urinary bladder [5] and colon [6, 7] carcinogenesis in laboratory animals. In addition, hesperetin shows blood lipid-lowering effect [8-10], anti-inflammatory activity towards the enzymes involved in arachidonate metabolism [11-13] and drug inhibition against cytochrome P-450 [14]. Besides, it is found to enhance microcirculation, assist recovering of venous ulcers, help in treatment of chronic venous insufficiency and hemorrhoids, and prevent post-operative thromboembolism [15]. In the cancer case, naringenin was reported to induce apoptosis in various cancer cell lines with no effect on normal cells (Park et al., 2008). Additionally, it has an insulin-like effect to decrease apolipoprotein B (Apo B) secretion in hepatocytes and to lower blood glucose levels in healthy male wistar rats (Zygmunt et al., 2010). From this point of views, there is a growing interest in applying hesperetin and naringenin in food products to enhance the health functions as well as used in developing nutraceutical and pharmaceutical products. Similarly to many flavonoids, their use in many applications is mostly limited by their low water solubility and stability.

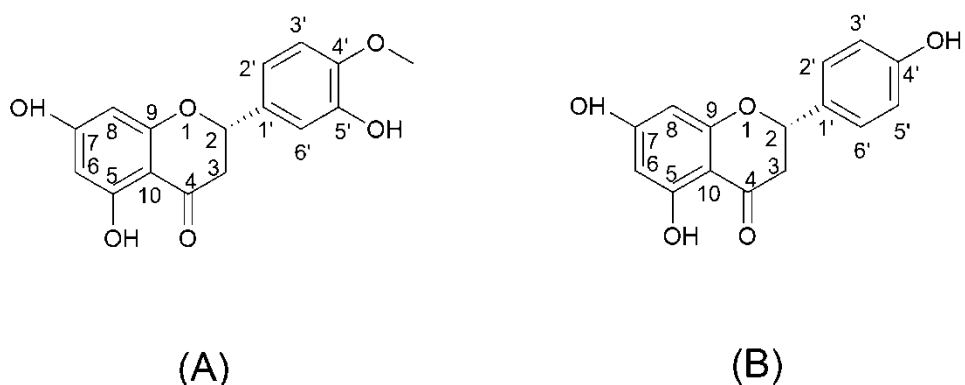


Figure 3. Chemical structures of (A) hesperetin and (B) naringenin

Physical properties of hesperetin

Empirical formular	: $C_{16}H_{14}O_6$
Molecular weight	: 302.2788
Chemical name	: (2S)-5,7-dihydroxy-2-(3-hydroxy-4-methoxyphenyl)-3,4-dihydro-2H-1-benzopyran-4-one
Melting point	: 227.5 °C
Solubility	: 138 mg in 1 L of water

Physical properties of naringenin

Empirical formular	: $C_{15}H_{12}O_5$
Molecular weight	: 272.2528
Chemical name	: (2S)-5, 7-dihydroxy-2-(4-hydroxyphenyl)-3,4-dihydro-2H-1-benzopyran-4-one
Melting point	: 251 °C
Solubility	: 214 mg in 1 L of water

1.2 Cyclodextrins structure and physicochemical properties

Cyclodextrins (CDs), are non-reducing cyclic glucose oligosaccharides resulting from the cyclomaltodextrin glucanotransferase (E.C. 2.4.1.19; CGTase) catalyzed degradation of starch [16]. The natural cyclodextrins (CDs) are a group of cyclic oligosaccharides, that consist of six (α -cyclodextrin or α -CD), seven (β -cyclodextrin or β -CD) or eight (γ -cyclodextrin or γ -CD) glucopyranose units linked by α -(1, 4) glycosidic bonds (Fig 4). From their geometry, the internal cavity is highly hydrophobic, whilst the external hydroxyl face establishes a hydrophilic character. The CDs are not perfectly cylindrical molecules but are toroidal or cone shaped. The secondary hydroxyl groups (on the C-2 and C-3 atoms of the glucose units) are situated on one edge of the ring and all primary hydroxyls on the other. The secondary hydroxyl side is wider than the primary hydroxyl side (Fig 5). In addition, the dimensions of the CDs alter with the number of glucose units. Because of their different internal cavity diameters, each CD shows a different ability of complex formation with guest molecules. The complex formed is called the “inclusion complex” [16]. Table 2 listed the important physicochemical properties of CDs and a dimethyl derivative.

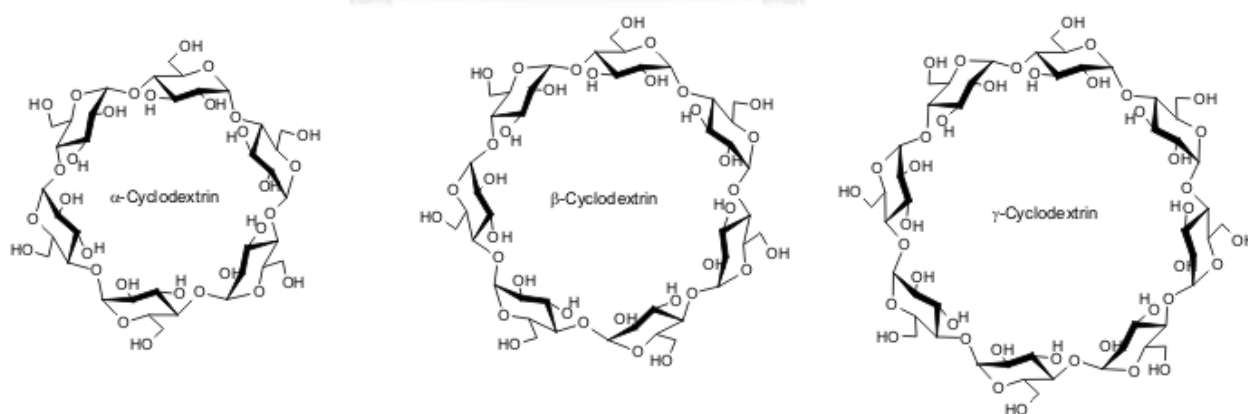


Figure 4. Chemical structure of three types of small ring cyclodextrins

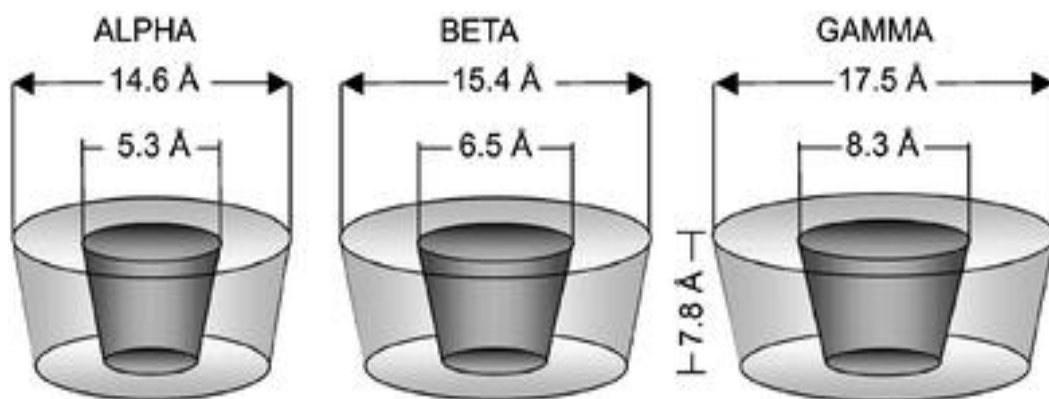


Figure 5. The dimensions of the three most common cyclodextrin molecules [17]

1.2.1 Cyclodextrin derivatives

However, the natural cyclodextrins, in particular β -cyclodextrin, have limited aqueous solubility meaning that complexes resulting from interaction of lipophiles with these cyclodextrins can be of limited solubility resulting in precipitation of solid cyclodextrin complexes from water and other aqueous systems. Therefore the more soluble cyclodextrin derivative was focused. The amorphous CD, 2,6-dimethyl- β -cyclodextrin (DM- β -CD) (Fig. 6), is a chemically modified cyclomaltoheptaose (β -CD) derivative obtained by methylation of the 2- and 6-hydroxyl groups. Compared to the native β -CD, DM- β -CD exhibits an increased solubility in water and organic solvents (Rajewski and Stella, 1996) which enable its use as a carrier for poorly soluble molecules in water or hydrophobic solvents (Szente and Szejtli, 1999; Merkus et al., 1999). In addition, DM- β -CD was found to be an effective absorption promoter for nasal glucagon in rabbit (Merkus et al., 1999) and has been reported in a European patent application for oral or parenteral administration (Szejtli, 1983). To date, the solubility enhancement of naringenin by natural cyclodextrin has been reported from experimentally and theoretically derived studies, but only a few studies on the DM- β -CD derivative are available.

Table 2. Physical properties of the CDs and derivatives of β -CD [16].

	α	β	γ	DM- β ¹⁾	HP- β ²⁾
*Number of glucose residues:	6	7	8	7	7
*Cavity dimension (Å)					
-Cavity diameter:	5	6	8	6	6
-Height of torus:	7.9	7.9	7.9	10.0	
-Diameter of periphery:	14.6	15.4	17.5		
*Molecular weight:	973	1135	1297	1331	± 1300
*Aqueous solubility ³⁾	14.5	1.85	23.2	57	>50
*Melting point (°C)	275	280	275	295-300	
*pKa ⁴⁾ :	12.3	12.2	12.1		
*Half-life of ring opening ⁵⁾ (hr)	6.2	5.4	3.0	8.5	
*Enzymatic hydrolysis ⁶⁾ :	negligible	slow	rapid		

¹⁾ heptakis-2,6-di-O-methyl- β -CD

²⁾ 2-hydroxypropyl- β -CD

³⁾ in grams per 100 ml water at ambient temperature

⁴⁾ pKa : by potentiometry at 25 °C

⁵⁾ Half-life of ring opening : in 1N HCl at 60°C

⁶⁾ by *Aspergillus oryzae* α -amylase

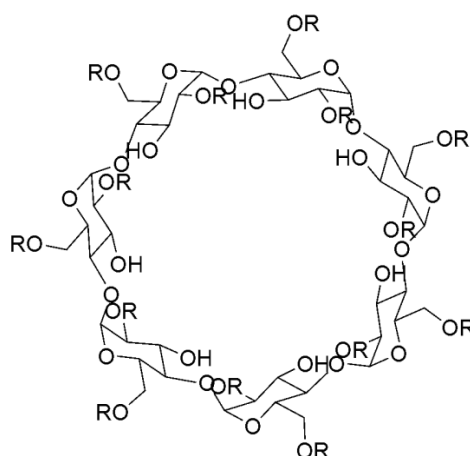


Figure 6. Chemical structure of 2,6-di-O-methyl- β -CD (DM- β -CD) where $-R$ is $-\text{CH}_3$

1.2.2 Complex formation and flavanone solubility

Cyclodextrins are able to form inclusion complexes with many guest molecules by taking up guest molecules into the central cavity. No covalent bonds are formed or broken during the guest-CD complex formation and in aqueous solutions [18]. In all complexation process including those associated with CDs, the measurement and knowledge of the stability constant (K_c) can be represented as follow.



Higuchi and Connors had classified different types of complex based on their effect on substrate solubility as indicated by phase-solubility profiles (Fig 6). A-type profiles: consist of three subtypes: A_L indicates a linear increase in solubility as a function of solubilizer concentration, A_p indicates an isotherm wherein the curve deviates in a positive direction from linearity (i.e. the CD is proportionally more effective at higher concentrations), A_N indicates a negative deviation from linearity (i.e. the CD is proportionally less effective at higher concentrations). B-type profiles indicate the formation of complexes with limited water solubility, there are two subclasses: B_S

and B₁ system. The B₅- type can be divided into three regions; In Region I the guest molecule solubility initially increases (linearly or non-linearly depending on the complex stoichiometry) with an increase in ligand concentration. Region II, representing the plateau portion, has both the complex and guest in solid phase, and the total solubility is the sum of intrinsic solubility of the guest molecule and that of the complex. Region III, begins when the ligand concentration becomes large enough to deplete the free guest concentration, thus decreasing the total guest solubility. At high cyclodextrin concentrations, complete removal of the free guest molecule leading to a solid phase containing pure complex and the total guest concentration will be equal to the solubility of the complex [19]. The B₁- types are similar to B₅- type except that the complexes being formed are so insoluble that they do not rise to the initial ascending component of the isotherm.

To date, the complexation between flavonoids and cyclodextrins has been experimentally and theoretically studied. For example, the data obtained from the NMR, FT-IR, DSC and X-ray studies showed that it is possible to obtain an inclusion complex (1:1), in solid state and in aqueous solution, between β -CD and hesperetin, hesperidin, naringenin and naringin [20]. From solubility and dissolution rate studies [21], the K_c stability constants of hesperetin- β -CD and naringenin- β -CD complexes were decreased as temperature increased. The solubility of the two flavonoids was influenced by changes of media pH: in basic pH hesperetin and naringenin were in the dissociated form and were more soluble. Tommasini et al. [22] studied the effect of (2-hydroxypropyl)- β -cyclodextrin (HP- β -CyD) on the solubility and antioxidant activity of hesperetin and its 7-rhamnoglucoside derivative. In both complexations, the antioxidant activity was higher than the free guest. These results are of great interest for their potential usefulness in pharmaceuticals. Choi et al. [23] applied the 6-ns molecular dynamic simulation (MD) to distinguish the aqueous solubility of hesperetin and naringenin in complex with β -CD. Based on phase solubility,

thermodynamic and highest occupied molecular orbital (HOMO) results [24], the hydrophobic interaction was found to be the main driving force for inclusion complexes of flavanones (hesperetin, naringenin, naringin, and dihydromyricetin) with (2-hydroxypropyl)-cyclodextrins (HP-CDs) [24]. The ^1H and 2D NMR data indicated that the phenyl ring of the naringenin preferentially inserted into β -CD, DM- β -CD and TM- β -CD cavity. In addition, the order of water solubility is: naringenin/DM- β -CD (1.60 mg/ml) > naringenin/TM- β -CD (1.52 mg/ml) > naringenin/ β -CD (1.34 mg/ml) > free naringenin (0.004 mg/ml) [25]. Although several research groups have reported the inclusion complex of flavanones formed with β -CD, only a few studies are focused on its derivatives.

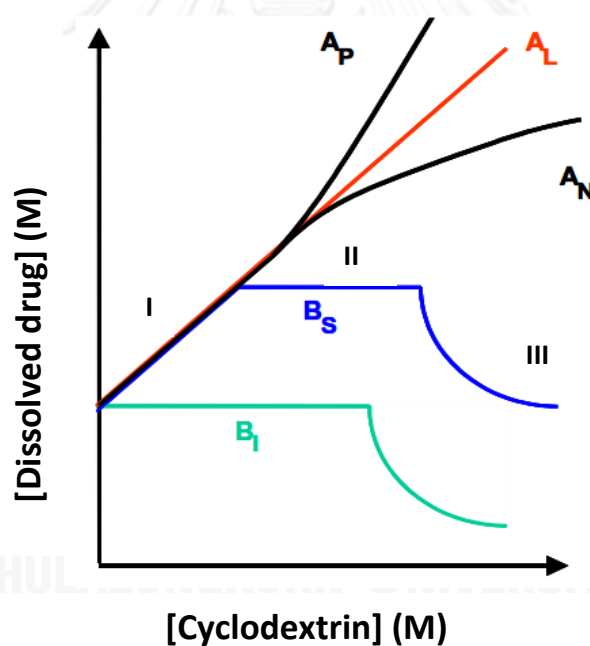


Figure 7. Phase solubility profiles and classification of complexes according to Higuchi and Connors [26]

1.3 Preparation methods of inclusion complex

In formation of the complexes (Fig 7), a guest molecule is held within the cavity of cyclodextrin host molecule. Several techniques are used to form cyclodextrin complexes [26-31]

1.3.1 Physical mixture method

A solid physical mixture of guest and CDs are prepared simply by mechanical trituration. In laboratory scale CDs and guest are mixed together completely by trituration in a mortar and passes through appropriate sieve to get the desired particle size in the final product. In industry scale, the preparation of physical mixture is based on extensive blending of the guest with CDs in a rapid mass granulator usually for 30 minutes. These powdered physical mixture is then stored in the room at controlled temperature and humidity condition [32].

1.3.2 Co-precipitation

Cyclodextrin is dissolved in water and the guest is added while stirring the cyclodextrin solution. The concentration of cyclodextrin can be as high as about 20% if the guest can tolerate higher temperatures. If a sufficiently high concentration is chosen, the solubility of the cyclodextrin–guest complex will be exceeded as the complexation reaction proceeds or as cooling is applied. In many cases, the solution of cyclodextrin and guest must be cooled while stirring before a precipitate is formed. The precipitate can be collected by decanting, centrifugation or filtration. The precipitate may be washed with a small amount of water or other water-

miscible solvent such as ethyl alcohol, methanol or acetone. Solvent washing may be detrimental with some complexes, so this should be tested before scaling up.

The main disadvantage of this method lies in the scale-up. Because of the limited solubility of the cyclodextrin, large volumes of water have to be used. Tank capacity, time and energy for heating and cooling may become important cost factors. [33, 34]

1.3.3 Kneading method

Only a small amount of water is added to form a paste, which is mixed with the cyclodextrin using a mortar and pestle, or on a large scale using a kneader. The amount of time required is dependent on the guest. The resulting complex can be dried directly or washed with a small amount of water and collected by filtration or centrifugation. Pastes will sometimes dry forming a hard mass instead of a fine powder. This is dependent on the guest and the amount of water used in the paste. Generally, the hard mass can be dried thoroughly and milled to obtain a powdered form of the complex.

1.3.4 Spray drying method

Spray drying is not a new technology as far as the pharmaceutical industry is concerned. It is useful method for the processing of pharmaceuticals since it offers a means for obtaining powders with predetermined properties, such as particle size and shape. Spray drying is also a convenient method of drying heat sensitive pharmaceuticals, such drugs, with minimal loss of activity. This is one area where the potential of spray drying has yet to be fully exploited [35]. The flavanones and CD are weighed in terms of equal molar ratios (1:1). This molar ratio was selected after

phase solubility studies. This first monophasic solution of flavanones & CD is prepared using a suitable solvent. The solution is then stirred to attain equilibrium following which the solvent is removed by spray drying.

1.3.5 Freeze-drying method

Freeze drying or lyophilization has been used in a number of applications for many years, most commonly in the food and pharmaceutical industries. Freeze drying involves the removal of water or other solvent from a frozen product by a process called “sublimation”. Sublimation occurs when a frozen liquid goes directly to the gaseous state without passing through the liquid phase. Freeze-drying is a complex process during which drying may proceed more or less rapidly within individual samples throughout the process batch, such that parts of the product will be frozen, whereas other areas are drying or will be dried depending on the nature of the sample and stage in the cycle. The advantages of freeze drying are obvious. Properly freeze dried product do not need refrigeration, and can be stored at ambient temperatures. However, freeze drying is an expensive form of dehydration for foods because of the slow drying rate and the use of vacuum [36].

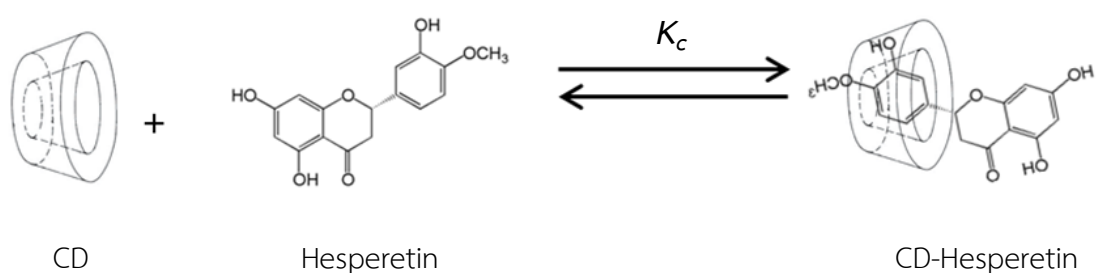


Figure 8. Inclusion complex formation

1.4 Characterization of inclusion complex

Most of the analytical techniques used to characterize solids can be divided into two categories: bulk and molecular. Bulk techniques provide information about the state of the material, and rely upon global properties such as the thermodynamics or particle morphology of the system. Bulk techniques include differential scanning calorimetry (DSC), thermogravimetric analysis (TGA). These techniques provide information about the global state of the material. Molecular-level techniques, such as diffraction, and spectroscopic techniques, provide information by probing the molecular-level interactions in the system [19].

1.4.1 Thermal analysis

Thermal analysis techniques are commonly used to characterize pharmaceutical solids. The advantage of most thermal techniques is that a very limited amount of sample is required to obtain the data. A disadvantage is the properties of the material that are being measured may be significantly different at higher temperatures compared to lower temperatures [19].

1.4.1.1 Differential Scanning Calorimetry (DSC)

DSC is a technique which is a part of Thermal Analysis (TA). Thermal Analysis is based upon the detection of changes in the heat content (enthalpy) or the specific heat of a sample with temperature. As thermal energy is supplied to the sample, its enthalpy increases and its temperature rises by an amount determined, for a given energy input, by the specific heat of the sample. The specific heat of a material changes slowly with temperature in a particular physical state, but alters discontinuously at a change of state. As well as increasing the sample temperature, the supply of thermal energy may induce physical or chemical processes in the

sample, e.g. melting or decomposition, accompanied by a change in enthalpy, the latent heat of fusion, heat of reaction etc. Such enthalpy changes may be detected by thermal analysis and related to the processes occurring in the sample [19].

1.4.1.2 Thermogravimetric Analysis

The technique is used to monitor loss of solvent or decomposition reactions. It is often used in conjunction with DSC to compare the enthalpy of transitions with the resulting weight gain or loss. The heating rate is typically comparable to that used for DSC [19].

1.4.2 Diffraction methods

1.4.2.1 Single-crystal X-ray Diffraction

Single-crystal XRD is one of the most powerful techniques to determine the structure of a molecule in a crystal. To acquire data from a single crystal, the sample is mounted and a narrow beam of X-rays is passed through it. The negative aspect of single-crystal XRD is that a crystal of sufficient size must be grown to be able to determine the crystal structure [19].

1.4.2.2 Powder X-ray Diffraction

PXRD is a common technique for the analysis of polymorphism in crystalline solids. The general principle behinds PXRD and single-crystal XRD is the same, except that in PXRD the material is a powder [19].

1.4.3 Vibrational Spectroscopy

Vibrational spectroscopy techniques include infrared, Raman, and near-infrared spectroscopy. The infrared and Raman both encompass the wavelength range from $400\text{-}4000\text{ cm}^{-1}$ and the near-infrared encompasses approximately $4000\text{-}14000\text{ cm}^{-1}$. The difference between the infrared and near-infrared region is that the infrared corresponds to the fundamental vibrations of the molecular species, and therefore many of the regions in the spectrum can be assigned to specific functional groups [19].

1.4.3.1 Fourier Transform Infrared Spectroscopy (FTIR)

FTIR is a measurement with IR light to analytical technique to qualify and quantify compounds utilizing infrared absorption of molecules. Absorption occurs when the energy of the beam of light (photons) are transferred to the molecule. The molecule gets “excited” and moves to a “higher” energy state. The energy transfer takes place in the form of electron ring shifts, molecular bond vibrations, rotations, and translations. The Fourier transform of the resulting intensities acquired at various path lengths results in an infrared spectrum.

1.4.4 Nuclear magnetic resonance spectroscopy

The NMR experiment makes the direct observation of atoms possible. The integral of an NMR signal is strictly linear by proportional to the amount of atoms in the probe volume. The signals are a measure of molar ratios of molecules, independent of the molecular weight. There are no response factors as in UV-detection caused by varying extinctions dependent on molecular structures; non-linear calibration curves as found with light scattering detectors are unknown to NMR

spectroscopy. There are several advantages of NMR; an NMR spectrum can simultaneously provide information on the quantity of an impurity. In most case, the integration of signals used for quantitation is more precise and accurate than the HPLC analysis. In most case, NMR spectroscopy is quicker (e.g. no equilibration of HPLC column), easy to perform. [37]

1.5 Dissolution studies

The drug dissolution testing is an analytical technique used to assess release profile of drugs from pharmaceutical products, generally solid oral products such as tablets and capsules. Drug dissolution testing plays an important role as a routine quality control test. The overall rate of dissolution depends on the slower of these two steps. In the first step of dissolution, the cohesive properties of the formulated drug play a key role. If the first step of dissolution is rate-limiting, then the rate of dissolution is considered *disintegration controlled*. In the second step (i.e., solubilization of drug particles), the physicochemical properties of the drug such as chemical form and physical form play an important role. If this step is rate-limiting , then the rate of dissolution is *dissolution controlled* [38].

1.6 Molecular Docking

Molecular docking is a method which predicts the preferred conformation and orientation of a ligand bound to a macromolecular target to form stable complex. Knowledge of the preferred orientation in turn may be used to predict the strength of stability or binding affinity between two molecules. Docking process has many algorithms but in this study use CDOCKER algorithm.

A CDOCKER algorithm is a grid-based molecular docking method that employs CHARMM. The receptor is held rigid while the ligands are allowed to be flexible during the refinement. Ligand conformations are randomly generated from the initial

ligand structure through high temperature molecular dynamics, followed by random rotations. The random conformations are refined by grid-based (GRID 1) simulated annealing and a final grid-based or full force field minimization.

Ahmadi and coworker studied stability constants of different guest molecules with beta-cyclodextrin using 3D-QSAR and also were approved and verified by the results of docking studies (CDOKER) [39]. In addition, Ghasemi B. J. and coworker studied stability constants of benzene derivatives as environmental pollutants with α -cyclodextrin using the same technique [40].

1.7 Molecular dynamics (MD) simulation

Molecular dynamic (MD) is a computer simulation technique which describes equilibrium and dynamics properties of a biological system. Configurations of the system by integration of Newton's laws of motion calculate the time dependence of the molecular system are generated. Computer simulations have altered the interplay between experiment and theory. The essence of the simulation is the use of the computer to model a physical system. Calculations implied by a mathematical model are carried out by the machine and the results are interpreted in terms of physical properties. MD simulation is one of most direct ways to theoretically investigate molecular behavior [41] that are not accessible to experimental approaches in complex system, such as in a system involving guest-host interactions [42]. During the past several years, many MD simulations of cyclodextrin and their complexes have been reported. For example, Choi and coworker used MD simulations to study the binding geometry of inclusion complex as a determinant factor for aqueous solubility of the of hesperetin/naringenin with β -CD complexes. They found that a bulky hydrophobic moiety (-OCH₃) of B-ring of hesperetin nearby the primary rim of β -CD was responsible for lower aqueous

solubility of hesperetin- β -CD complex [23]. Fernandes and coworkers studied inclusion complex formation between cyaniding-3-O-glucoside and β -CD using a combined approach of NMR spectroscopy and molecular dynamics simulation [43]. Zhang and coworkers investigated the inclusions of Puerarin and Daidzin with β -CD by molecular dynamics simulation [42]. They found that both compounds could induce a conformation change of β -CD. The conformational change is related to hydrogen bonding interaction.

1.8 Umbrella Sampling simulations

Umbrella Sampling, biased molecular dynamics, is one of the methods that provides the free energy along a reaction coordinate. The method uses molecular dynamic simulation to determine the probability for the system to be in a given conformation [44]. The binding energy (ΔG_{bind}) is derived from the potential of mean force (PMF), extracted from a series of umbrella sampling simulations. A series of initial configurations is generated, each corresponding to a location wherein the molecule of interest (generally referred to as a "ligand") is harmonically restrained at increasing center-of-mass (COM) distance from a reference molecule using an umbrella biasing potential. This restraint allows the ligand to sample the configurationally space in a defined region along a reaction coordinate between it and its reference molecule or binding partner. The windows must allow for slight overlap of the ligand positions for proper reconstruction of the PMF curve. For sampling, an important factor is a proper choice of the reaction coordinate. If the reaction coordinates misses important structural changes, it can lead to artificial lowering or raising of the result obtained by umbrella sampling [45]. A too high barrier may be the result of an unfavorable path being taken.

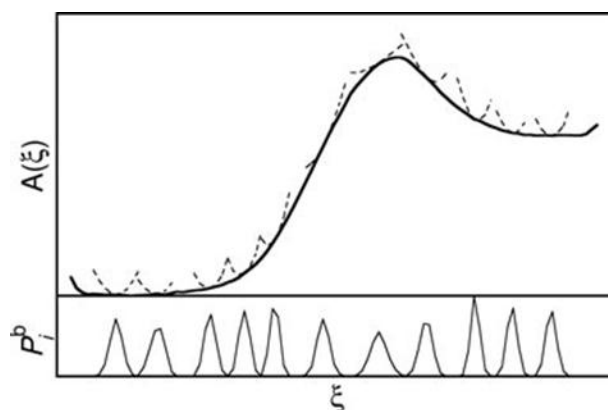


Figure 9. Free energy (black solid curve), the contributions A of some of the windows (dashed curves) and the biased distribution P_i (grey solid curve) [44]

In 2006, Yu and coworkers [46] studied interaction of three cyclodextrin (β -CD, DM- β -CD and HP- β -CD) with cholesterol using MD simulations. The free energy were calculated by ABF calculation and compared to umbrella sampling method. Barghouthi and coworkers [47] used MD simulation to study the dynamics of the inclusion complexes of methyl viologen (MV) with cucurbit[n]uril, CB_n (where $n=6, 7$ and 8) in aqueous solution. The PMF for the host-guest distance was obtained by umbrella sampling.

In addition, this technique was used in publication of Zhang and co-workers [48], they studied binding process of β -CD (host) and the four guest molecules puerarin, daidzin, daidzein and nabumetone. These four molecules have been reported to possess potential medicinal values. Steered molecular dynamics (SMD) was used to generate a formation process of complex, PMF was computed with umbrella sampling [48].

1.9 Potential Energy Surface (PES)

Potential energy surface (PES) is a theoretical concept used to describe the energy of a system, especially a collection of atoms, in terms of certain parameters, normally the positions of the atoms. This method depends in a fundamental way on the Born-Oppenheimer approximation. The surface might be in one or more dimensions. The plot of formation of a PES which records how the energy varies with respect to the nuclear coordinates. A molecular PES suggests how the potential energy changes with respect to the variety of configurations that are plausible for a particular molecule. The regions of high potential energy indicate a high-energy nuclear arrangement, which are molecular conformations that have unfavorable electronic or steric interactions. Conversely, regions of low potential energy indicate nuclear arrangements that are in low energy molecular conformations. Examination of the reaction PES gives many clues as to the nature of the reaction. As known that reactants and products are stable structures having relatively low potential energies, they are expected to be associated with minima on the PES.

1.10 The objectives of this thesis

1. To investigate interactions between CDs and flavanones in the inclusion complexes by molecular dynamics simulation.
2. To determine enhancement of flavanone solubility by complex formation
3. To form inclusion complex between CDs and flavanones and to characterize the complexes.
4. To investigate release of flavanones by umbrella sampling and dissolution of solid complex in comparison to free flavanones

CHAPTER II

MATERIALS AND METHODS

2.1 Equipments

- Analytical balance : AB204-S, Mettler Toledo, Switzerland.
PB303-S, Mettler Toledo, Switzerland.
- Centrifuge :Centrifuge 5430 R, Eppendorf, Germany.
- High Performance Liquid Chromatography : Waters 600, USA.
- Column : Reversed-phase C18 column (25 cm × 4.6 mm), Japan
- Syringe : Nipro Syringe, Thailand.
- Nylon Syringe Filter : 0.45 μm Sigma-Aldrich, USA.
- UV-VIS Spectrophotometer : DU650, Spectrophotometer, Beckman, USA.
- Vortex : Model G-560E, Scientific Industries USA.
- Shaker water bath : Memmert, Germany.
- Differential Scanning Calorimeter (DSC) : Netzsch, 204 F1 Phoenix.
- Fourier Transform Infrared Spectrometer (FT-IR): Perkin Elmer, Spectrum One, USA.
- Freeze dryer : LYO-LAB, Lyophilization Systems, Inc USA.

2.2 Chemicals

Hesperetin : Cayman Chemical Company, USA.

Naringenin : Sigma-Aldrich Chemie, UK

Cyclodextrin : β -cyclodextrin (HPLC grade), MW=1135,
DM- β -cyclodextrin, MW=1331,
(Wako Pure Chemical Industries, Japan)

Methanol : Analytical grade: Loba Chemie, Mumbai, India.

Acetonitrile : (HPLC grade): LAB-SCAN Analytical Science, Ireland.

2.3 Computational methods

2.3.1 Molecular simulation method

The starting configurations of hesperetin and naringenin were created and fully optimized with the *ab initio* calculation using the HF/6-31G* basis set in the Gaussian09 program, [49] while the optimized structures of β -CD and DM- β -CD were taken from Cambridge structural database. Prediction of hesperetin and naringenin inclusion complex with these two CDs was performed via a docking procedure with 500 independent runs using the CDOCKER module of Accelrys Discovery Studio 2.5 (Accelrys, Inc.). The three docked inclusion complexes with the best ranked interaction energy and hydrogen bond (H-bond) formation between flavanone and each CD were then chosen for the MD study. The following system preparation and MD simulations on all inclusion complexes were performed with the Amber 12 software package [50]. The Glycam-06 bimolecular force field [51] was applied for the β -CD and DM- β -CD. In case of hesperetin and naringenin, the atomic charges and parameters were developed according to standard procedures [52-54]. The electrostatic potential (ESP) charges around the optimized molecules were evaluated by the HF/6-31G* calculation using Gaussian09. The restrained electrostatic potential (RESP) charges of hesperetin and naringenin were then evaluated by a charge fitting procedure using the antechamber module implemented in the Amber 12, while their parameters were obtained using the parmchk module. The hydrogen atoms of each inclusion complex were minimized with the 1000 steps of steepest descents (SD) followed by 3000 steps of conjugated gradients (CG) to relax the structure and release bad contacts. The complex was solvated by SPC water molecules with a spacing distance of 12 Å around the system surface. The hesperetin- β -CD and hesperetin-DM- β -CD, naringenin- β -CD and naringenin-DM- β -CD complexes consisted of 1362 ± 5 , 1701 ± 14 , 1480 ± 10 and 1750 ± 3 water molecules in the 40 x 40 x 40

Å, 43.0 x 43.0 x 43.0 Å, 41 x 41 x 41 Å and 44.0 x 44.0 x 44.0 Å truncated octahedron periodic boxes, respectively. The water molecules alone were minimized with the SD (1000 steps) and CG (3000 steps) and then minimization with the same process was applied on the whole system. In the next step, the MD simulation with periodic boundary condition using the NPT ensemble and a time step of 2 fs. The electrostatic interactions were taken into account by the particle mesh Ewald approach [55] with a cutoff distance of 12 Å. The SHAKE algorithm was used to constrain all bonds with hydrogen atoms. Each system was heated up to 298 K with a relaxation time of 100 ps and then simulated at the same temperature for 80 ns. The coordinates were recorded every 500 steps for analysis. The root means square displacement (RMSD), distance between the centers of gravity of the hesperetin and naringenin ring and CD ($d(C_{\text{chromone/phenyl ring}}-C_{\text{gCD}})$) along the simulation time were analyzed by the ptraj module. The 30 MD trajectories of inclusion complex extracted from simulation (discussed later) were used for the binding free energy prediction. MM/PBSA and MM/GBSA approaches, the acceptable methods for predicting the absolute binding free energy of molecules in solution [56] were adopted for calculating the free energy of flavanones binding to β -CD and DM- β -CD. The methodology details of both methods have been described elsewhere [53, 57-59]. To correct the MM energy, the single point M06-2X/6-31+G(d,p) calculations were applied to the structures of the inclusion complex, CD and naringenin/hesperetin used in MM/PBSA and MM/GBSA calculations.. Note that the DFT M06-2X functional energy includes the empirical dispersion correction energy, [60] which is an important factor in the guest-host interaction.

the calculation of salvation. The difference of free energies between complexes ($\Delta G_{\text{complex}}$), cyclodextrin ($\Delta G_{\text{cyclodextrin}}$) and hesperetin or naringenin ($\Delta G_{\text{hesperetin or naringenin}}$) is used to calculate the binding free energy of system as Eq. (1)

$$\Delta G_{\text{bind}} = \Delta G_{\text{complex}} - \Delta G_{\text{cyclodextrin}} - \Delta G_{\text{ligand}} \quad (1)$$

In thermodynamics, the total free energy of a system is the sum of its enthalpy term (ΔH) and entropy term with constant temperature ($T\Delta S$).

$$\Delta G = \Delta H - T\Delta S \quad (2)$$

In solution, the ΔH term can be calculated from molecular mechanics energy of formation of complex (ΔE_{MM}) in the gas phase and term of solvation free energy (ΔG_{sol}). Eq. (2) can be rewritten as:

$$\Delta G = (\Delta E_{\text{MM}} + \Delta G_{\text{sol}}) - T\Delta S \quad (3)$$

In Eq. (3), ΔE_{MM} is the sum of the bonded and non-bonded from electrostatic (ΔE^{ele}) and van der Waal interaction energies (ΔE^{vdw})

$$\Delta E_{\text{MM}} = \Delta E^{\text{bonded}} + \Delta E^{\text{ele}} + \Delta E^{\text{vdw}} \quad (4)$$

The solvation free energy term, ΔG_{sol} , contains both polar and non-polar terms. The non-polar term is assumed to the surface accessible surface area (SASA) in Eq. (5). The polar term is calculated from the Poisson Boltzmann (PB) equation in Eq. (6) or the generalized Born (GB) in Eq. (7). The increasing in SASA is associated with an increase in solvation free energy, which is partly calculated for non-polar and excluded in term of solvent, using Eq. (8). The salvation parameters, γ and β , depend on the methods and solvation models.

$$\Delta G_{sol} = \Delta G_{PB(GB)} + \Delta G_{SASA} \quad (5)$$

$$\Delta G_{PB} = \frac{1}{2} \sum q_i (\varphi_i^{80} - \varphi_i^1) + \Delta G_{SASA} \quad (6)$$

$$\Delta G_{GB} = -166 \left(1 - \frac{1}{\epsilon}\right) \sum_{i=1}^n \sum_{j=1}^n \frac{q_i q_j}{f_{m2GB}} + \Delta G_{SASA} \quad (7)$$

$$\Delta G_{SASA} = \gamma SASA + \beta \quad (8)$$

2.3.2 Umbrella sampling method

The umbrella sampling simulation has been performed with the GROMACS software package (version 4.5.5). The geometry of β -CD was taken from a systematic investigation on the structure of β -CD (Snor et al., 2007) and the structure of DM- β -CD was obtained by adding methyl groups to β -CD and subsequent geometry optimization with the B3LYP/6-31G**. The starting configurations of hesperetin and naringenin were created and fully optimized with the *ab initio* calculation using the HF/6-31G* basis set in the Gaussian09 program, [49]. The topology parameters of β -CD and DM- β -CD were obtained from the GROMOS96 53a6 while those of hesperetin and naringenin were built by the Dundee PRODRG Server. Then, we defined the unit cell for pulling simulation. The box length was $7 \times 7 \times 6 \text{ nm}^3$, containing one host, one guest, and 12,000 water molecules. Here, the steepest descents minimization followed by equilibration with NPT ensemble, where the number of molecules, N; the pressure, P; and the temperature, T, were kept constant. The production with NVT ensemble was applied. The CD host molecule was centered in the box and the cavity axis defined by its seven glycosidic oxygen atoms was oriented in the parallel direction to the Z-axis. The distance between the center of mass of the B-ring of guest molecule and that of the seven glycosidic oxygens of CD along the Z-axis was defined as the reaction coordinate. The values of the reaction coordinate were set

from -2 nm to 2 nm (Fig. 8) with reaction coordinate interval of 0.1 nm. Each simulation was firstly performed for 2 ns in which the pressure was sustained at 1 bar with the semi-isotropic Parrinello-Rahman barostat. The seven glycosidic oxygen atoms of CD and phenyl ring of flavanone were restrained with an isotropic force constant of $1000 \text{ kJ}\cdot\text{mol}^{-1}$. The B-ring of guest was pulled through CD cavity from the secondary rim (Fig. 8) along the Z-axis with harmonic force constant of $5000 \text{ kJ}\cdot\text{mol}^{-1}\cdot\text{nm}^{-2}$. The total simulation time for a single PMF profile was 400 ns (10 ns for each window). The potential means force (PMF) profile for release process was estimated by the weighted histogram analysis method (WHAM) using the 2-10 ns simulations.

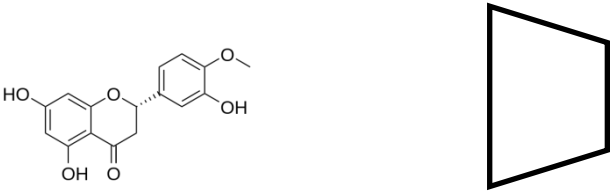
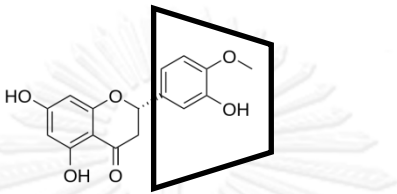
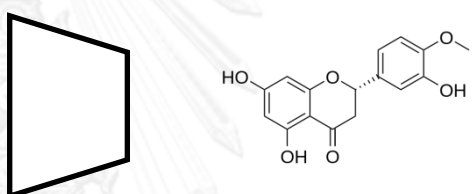
	Starting geometry at -2 nm
	Starting geometry at 0 nm
	Starting geometry at 2 nm

Figure 10. Definition of the reaction coordinates distance used in umbrella sampling

2.4 Experimental methods

2.4.1 Analysis of hesperetin and naringenin

2.4.1.1 Spectrophotometric Method

2.4.1.1.1 The maximum absorption of hesperetin and naringenin

The UV absorption spectra for hesperetin, naringenin, cyclodextrins and its soluble complex with cyclodextrin were compared. The solution of 1mg/20ml flavonaone, β -CD, DM- β -CD and their soluble complexes were

prepared using distilled water (pH ~5.8). The flavanones solutions were boiled at 60 °C for 10 minutes. Then all samples were filtered through 0.45 µm membrane and scanned for absorbance in the wavelength range of 200-400 nm.

2.4.1.1.2 Calibration curves of hesperetin and naringenin

Prepare a stock solution of hesperetin and naringenin with a concentration of 0.16 and 0.18 mM, respectively by accurately weighed 1 mg of both solid samples and dissolved in 20 ml of distilled water. Standard solutions of hesperetin and naringenin were prepared by diluted to the final concentrations of 0.01, 0.02, 0.03, 0.04, 0.05 and 0.06 mM, respectively. All standard solutions were analyzed spectrophotometrically at λ_{\max} obtained from 2.4.1.1.1. Standard calibration curve was plotted.

2.4.1.2 High performance liquid chromatography Method

2.4.1.2.1 Calibration curves of hesperetin and naringenin

Prepare a stock solution of hesperetin and naringenin with a concentration of 1 mM by accurately weighed 3.0 and 2.7 mg, respectively of both solid samples and dissolved in 10 ml of distilled water. Standard solutions of hesperetin and naringenin were prepared by dilute to the final concentrations of 0.04, 0.08, 0.12, 0.16, 0.4, 0.6, 0.8 and 1 mM for hesperetin and 0.04, 0.08, 0.12, 0.16, 0.3, 0.5, 0.7 and 1 mM for naringenin. All standard solutions were analyzed by HPLC at 37 °C. Standard calibration curve was plotted.

2.4.2 Phase-solubility diagram

Phase solubility studies were carried out according to Higuchi and Connors (1965). The data was used to determine the stability constant of the complexes. For this study, the stock solution of 0.015 M β -CD or DM- β -CD was prepared using distilled water. These stock solutions were diluted with distilled water to give concentration in the range 0.002 to 0.0014 M cyclodextrin. Excess hesperetin or naringenin was added to aqueous β -CD or DM- β -CD solution. The mixtures were shaken at 30 ± 0.5 , 37 ± 0.5 and 45 ± 0.5 °C for 72 hours, by water bath shaker. After equilibrium, the samples were centrifuged at 12,000 rpm for 15 minutes; the upper liquid portion was determined for absorbance using UV visible spectrophotometer. Since no detectable changes in λ max of flavanones were found after complexation with cyclodextrins. Therefore, absorbance of the resultant solution was recorded at 286 nm, which was λ max of the flavanones.

Calculation of the stability constants (K_c) from the straight-line portion of the phase solubility diagram was performed according to Higuchi-Connors equation in Eq. (9).

$$K_c = \frac{\text{slope}}{\text{intercept}(1-\text{slope})} \quad (9)$$

2.4.3 Preparation of the inclusion complexes

Inclusion complex of hesperetin and naringenin with β -CD and DM- β -CD were prepared by the kneading and Freeze drying methods.

2.4.3.1 Kneading method

In the kneading method, hesperetin or naringenin and β -CD or DM- β -CD were weighed accurately and mixed in a molar ratio of 1:1 (56.0 mg β -CD or 66.5 mg DM- β -CD : 15.0 mg hesperetin or 13.6 mg naringenin). A homogenous paste of cyclodextrin was prepared in a mortar by adding water in small quantities. Hesperetin or naringenin was added to this paste in portions, with continuous kneading for 15 minutes. After that these pastes were dried in hot air oven at 45 °C for 10 hours. The dried complexes were grinded to fine powder and stored in a desiccator till further use.

2.4.3.2 Freeze drying method

Solid-stage hesperetin or naringenin complexes with β -CD or DM- β -CD in 1:1 molar ratio were prepared. Each compound was accurately weighed, then dissolved in distilled water (10 ml) and sealed in a flask. The mixture was magnetic stirred at room temperature for 24 hours. Then, the solution was filtered (0.45 μ m pore size). The solution was frozen overnight and then lyophilized over the period of 24 hours using a freeze-dryer apparatus. The dried powder was stored in a desiccator.

2.4.4 Characterization of the inclusion complexes

The interaction of the guest and CD molecules can be monitored. Some useful techniques are used in this study.

2.4.4.1 Differential scanning calorimetric analysis (DSC)

The differential scanning calorimetry, DSC (Netzsch, 204 F1 Phoenix) at The Technological Research Equipment Center of Chulalongkorn University was used for recording DSC thermograms of the free hesperetin and naringenin, the inclusion complexes prepared by kneading method as well as the freeze-drying method. The

thermal behavior was studied by heating samples (2-5 mg) in closed aluminum crimped pans at a rate of $10^{\circ}\text{C min}^{-1}$ between 25 and 250 $^{\circ}\text{C}$ temperature range for hesperetin and 25 to 300 $^{\circ}\text{C}$ for naringenin [21].

2.4.4.2 Fourier transforms infrared (FT-IR) spectroscopy

An IR spectrophotometer (FTIR Perkin Elmer) at The Technological Research Equipment Center of Chulalongkorn was used to obtain spectrum of free flavanones and all solid complexes using potassium bromide (KBr) disc in the range of 400-4000 cm^{-1}

2.4.5 Dissolution study

Dissolution studies of all samples were carried out in 20 ml of distilled water (as a medium solution). Hesperetin or naringenin and its solid complexes were added in the distilled water and shaken at 37 $^{\circ}\text{C}$, 1 ml was withdrawn at different time intervals (0, 5, 10, 20, 30, 60 and 120 minutes) for analysis of hesperetin or naringenin content. The sampling was diluted for appropriate concentration, and analyzed by UV spectrophotometer and HPLC at 286 nm. The dissolution studies were performed in triplicate.

CHAPTER III

RESULTS

3.1 Molecular dynamics simulations of hesperetin-CD complexes

3.1.1 Docked hesperetin-CD inclusion complex

From the 500 independent docking runs, the two major different orientations of the guest molecule, hesperetin, occupied in the β -CD cavity were observed. For inclusion complex A, its chromone ring was located inside the β -CD's cavity close to the primary rim, whereas for complex B the phenyl ring was inserted instead. On the other hand, hesperetin preferentially formed the inclusion complex with DM- β -CD through its B-ring. The percentage of conformational occurrences, interaction energy and hydrogen bond (H-bond) formation of hesperetin inside the hydrophobic cavity of cyclodextrin are given in Table 3. The phenyl ring of hesperetin molecule preferentially dipped to β -CD (89 % docked conformation) and its dimethyl derivative (100 %) and located close to the primary rim. The obtained information was in good agreement with the theoretical studies by 6-ns MD simulation [23] as well as the semi-empirical AM1 method [61] on hesperetin- β -CD complex. Based on the interaction energy and number of H-bonds formation between hesperetin and cyclodextrin, the best formed inclusion complex with β -CD and DM- β -CD (Fig. 11) were focused and compared. In chromone ring complex, hesperetin has no H-bond interaction with β -CD, while two strong H-bonds were found in phenyl ring complex. In Fig. 11B, the hydroxyl oxygen (O7) on its chromone ring interacted with the 3-OH group located in the interior of β -CD (2.2 Å), and the H7 group on the same ring formed a H-bond with the hydroxyl oxygen (O3) of one of the other D-glucopyranose units (2.4 Å). This leads to a more stable phenyl ring complex than chromone ring

complex in gas phase as seen by interaction energy of $-30.81 \text{ kcal}\cdot\text{mol}^{-1}$ and $-26.91 \text{ kcal}\cdot\text{mol}^{-1}$, respectively. In comparison on the H-bond interaction of our results and previous study, we found that H-bond interactions were occurred between the chromone ring and β -CD whereas in the previous study the interactions were found with the phenyl ring. Although, the H-bond strength of hesperetin-CD complex more than DM- β -CD complex the interaction energies were not significantly different in gas phase. The top three ranked conformations of each inclusion complex from the docking results were chosen for study the dynamics behaviors of complex in aqueous solution.

Table 3. Percentage of docked conformation and interaction energy ($\text{kcal}\cdot\text{mol}^{-1}$) of hesperetin into the interior of β -CD and DM- β -CD cavities

Inclusion complex	% Docked conformation	Interaction	
		energy ($\text{kcal}\cdot\text{mol}^{-1}$)	# H-bond (distance)
Hesperetin- β -CD	89 % phenyl ring inserted	-30.81	O7-H7...O3 (β -CD) 2.2
	11% chromone ring inserted	-26.91	O7-H7...O2 (β -CD) 2.4
Hesperetin-DM- β -CD	100 % phenyl ring inserted	-30.83	O7-H7...O3 (DM- β -CD) 2.3

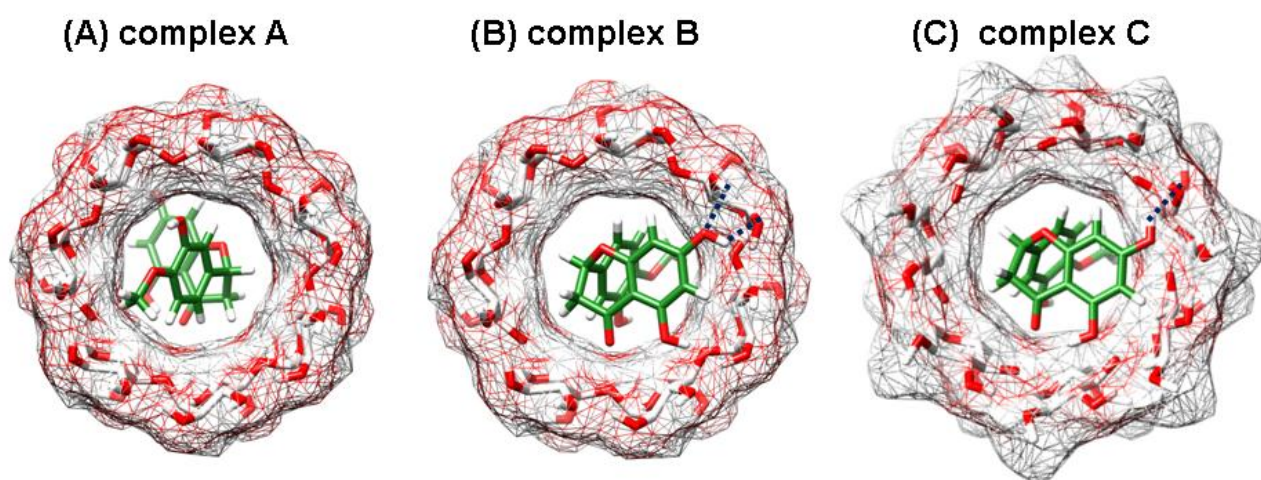


Figure 11. Top views of (A) the chromone ring and (B) phenyl ring of hesperetin inserted into β -CD's cavity, while (C) phenyl ring inserted into DM- β -CD's cavity where the H-bonds were shown by dashed line

3.1.2 Stability of simulated system

The system stability of the simulated hesperetin-CD inclusion complexes in solution was monitored using the root-mean-square displacement (RMSD) calculation. Fig. 12 shows the RMSD plots for all atoms of inclusion complex (black), cyclodextrin (dark gray) and hesperetin (light gray) relative to those of the docked structure for the β -CD (A1-A3) and DM- β -CD (B1-B3) complexes along the simulation time. Onwards the three modeled systems in type of phenyl ring inserted into β -CD's cavity of each inclusion complex with the lowest binding energy and highest hydrogen bond formation between ligand and cyclodextrin were chosen as the initial structures for performing MD simulation. In comparison between the RMSD values of inclusion complex with the two cyclodextrins (black) during the 25-80 ns of simulation. The RMSD plots of the 6 simulated inclusion complexes (black) suggested that all systems had reached equilibrium at 25 ns and thus the obtained results from

the last 55 ns were mainly discussed as follows. From the averaged RMSD of β -CD complexes of ~ 2.5 Å in A1-A3 and DM- β -CD complexes of ~ 2.6 Å in B1 and ~ 3.2 Å in B2 and B3, the lower RMSD value and fluctuation in the DM- β -CD complexes implied that hesperetin might be better formed the inclusion complex with its dimethyl derivative than the native β -CD. Interestingly, for the DM- β -CD host molecule, the methyl substitutions on the 2- and 6- positions of each D-glucopyranose did not affect to the RMSD fluctuation in comparable to that of β -CD, dark gray). The RMSD value of hesperetin (light gray) in the cavity of cyclodextrins enhanced from ~ 0.5 Å in β -CD to ~ 1.5 Å in DM- β -CD.

3.1.3 Hesperetin binding inside the CD cavity

To show the binding mode and dynamics behavior of hesperetin molecule inside of the cyclodextrin's cavity, the distance measured from the center of gravity of each hesperetin ring ($C_{g_{\text{chromone/phenyl ring}}}$) to the center of gravity of β -CD ($C_{g_{\text{CD}}}$) was determined along the simulation time. The results are plotted in Fig. 13 where the horizontal dashed lines at -3.95 Å and 3.95 Å indicates the approximated positions of the primary and secondary rims of β -CD. In other words, the distance ranged from -3.95 Å to 3.95 Å represents the β -CD height of 7.9 Å as reported in the previous study [16]. The representative MD structures of the inclusion complexes with β -CD and DM- β -CD taken from MD snapshots were depicted in Fig. 14. Although the simulations of each inclusion complex were started from the three different starting structures resulted from docking procedure, the relatively similar mobility of hesperetin in the CD cavity was observed. For hesperetin- β -CD complex (Fig. 14A and 14B), the phenyl ring (gray) stayed close to the primary rim ($\sim -1.0 \pm 1.8$ Å) leading to the chromone ring (black) likely positioned nearby the secondary rim ($\sim 3.5 \pm 1.0$ Å, see also Fig. 12A) and rarely phenyl ring moved deeper through and stayed outside the primary rim (Fig. 12B). Note that in complex B both rings of hesperetin were well

occupied inside the cavity of β -CD. Since an increase in the height of cavity with narrower primary rim and wider secondary rim was established due to the 2,6-dimethyl substitutions on β -CD 10 Å [16], the different dynamics behavior of hesperetin binding was under expected. The phenyl ring mainly occupied and moved within the interior of DM- β -CD in a range of -3.0 Å and 1.0 Å for B1 and B3 simulations. The structure of chromone ring was supported by the methyl groups at the secondary rim (Fig. 14C) but in somewhat it can be seen that the chromone ring moving up to secondary rim or stayed outside the cavity of DM- β -CD at 50 ns in B1 and 25, 75 ns in B3 (see also Fig. 14D). In view of Fig. 14, hesperetin molecule was significantly better fitted in the DM- β -CD's cavity compared with β -CD complex.

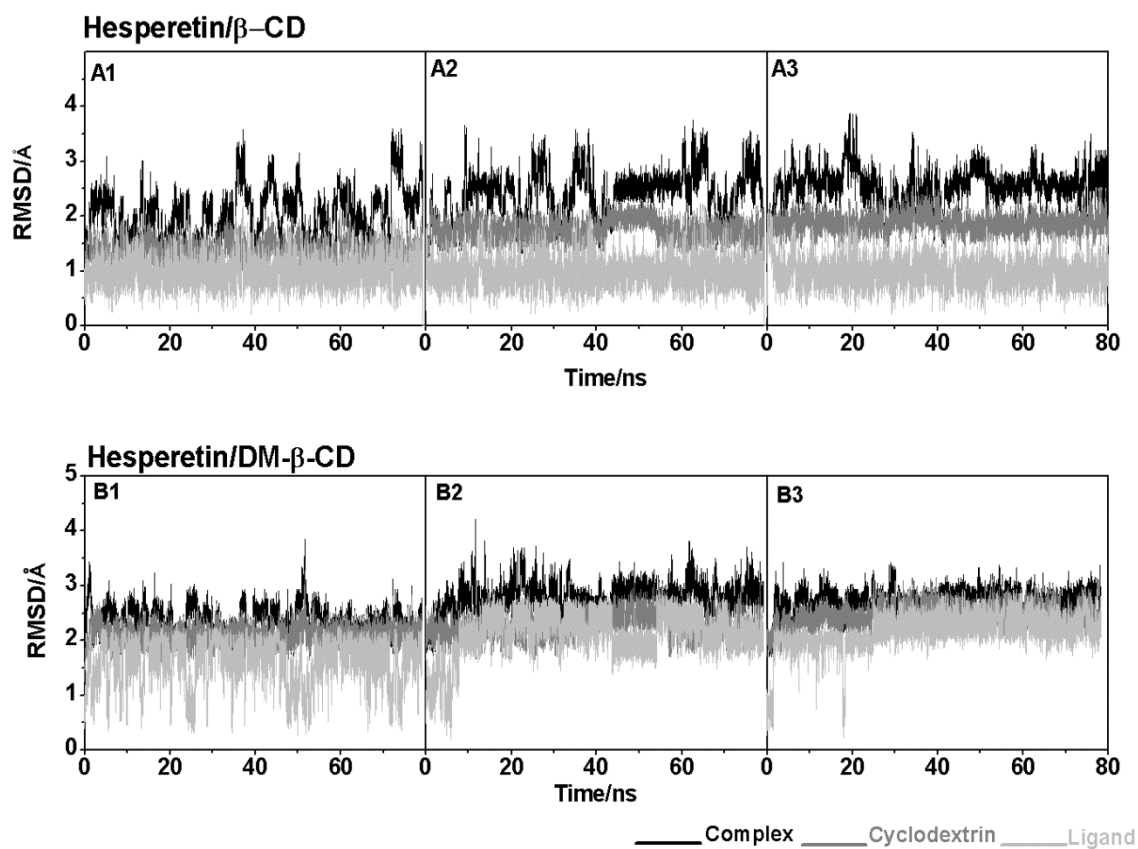


Figure 12. RMSD plots of all atoms for the simulated systems of the hesperetin in complex with β -CD and DM- β -CD started from the best three different docked conformations: (A1-A3) for hesperetin- β -CD and (B1-B3) for hesperetin-DM- β -CD

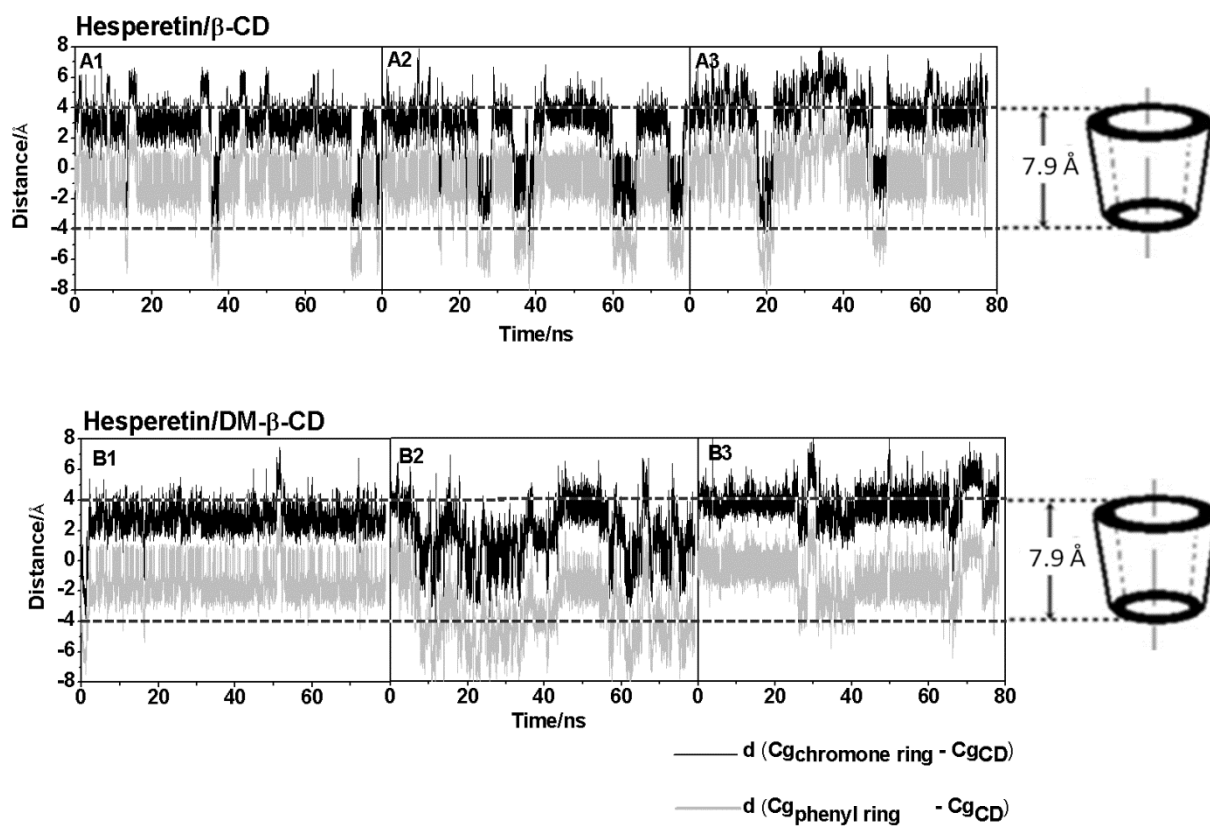


Figure 13. Distance from the center of gravity of each hesperetin ring ($C_{g_{\text{chromone ring}}}$ or $C_{g_{\text{phenyl ring}}}$) to the center of gravity of cyclodextrin ($C_{g_{\text{CD}}}$) for the two systems of (A1-A3) hesperetin- β -CD and (B1-B3) hesperetin-DM- β -CD. Dash line represents the cavity height of β -CD.

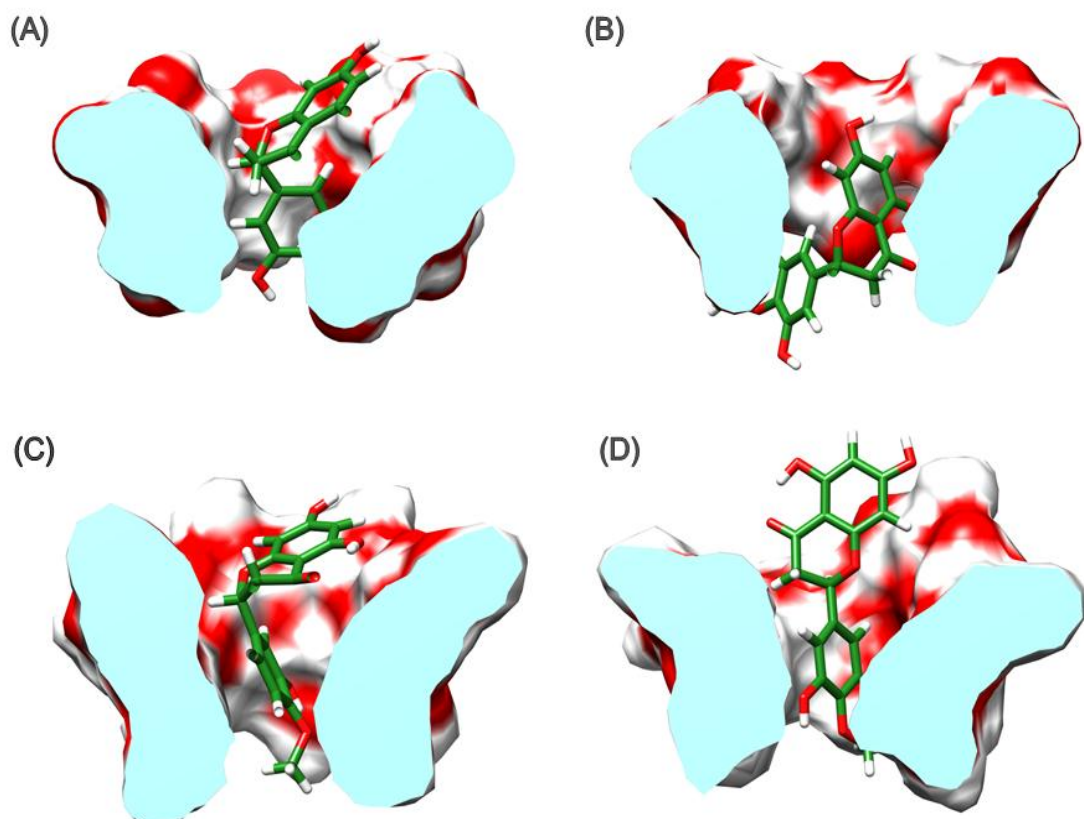


Figure 14. The possible orientations of hesperetin in the hydrophobic cavity of (A and B) β -CD (C and D) and DM- β -CD taken from MD simulations

3.1.4 Binding free energy

In this study we applied a molecular mechanics and continuum solvation method to estimate the binding free energies or calculate the free energies of molecules in solution ΔG_{bind} using the MM-PBSA/GBSA method. The 25-80 MD snapshots were used. The free energy decomposition of each complex in terms of gas phase energy (ΔE_{MM}) including ΔE_{ele} and ΔE_{vdw} energies, solvation free energy (ΔG_{Sol}) and entropic term ($T\Delta S$) is shown in Table 4. It seems that the hesperetin prefer interacted with cyclodextrin through van der waals force stronger than electrostatic interaction by 2 to 5 folds in the two inclusion complexes (ΔE_{vdw} of -23.58 and -31.30 kcal•mol⁻¹; ΔE_{ele} of -9.95 and -5.90 kcal•mol⁻¹ for hesperetin- β -CD and hesperetin-DM- β -CD, respectively). Thus, the vdW interaction played an important role in forming the inclusion complex. For the summation of entropic and terms solvation, both MM/PBSA and MM/GBSA methods predicted the binding free energy of hesperetin- β -CD (-6.32 and -7.26 kcal•mol⁻¹) > hesperetin-DM- β -CD (-14.54 and -14.17 kcal•mol⁻¹). Nevertheless, the MM-PBSA/GBSA binding free energies of two inclusion complexes might be overestimated due to MM energy. To correct this energy section, the same set of 25 to 80 MD snapshots was carried out by the single point DFT M062X/6-31+g (d,p) calculation. Although, the results of QM/PBSA and QM/GBSA binding free energy were relatively related to MM/PBSA and MM/GBSA energies, the absolute values of hesperetin- β -CD were closer to the experimental ΔG obtained from our study and the previous study [21]. These results can suggest that hesperetin binds to and interacts with DM- β -CD stronger than that with β -CD.

Table 4. Binding free energy ($\text{kcal}\cdot\text{mol}^{-1}$) and its calculated energy components of the hesperetin- β -CD and hesperetin-DM- β -CD complexes by MM-PBSA/GBSA method in comparison to experimental values

Energy ($\text{kcal}\cdot\text{mol}^{-1}$)	Hesperetin- β -CD	Hesperetin-DM- β -CD
ΔE_{ele}	-9.95 ± 0.73	-5.90 ± 0.46
ΔE_{vdw}	-23.58 ± 2.97	-31.30 ± 0.44
ΔE_{MM}	-33.86 ± 3.23	-38.23 ± 0.60
ΔE_{QM}	-28.80 ± 0.03	-31.33 ± 0.03
$T\Delta S$	-12.46 ± 0.37	-11.27 ± 0.07
$\Delta G_{Sol} (PBSA)$	15.08 ± 1.78	12.42 ± 2.73
$\Delta G_{Sol} (GBSA)$	14.14 ± 1.71	12.79 ± 2.10
$\Delta G_{MM/PBSA}$	-6.32 ± 1.08	-14.54 ± 2.06
$\Delta G_{MM/GBSA}$	-7.26 ± 1.15	-14.17 ± 1.30
$\Delta G_{QM/PBSA}$	-1.26 ± 1.44	-7.64 ± 2.69
$\Delta G_{QM/GBSA}$	-2.20 ± 1.37	-7.27 ± 2.06
$\Delta G_{experiment \text{ of this study}}$	-3.50	-4.27
$\Delta G_{experiment} [21]$	-3.39	N/A

3.2 Molecular dynamics (MD) simulations of naringenin

3.2.1 Docked naringenin-CD inclusion complex

From the 500 independent docking runs, the conformation, interaction energy and H-bond formation of naringenin inside the hydrophobic cavity of the CDs are given in Table 5.

Table 5. Percentage of docked conformation, interaction energy ($\text{kcal}\cdot\text{mol}^{-1}$) and number of H-bond formation of naringenin in the interior of β -CD and DM- β -CD.

Inclusion complex	% Docked conformation	Interaction energy ($\text{kcal}\cdot\text{mol}^{-1}$)	# H-bond (distance)
Naringenin- β -CD	99 % phenyl ring inserted	-26.70	1 (1.9 Å)
	1% chromone ring inserted	-25.00	-
Naringenin-DM- β -CD	100 % phenyl ring inserted	-28.76	1 (2.5 Å)

Note that the interaction energy of inclusion complex was calculated by the energy difference between inclusion complex, cyclodextrin and naringenin using the CHARMM-based docking algorithm [62]. It can be clearly seen that the phenyl ring of naringenin molecule (Fig. 3B) preferentially dipped to β -CD (99 % docked conformation) and DM- β -CD (100 %) with a location close to the primary rim. The obtained information was in good agreement with the recent ^1H and 2D NMR study of naringenin in complex with β -CD and DM- β -CD [25] and the

theoretical studies by 6-ns MD simulation [23] as well as the semi-empirical AM1 method (Kano et al., 2002) on naringenin- β -CD complex.

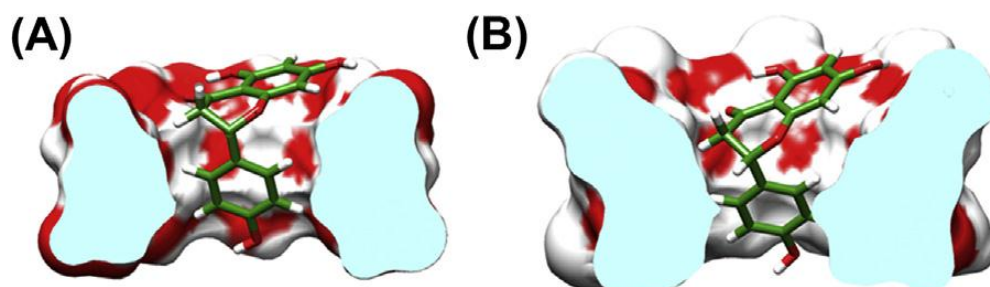


Figure 15. Cutaway views of the CD hydrophobic cavity showing naringenin occupied in (A) β -CD and (B) DM- β -CD from docked structures

Based on docked interaction energy and H-bond between naringenin and cyclodextrin, the best formed inclusion complex with β -CD and DM- β -CD were depicted in Fig. 13. It is worth noting that the DM- β -CD encapsulates this flavanones molecule better than the native β -CD by $2 \text{ kcal}\cdot\text{mol}^{-1}$ in the gas phase. For naringenin- β -CD complex, the hydroxyl oxygen (O7) on its chromone ring formed a H-bond with the 3-OH group located in the interior of β -CD (1.9 \AA). Differentially, a weaker H-bond was detected in the naringenin-DM- β -CD complex (2.5 \AA) between the O1 atom and the 3-OH group. The decreased H-bond strength in the DM- β -CD is due to the larger and deeper cavity, as previously discussed [25, 61]. By the two mentioned criteria, the top three ranked conformations of each inclusion complex from the docking results were chosen for further study on dynamics behaviors of complex in aqueous solution.

3.2.2 Stability of the simulated system

The system stability of the simulated inclusion complex in solution was monitored using the RMSD calculation. Fig. 14 shows the RMSD plots for all atoms of the inclusion complex (black), CD (dark grey) and naringenin (light grey) relative to those of the docked structure for the three different conformations of naringenin- β -CD (A1–A3) and naringenin-DM- β -CD (B1–B3) along the simulation time. The RMSD plots of the six simulated inclusion complexes (black) suggested that all systems had reached equilibrium at 25 ns and so the obtained results from the last 55 ns were mainly discussed. Comparing the RMSD values of the inclusion complex with the two CDs (black) during the 25–80 ns of simulation, the decreased fluctuation of the naringenin-DM- β -CD complex (1.8–3.4 Å in B1; 1.4–3.6 Å in B2 and B3) implied that naringenin might form a better inclusion complex with DM- β -CD than with native β -CD (1.25–4.0 Å in A1–A3). Interestingly, for the DM- β -CD host molecule, the methyl substitutions on the C2 and C6 positions of each D-glucopyranose did not affect the RMSD value (\sim 2.0 Å, comparable to that of β -CD, dark grey). The RMSD value of naringenin (light grey) in the cavity of both CDs was enhanced from \sim 0.5Å to \sim 2.0Å, but its fluctuation was considerably larger in the DM- β -CD based complex (except for the B1 system). This is probably because the increased height of the DM- β -CD's cavity may allow for a higher conformational flexibility of naringenin.

3.2.3 Ligand binding inside the CD cavity

To understand the binding mode and dynamics behavior of naringenin in the interior of the two CDs, the distance measured from the center of gravity of each naringenin ring ($C_{g_{\text{chromone/phenyl ring}}}$) to the center of gravity of CD ($C_{g_{\text{CD}}}$) was determined along the simulation time. The results (Fig. 15) reveal that the

approximated positions of the primary and secondary rims of β -CD (the horizontal dashed lines) ranged from -3.95 \AA to 3.95 \AA and so represent a β -CD height of 7.9 \AA as previously reported [25, 63, 64]. The representative MD structures of the two inclusion complexes are shown in Fig. 16.

Although the simulations of each naringenin/CD complex were initiated from three different structures obtained from the docking procedure, a relatively similar mobility of naringenin in the CD cavity was observed in each case. For the naringenin- β -CD complex, the phenyl ring (grey, Fig. 15) mostly stayed at the β -CD center ($\sim 0.0 \pm 1.8 \text{ \AA}$ in the A1 and A2 simulations, and $\sim 1.0 \pm 1.0 \text{ \AA}$ in A3) while the chromone ring (black) was likely to be located nearby the secondary rim ($\sim 3.5 \pm 1.0 \text{ \AA}$ and $\sim 2.5 \pm 1.0 \text{ \AA}$, respectively) in the first 30 ns (A1) or 40 ns (A2 and A3) of simulation (see also Fig. 15A, left). Afterwards, the phenyl ring moved deeper and feasibly passed through the primary rim ($\sim -6.0 \pm 2.0 \text{ \AA}$) with a result that the chromone ring occupied inside the cavity instead ($\sim 0.0 \pm 2.0 \text{ \AA}$) in the A1 and A2 simulations (Fig. 16A, right). However, the phenyl ring was able to move back into the cavity as well, which was found in all three simulations but in particular in A3. Since an increased height of the cavity ($> 7.9 \text{ \AA}$) with a narrower primary and wider secondary rim (Fig. 13B) was established in the DM- β -CD, different dynamic behavior of naringenin binding was expected for the naringenin-DM- β -CD inclusion complex. All three simulations (B1–B3) suggested that the phenyl ring mainly occupied and moved within the interior of DM- β -CD in a range of -3.5 \AA and 2.0 \AA , while the chromone ring structure was supported by the methyl groups at the secondary rim (Figure. 16B, left). Among the three simulations (B1–B3), there was a low possibility of the phenyl ring moving down to the primary rim or staying outside the cavity of DM- β -CD (Figure. 16B, right), as seen in the B1 simulation at the early stage and again at ~ 62 – 73 ns and shortly in the B3 simulation at $\sim 73 \text{ ns}$. Therefore, it can be presumed that naringenin

significantly better fitted in the cavity of DM- β -CD to form a more stable naringenin/DM- β -CD complex.

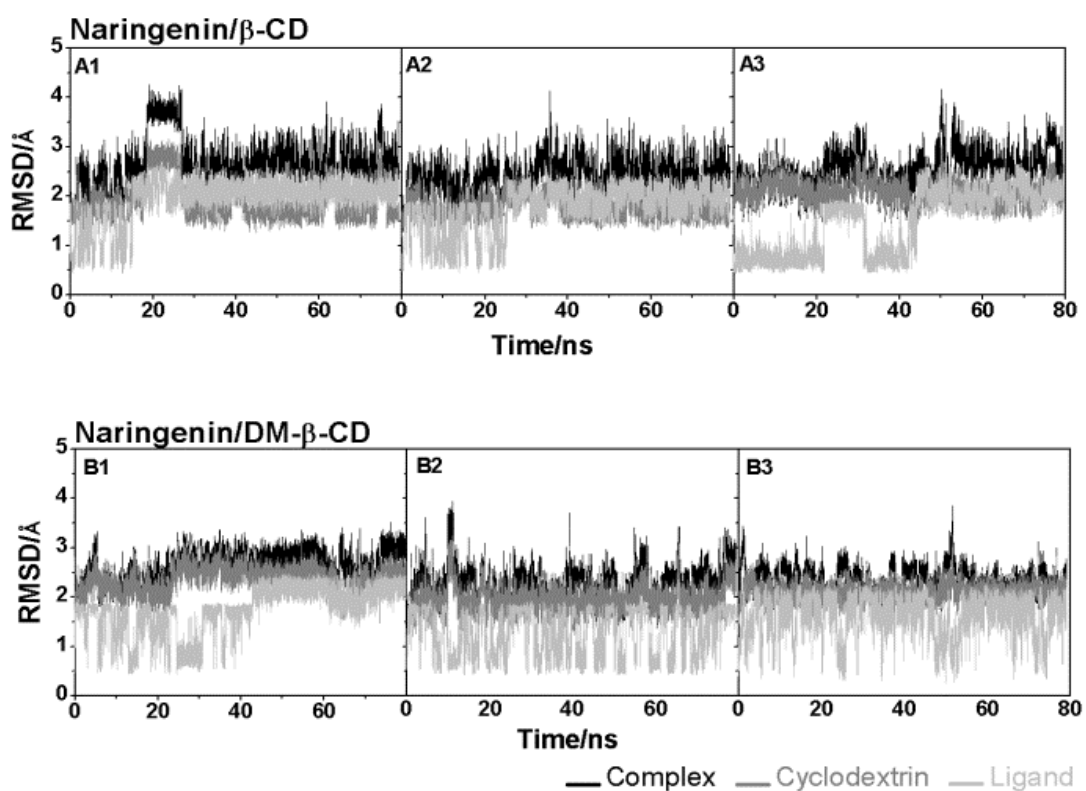


Figure 16. RMSD plots for the simulated systems of naringenin complexes with β -CD and DM- β -CD from the three different (best) docked conformations for (A1–A3) naringenin- β -CD and (B1–B3) naringenin-DM- β -CD

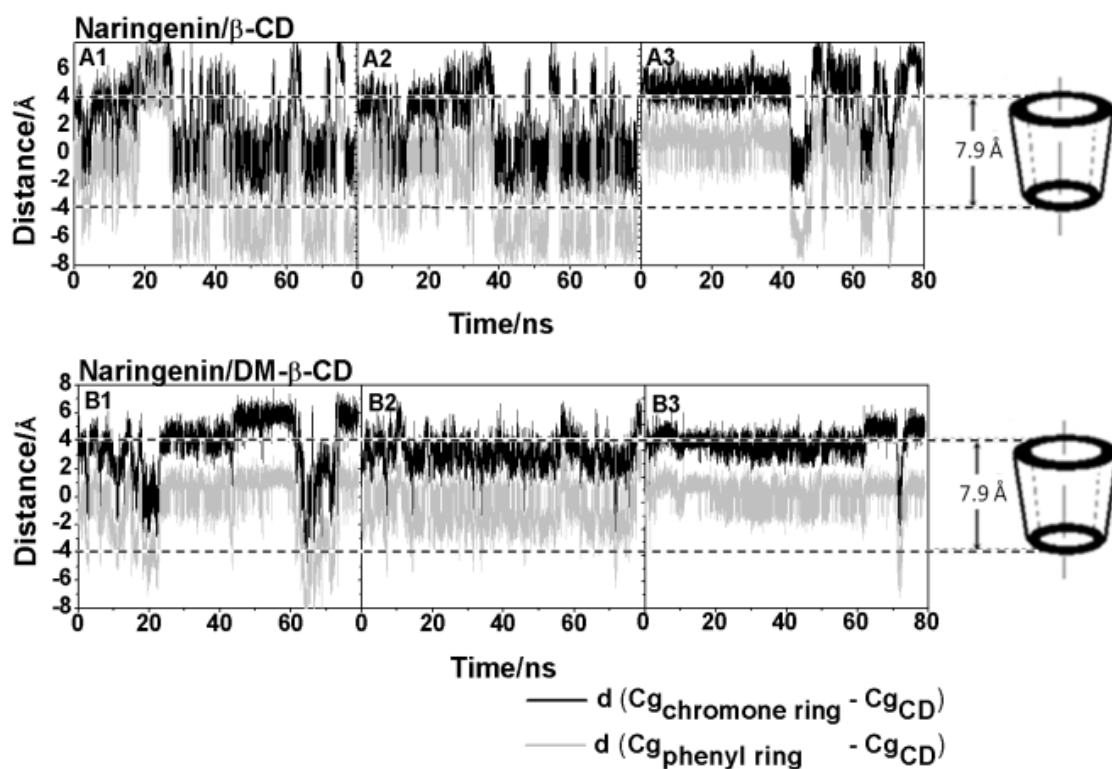


Figure 17. Distance from the center of gravity of each naringenin ring ($Cg_{\text{chromone ring}}$ or $Cg_{\text{phenyl ring}}$) to the center of gravity of cyclodextrin (Cg_{CD}) for the three systems of (A1-A3) naringenin- β -CD and (B1-B3) naringenin-DM- β -CD inclusion complexes. Dash line represents the cavity height of β -CD

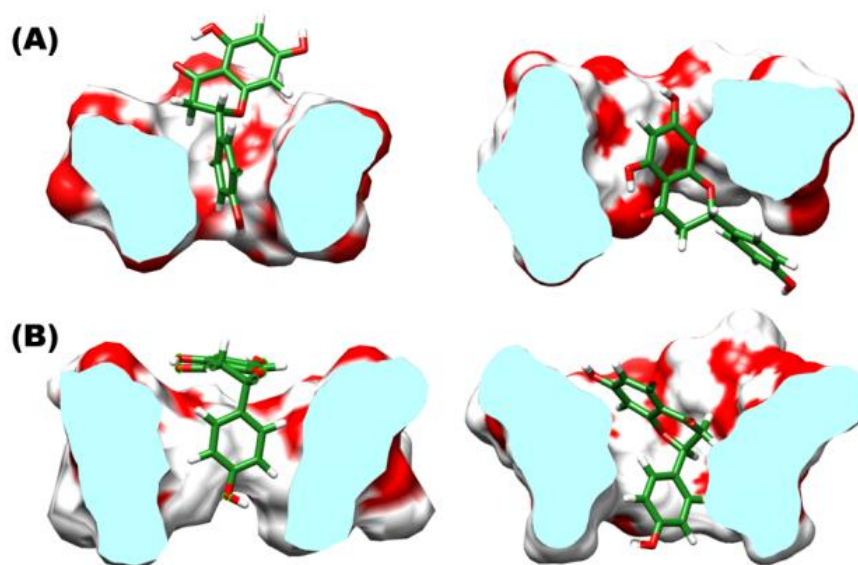


Figure 18. Cutaway views on the MD structures of (A) naringenin- β -CD and (B) naringenin-DM- β -CD showing possible orientations of naringenin in the inner surface of CD

3.2.4 Binding free energy

The molecular mechanic with two different continuum solvation methods, PBSA and GBSA, was applied to estimate the absolute binding free energies of the naringenin- β -CD and naringenin-DM- β -CD inclusion complexes. The binding free energies ($\Delta G_{MM/PBSA}$ and $\Delta G_{MM/GBSA}$) and their energetic components, including the gas phase energy (ΔE_{MM}) from a summation of ΔE_{ele} and ΔE_{vdW} , solvation free energies (ΔG_{PBSA} and ΔG_{GBSA}) and entropic term ($T\Delta S$) are summarized in Table 6. In the gas phase, the contribution of the attractive electrostatic interaction was almost equal in the naringenin- β -CD and naringenin-DM- β -CD complexes (ΔE_{ele} of -4.09 and -4.73 kcal \cdot mol $^{-1}$, respectively). The van der Waals (vdW) energy was some six-fold greater

than the ΔE_{ele} in both of the naringenin/CD complexes (ΔE_{vdW} of -25.69 and -29.71 kcal•mol⁻¹), which implied that the vdW interaction played an important role in forming/stabilizing the inclusion complex. The obtained information was in good agreement with the previous studies in which the hydrophobic interaction was found to be the main driving force for flavanones-CD inclusion complexes [24]. From the two interaction energies, the MM energy (ΔE_{MM}) suggested a better binding of naringenin in the cavity of DM- β -CD than in that of β -CD by ~ 4.6 kcal•mol⁻¹. However, the absolute MM energy can overestimate the binding interaction, and so QM calculations with the DFT M06-2X/6-31+g(d,p) level of theory was applied on the same set of MD trajectories. With energy correction, the QM energy also indicated a more stable complexation of naringenin-DM- β -CD than naringenin- β -CD (~ 3.5 kcal•mol⁻¹). By including the solvation free energy and entropic terms, all four approaches (MM/PBSA, MM/GBSA, QM/PBSA and QM/GBSA) predicted the same trend of absolute binding free energy of naringenin-DM- β -CD \gg naringenin- β -CD, and so strongly suggest that the DM- β -CD derivative could better encapsulate naringenin with an enhanced complex stability. In addition, the calculated ΔG values of the naringenin- β -CD complex were somewhat close to the previously reported experimental ΔG value (-3.45 kcal•mol⁻¹) [21].

Table 6. Binding free energy ($\text{kcal}\cdot\text{mol}^{-1}$) and its calculated energy components of the naringenin- β -CD and naringenin-DM- β -CD complexes in comparison to experimental values

Energy ($\text{kcal}\cdot\text{mol}^{-1}$)	Naringenin/ β -CD	Naringenin/DM- β -CD
ΔE_{ele}	-4.09 ± 2.89	-4.73 ± 3.65
ΔE_{vdw}	-25.69 ± 2.85	-29.71 ± 2.61
ΔE_{MM}	-29.78 ± 4.32	-34.43 ± 3.54
ΔE_{QM}	-23.51 ± 0.01	-27.05 ± 0.03
$T\Delta S$	-11.70 ± 1.31	-14.1 ± 5.82
$\Delta G_{Sol} (PBSA)$	11.65 ± 2.12	11.64 ± 1.97
$\Delta G_{Sol} (GBSA)$	10.64 ± 2.19	9.28 ± 1.63
$\Delta G_{MM/PBSA}$	-6.43 ± 1.25	-8.70 ± 2.57
$\Delta G_{MM/GBSA}$	-7.44 ± 1.46	-11.06 ± 2.69
$\Delta G_{QM/PBSA}$	0.16 ± 0.82	-1.31 ± 3.82
$\Delta G_{QM/GBSA}$	-1.17 ± 0.89	-3.67 ± 4.16
$\Delta G_{experiment \text{ of this study}}$	-3.64	-4.27
$\Delta G_{experiment} [21]$	-3.45	N/A

3.3 Potential mean force of flavanone-CD complexation

The PMF profiles of flavanones-CD complexation along the z coordinate (described in Fig. 8) are shown in Figs. 19 and 20. Note that the force was applied on the phenyl ring moving towards cavity axis of cyclodextrin. For hesperetin- β -CD complex (Fig. 19 left), firstly the phenyl ring of hesperetin interacted with the wider rim at the z of -0.1 nm. The local minimum of such complex with the lowest energy of $-9.0 \text{ kcal}\cdot\text{mol}^{-1}$ was likely observed at the CD center in a range of -0.3-0.1 nm. It can be implied that the hesperetin can feasibly move up and down within the interior of β -CD in range 0.4 nm. The stable naringenin- β -CD complex (Fig. 20 left) was found at in a range of -0.1-0.4 nm. Interestingly, the chromone ring of naringenin firstly interacted with the wider rim of β -CD by ~ 2 hydrogen bonds at the z of -0.5 nm. Afterwards, naringenin consumed the energy of $4.0 \text{ kcal}\cdot\text{mol}^{-1}$ (at z of -0.5 nm) to change its orientation by flipping the phenyl ring to form the stable inclusion complex at the β -CD center instead. This was in contrast to the case of hesperetin in which a broader PMF was observed in the naringenin- β -CD complex with the higher standard deviation of PMF values at center of cyclodextrin. Besides, hesperetin-DM- β -CD complex (Fig.19 right), at the first minimum z of -0.5 nm the chromone ring of hesperetin interacted with the wider rim of DM- β -CD and then it consumed the energy of $4.2 \text{ kcal}\cdot\text{mol}^{-1}$ to move its phenyl ring to form the stable inclusion complex at z of 0.3 nm and then the phenyl ring of hesperetin moved deeper pass through the narrow rim of DM- β -CD. Afterwards, the chromone ring of hesperetin interacted with its narrow rim at z= 0.8 nm before moving out from the cavity of DM- β -CD. The naringenin-DM- β -CD complex (Fig. 20, right) was formed at z of -0.2 nm where the phenyl ring of naringenin interacted with the wider rim of DM- β -CD (the first local minimum), while at the second minimum both rings of naringenin likely occupied within the interior of DM- β -CD (z of 0.3 nm). Aforementioned, both flavanones in complex with β -CD had high flexibility within the cavity, while a lower flexibility of DM- β -CD complex was suggested by a sharper PMF.

In the release process, the β -CD complex had to consume the energy for releasing the guest molecule from the cavity more than DM- β -CD complex ($1-2 \text{ kcal}\cdot\text{mol}^{-1}$). This result suggested that the flavanone molecules was easily released

from the cavity of DM- β -CD which was somewhat supported by number of H-bonding between guest molecule and CD in Figs. 21 and 22. In the β -CD complex, the hesperetin can form the strongest H-bond (1.8) with β -CD at z of 0.0 nm, while for DM- β -CD complex, almost no H-bond was observed. In contrast, low H-bond interaction between naringenin and the two CDs was found. In comparison between the formed β -CD (z from -0.5 nm to 0.5 nm) and DM- β -CD (z from -0.5 to 0.5 nm) complexes, the flavanones can establish more H-bonds with water molecules in the DM- β -CD complex suggesting that the higher water molecules solvated around the flavanones may help it better releasing from the DM- β -CD.

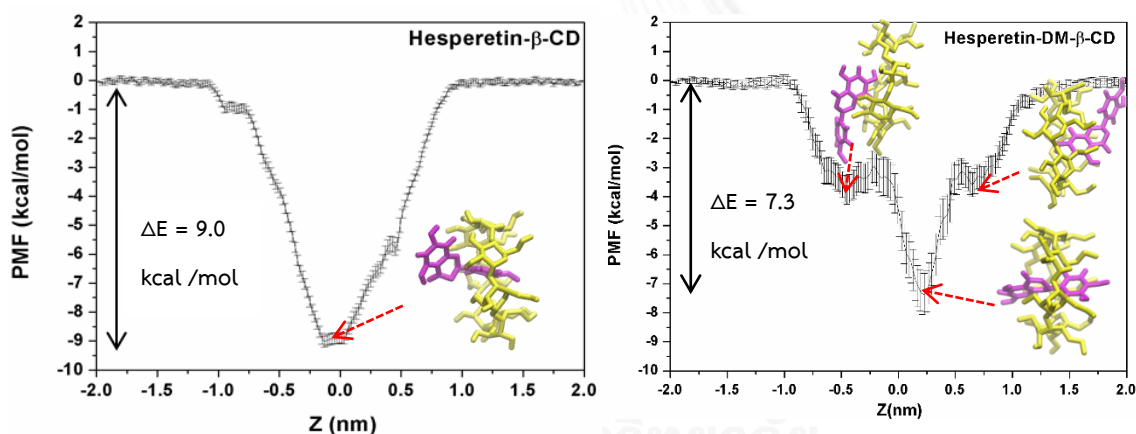


Figure 19. Potential of mean force (PMF) profiles for the hesperetin- β -CD (left) and hesperetin-DM- β -CD (right) complexes

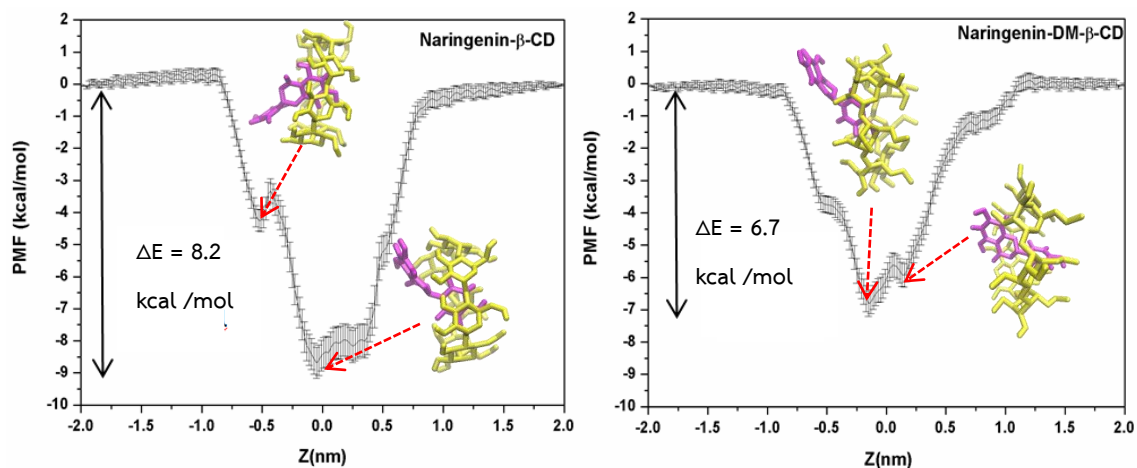


Figure 20. Potential of mean force (PMF) profiles for the naringenin- β -CD (left) and naringenin-DM- β -CD (right) complexes

3.4 Potential energy surface (PES)

To understand and conformational change of CD with guest molecule occupied, the distance between the secondary hydroxyl groups of adjacent glucopyranose units $d_1[\text{O}2(n)\text{-O}3(n+1)]$ and distance between the adjacent glycosidic oxygen atoms $d_2[\text{O}4(n)\text{-O}4(n+1)]$ for the 7 connecting glucopyranose units were monitored and compared to those of the CD structure without guest molecules. The free energy of CD conformational change was calculated as a function of these two parameters by

$$F(x, y) = -k_B T \log[P(x, y)] \quad (10)$$

where k_B , T and $P(x,y)$ are the Boltzmann constant, the temperature and the probability of a conformation whose parameters x and y are $d_1[\text{O}2(n)\text{-O}3(n+1)]$ and $d_2[\text{O}4(n)\text{-O}4(n+1)]$, respectively.

The snapshots from simulations of CD alone and complex between CD and guest molecule (hesperetin naringenin) were used for analysis. The potential energy

surfaces of β -CD and DM- β -CD without guest molecule and with hesperetin and naringenin are shown in Figs. 23-25. The surface plot of free form of β -CD showed three local minima M1, M2, M3 observed at (3.5 Å, 4.7 Å), (5.6 Å, 4.9 Å), and (5.0 Å, 5.5 Å). The surface plot of free form of DM- β -CD also showed three local minima M1, M2, M3 observed at (3.7 Å, 4.5 Å), (5.6 Å, 4.7 Å), and (4.8 Å, 5.5 Å). The distance between the glycosidic oxygen atoms (d_2 [O4(n)-O4(n+1)]) of the M2 structure was in the same length as that of M1, but its d_1 [O2(n)-O3(n+1)] was increased. It can suggest that the conformation of M2 was likely similar to M1 but no intrahydrogen bonds between the hydroxyl groups at secondary hydroxyl rim can be formed. For M3, the d_1 [O2(n)-O3(n+1)] of 5.0 Å was fallen in between those of M1 and M2, while the d_2 [O4(n)-O4(n+1)] was increased to 5.6 Å. Therefore, the M1 and M2 were so-called the closed-form of CD with and without intrahydrogen bonds, respectively, whilst the M3 represented the open-form of CD. For hesperetin in complex with β -CD, we mainly found M1 (Fig. 24 left) whereas in DM- β -CD complex (Fig. 24 right) M1, M2 and M3 were observed. Moreover, we detected the new conformation of DM- β -CD (M4) in the same length of d_2 [O4(n)-O4(n+1)] as that of M3 but increasing d_1 [O2(n) - O3(n+1)]. Therefore this M4 structure showed the open-form as same as M3. For naringenin complex with β -CD, we found the M1 and M2 structures which represented the closed form (Fig. 25, left), while DM- β -CD complex gave a result similar to hesperetin-DM- β -CD complex (Fig. 25, right).

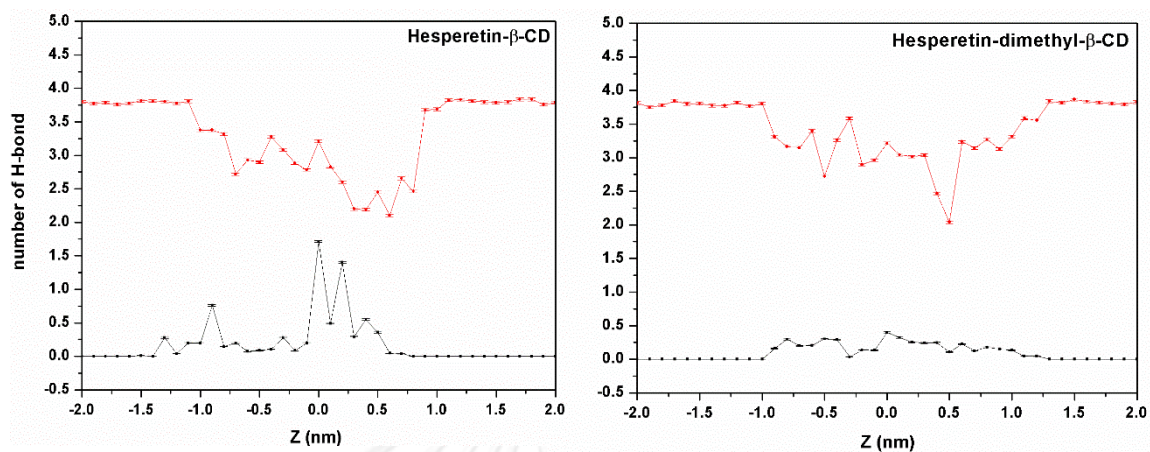


Figure 21. H-bond between hesperetin and β -CD (left) and DM- β -CD complex (right) along the reaction coordinate

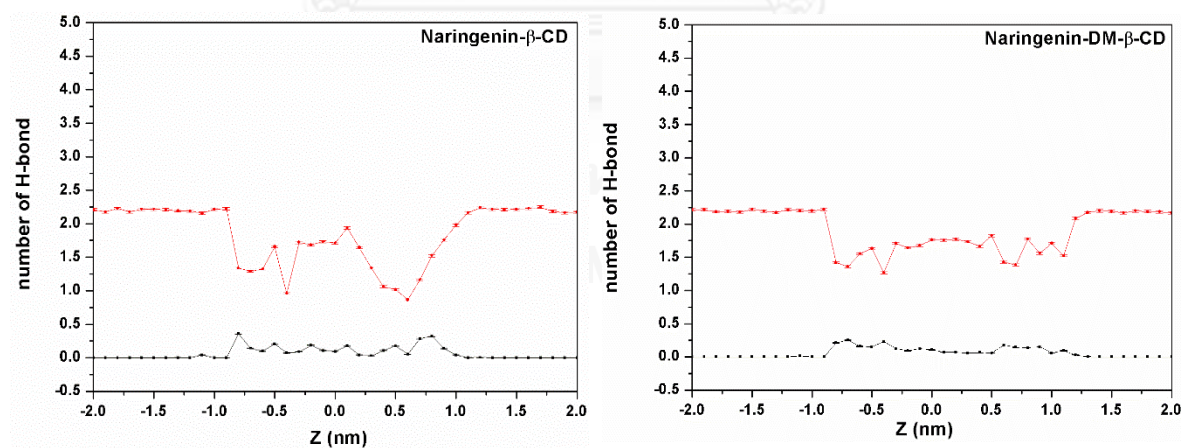


Figure 22. H-bond between naringenin and β -CD (left) and DM- β -CD complex (right) along the reaction coordinate

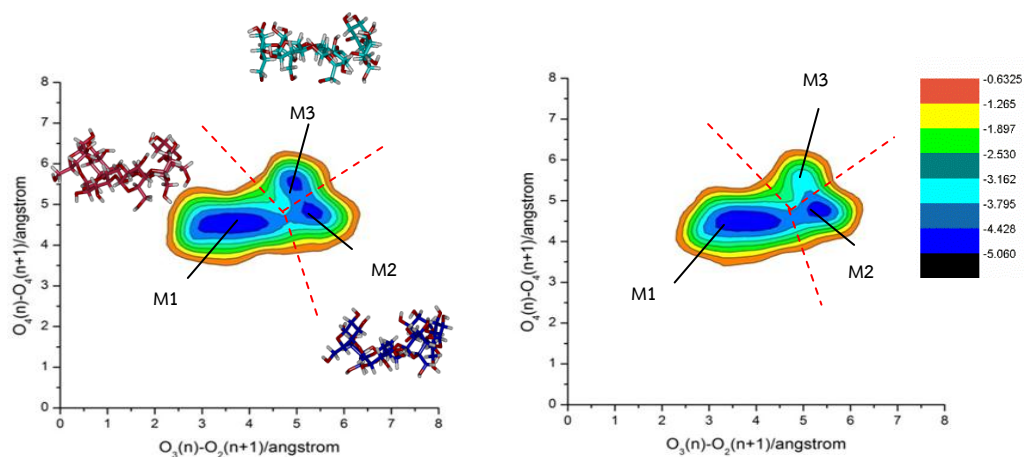


Figure 23. Potential energy surface of β -CD (left) and DM- β -CD (right) without guest molecule

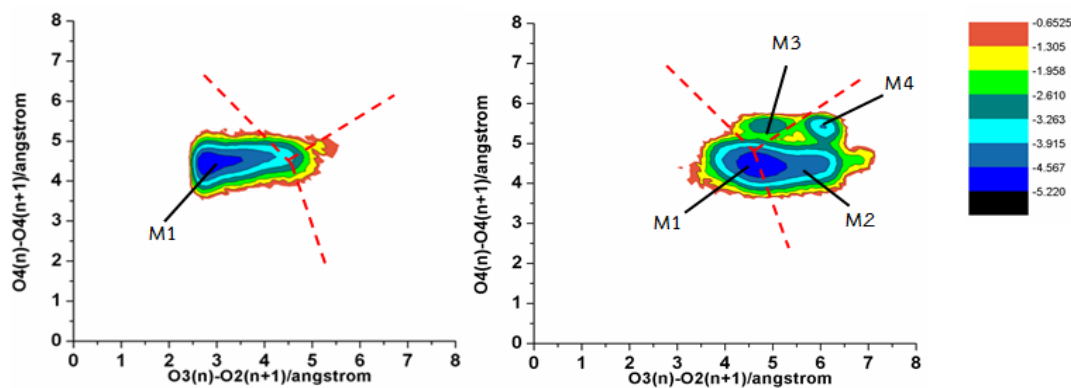


Figure 24. Potential energy surface of hesperetin- β -CD complex (left) and hesperetin-DM- β -CD complex (right)

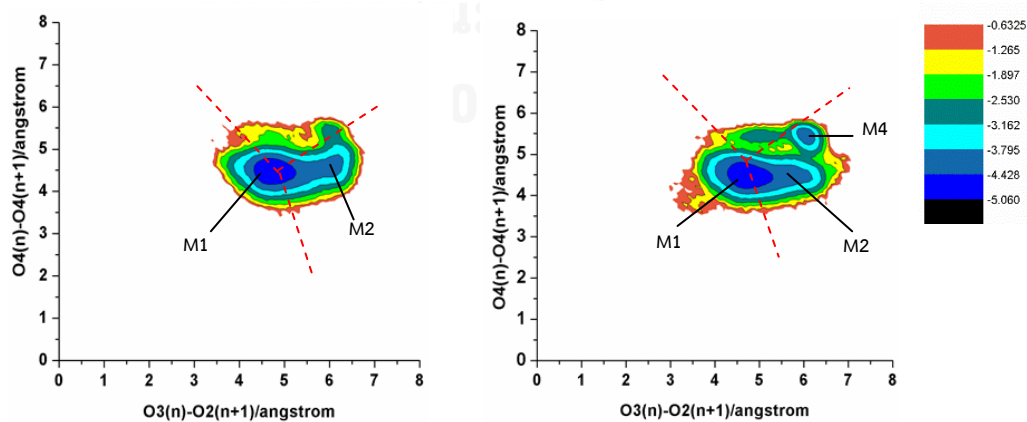


Figure 25. Potential energy surface of naringenin- β -CD complex (left) and naringenin-DM- β -CD complex (right)

3.5 Analysis of flavanones

3.5.1 Spectrophotometric Method

3.5.1.1 The maximum absorption of flavanones and flavanone-CD complexes

Solutions of flavanones and flavanone-CD complexes were prepared in distilled water at the concentration of 1mg/20 ml. The complex was formed by freeze-drying method. In this study, UV spectrophotometer was used for the determination of maximum absorption of hesperetin and naringenin. The absorption spectrum in the range of 200-400 nm was determined. For both flavanones, the maximum absorption at 286 nm (Fig 19 and 20) was found while free β -CD and DM- β -CD displayed no UV absorbance. No change in UV spectra of hesperetin was observed when it formed complex with the CD. In contrast, the maximum wavelength of the naringenin-CD complex was shifted from 286 to 288 nm.

3.4.1.2 Calibration curve of hesperetin and naringenin

The calibration curves of hesperetin and naringenin were determined at 286 nm as shown in Fig 23 and 24, respectively. The regression coefficient of the linear relationship was highly significant ($R^2 = 0.9925$ and 0.9926 , respectively).

3.4.2 High performance liquid chromatography Method

3.4.2.1 Calibration curve of hesperetin and naringenin

Analysis of hesperetin and naringenin was dissolved in the dissolution medium (see section 3.8) also determined by HPLC using C18 column and 70% methanol as mobile phase. The retention time of hesperetin was at 13 minutes while that of naringenin was at 16 minutes. The chromatograms of standard hesperetin and naringenin are as shown in Fig. 21 and 22, respectively. The calibration curve of

hesperetin and naringenin were then plotted (Fig. 25 and 26). The regression coefficient of the linear relationship was highly significant ($R^2 = 0.9907$ and 0.9902 , respectively). When compared the sensitivity of HPLC and spectrophotometer technique for determining the concentration of the two flavanones, we found that the concentration of flavanones that could be detected spectrophotometrically was around $5 \mu\text{M}$ while as low as $0.05 \mu\text{M}$ could be detected by HPLC obviously gave higher sensitivity than spectrophotometry.



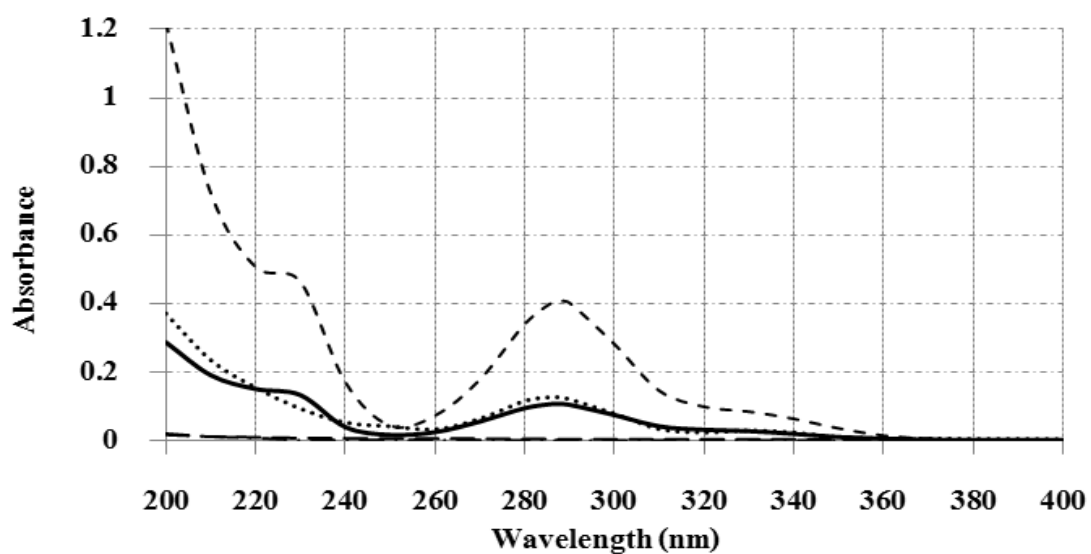


Figure 26. The UV spectra of hesperetin (—), hesperetin- β -CD (.....), hesperetin-DM- β -CD complex (---), β -CD (— ·) and DM- β -CD (— · ·)

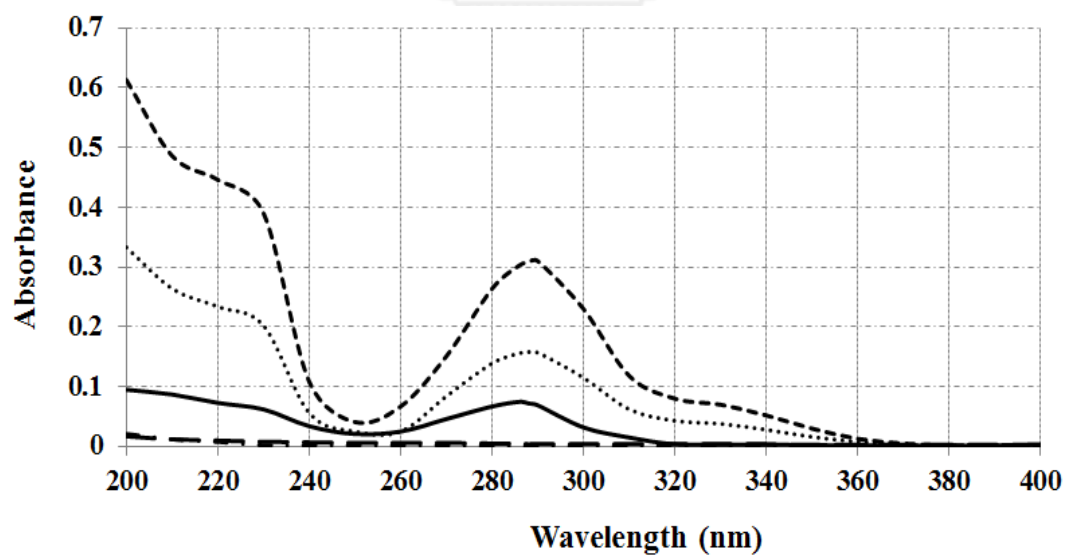


Figure 27. The UV spectra of naringenin (—), naringenin- β -CD (.....), naringenin-DM- β -CD complex (---), β -CD (— ·) and DM- β -CD (— · ·)

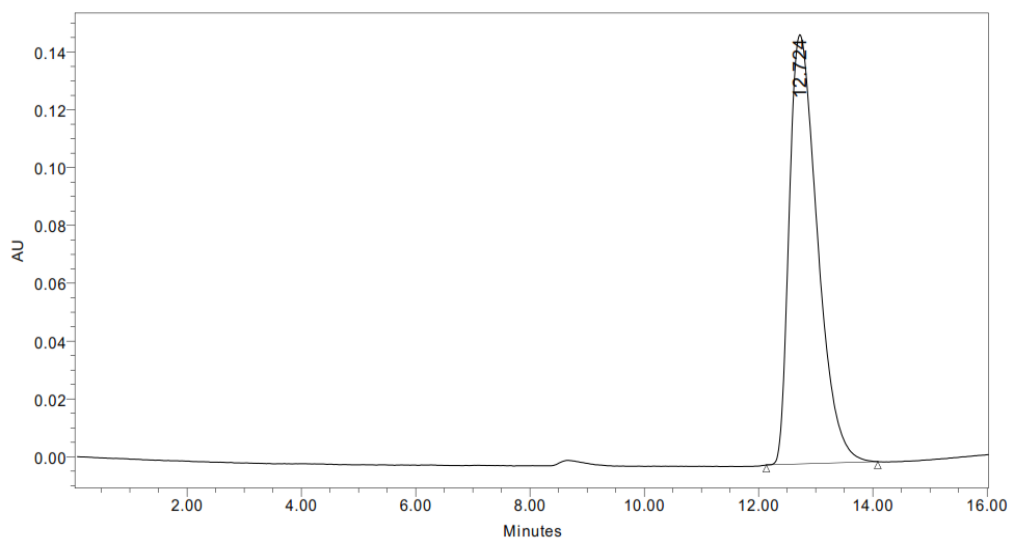


Figure 28. HPLC chromatogram of 0.12 mM hesperetin

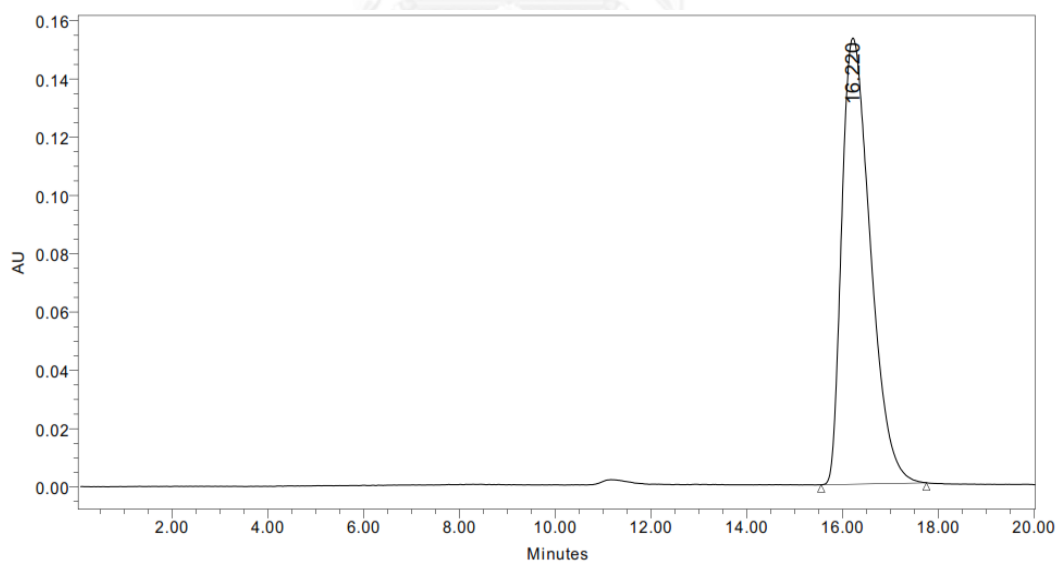


Figure 29. HPLC chromatogram of 0.12 mM naringenin

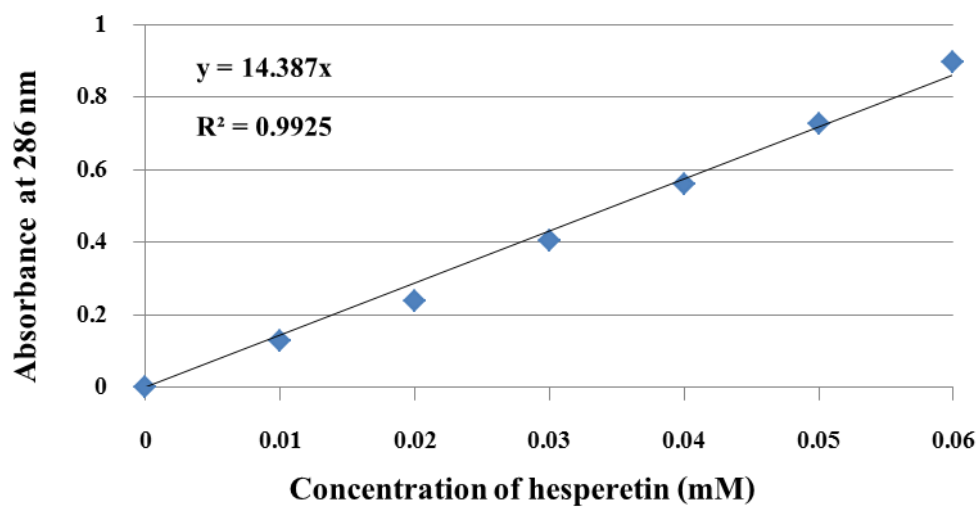


Figure 30. Calibration curve of hesperetin by spectrophotometric method

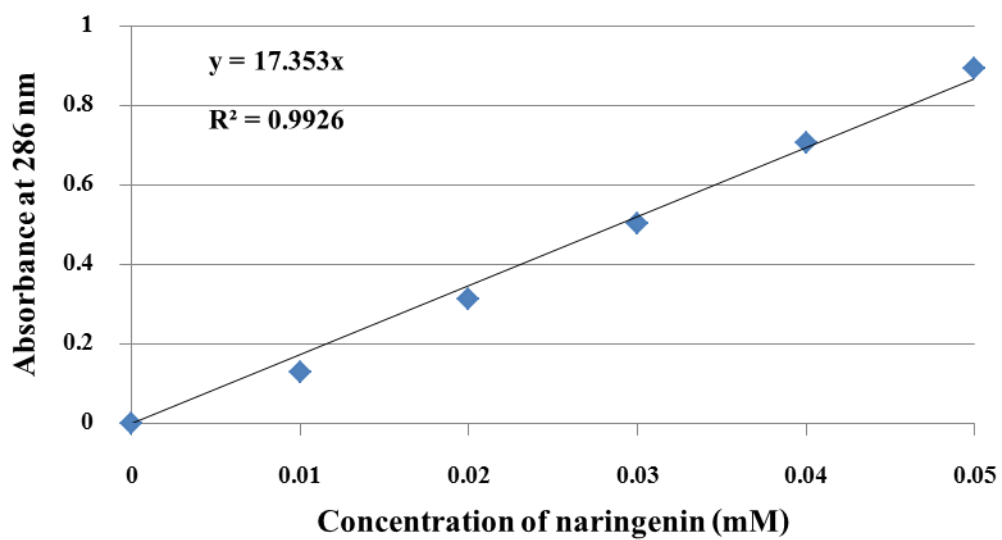


Figure 31. Calibration curve of naringenin by spectrophotometric method

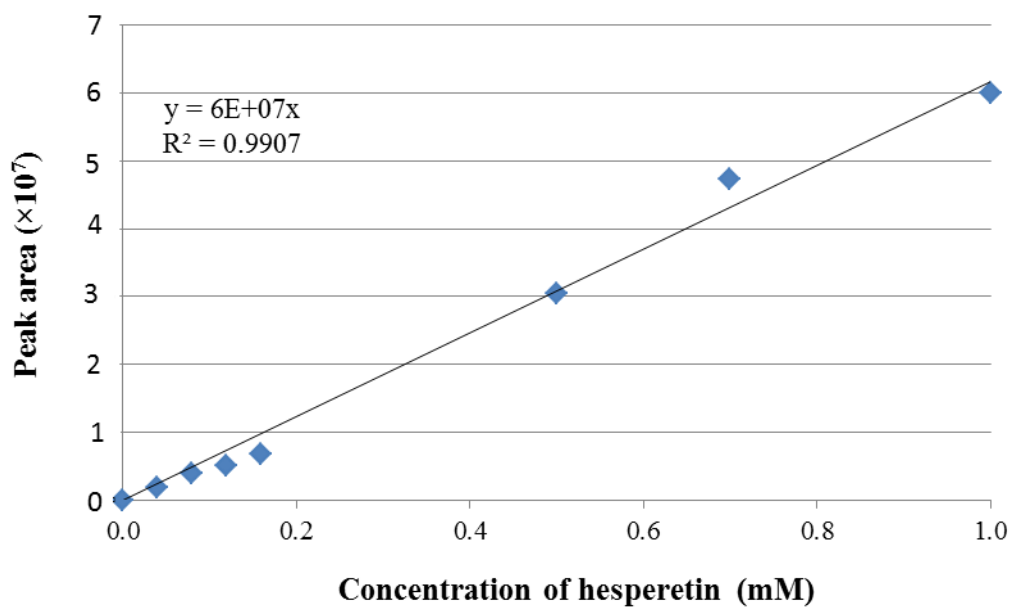


Figure 32. Calibration curve of hesperetin by High performance liquid chromatography method

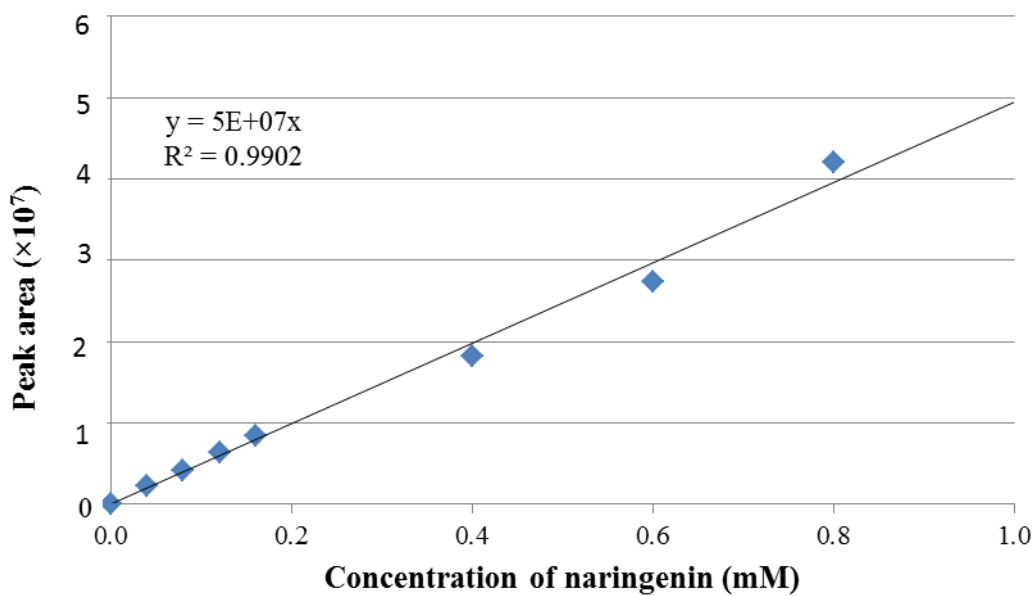


Figure 33. Calibration curve of naringenin by High performance liquid chromatography method

3.6 Phase solubility studies

The phase solubility studies were carried out according to the method of Higuchi and Connors. The determination of the phase-solubility diagram is a widely accepted method for evaluation of the effect of CD complexation on the guest solubility. The 1:1 flavanone-cyclodextrin complex is the most common type of association where a single guest molecule is included in the cavity of one cyclodextrin molecule, with a stability constant $K_{1:1}$ for the equilibrium between the free and associated species. Fig 27 and Fig 28 show the phase-solubility diagram for the hesperetin-CD complex and naringenin-CD complex at different temperature. The solubility of hesperetin and naringenin increased linearly as a function of the CD concentration, a feature of A_L -type diagram. The summarized data for stability constants (K_c) of the hesperetin-CD complex and naringenin-CD complex at different temperature are shown in Table 7. The stability constant (K_c) was calculated by Eq. 9, where the S_0 value was obtained from averaged intercept values of the between β -CD and DM- β -CD complexes. The results showed that the binding energy and solubility of both flavanones with two β -CDs followed the same rank of order of DM- β -CD > β -CD, reflecting an enhancement of binding and solubility of both flavanones. In addition, it can be observed that these values decreased as the temperature increased, revealing the temperature influence on stability of the complexes. The stability constants of the inclusion complexes of DM- β -CD with both flavanones were about three to four times greater than those of the β -CD complexes. In addition, increasing the temperature about 15 °C had a higher effect on the stability constants of β -CD's system than the DM- β -CD's system.

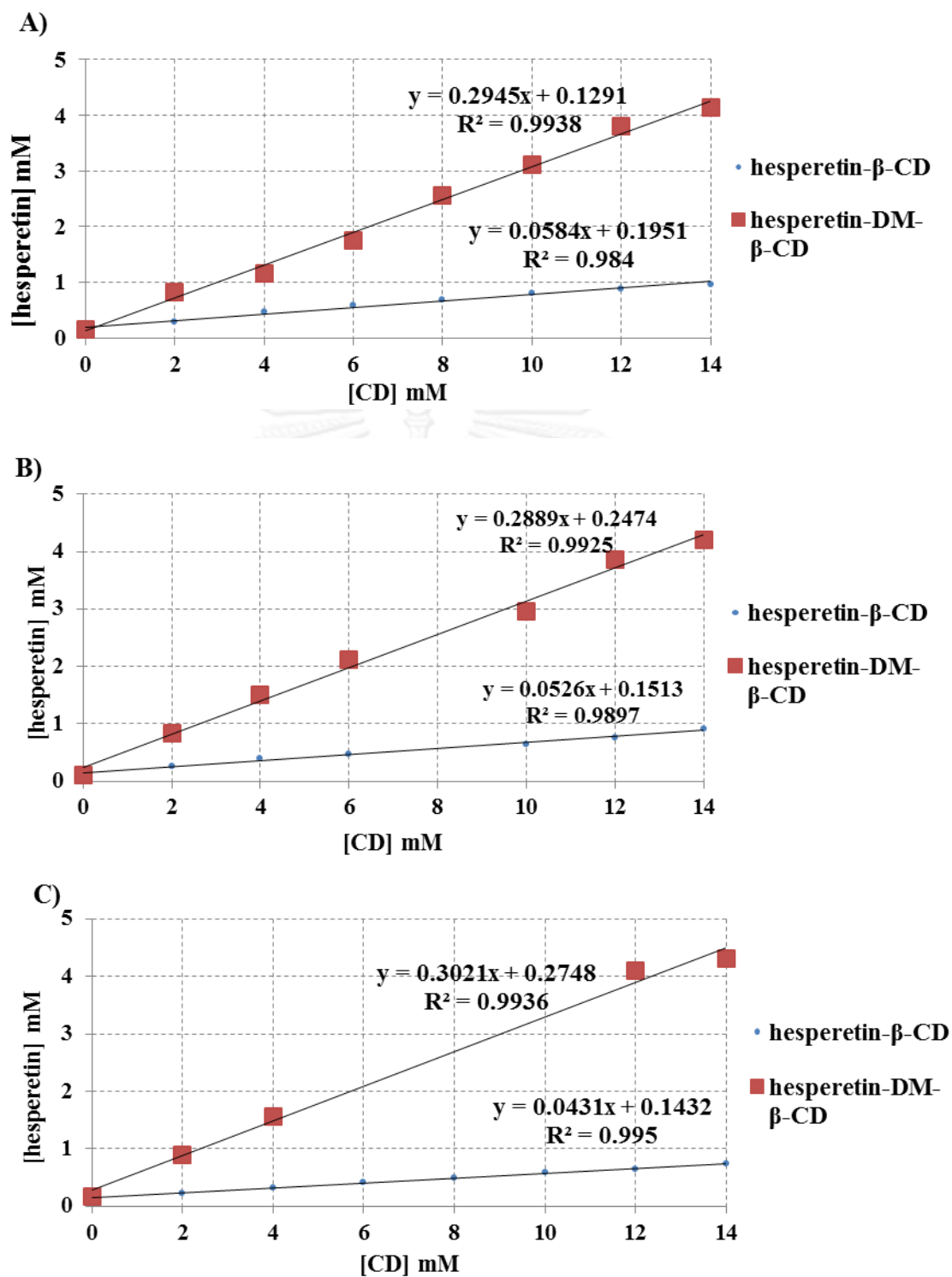


Figure 34. Phase solubility study of hesperetin with β -CD (●) or DM- β -CD (■) in water at A) 30°C, B) 37°C and C) 45 °C

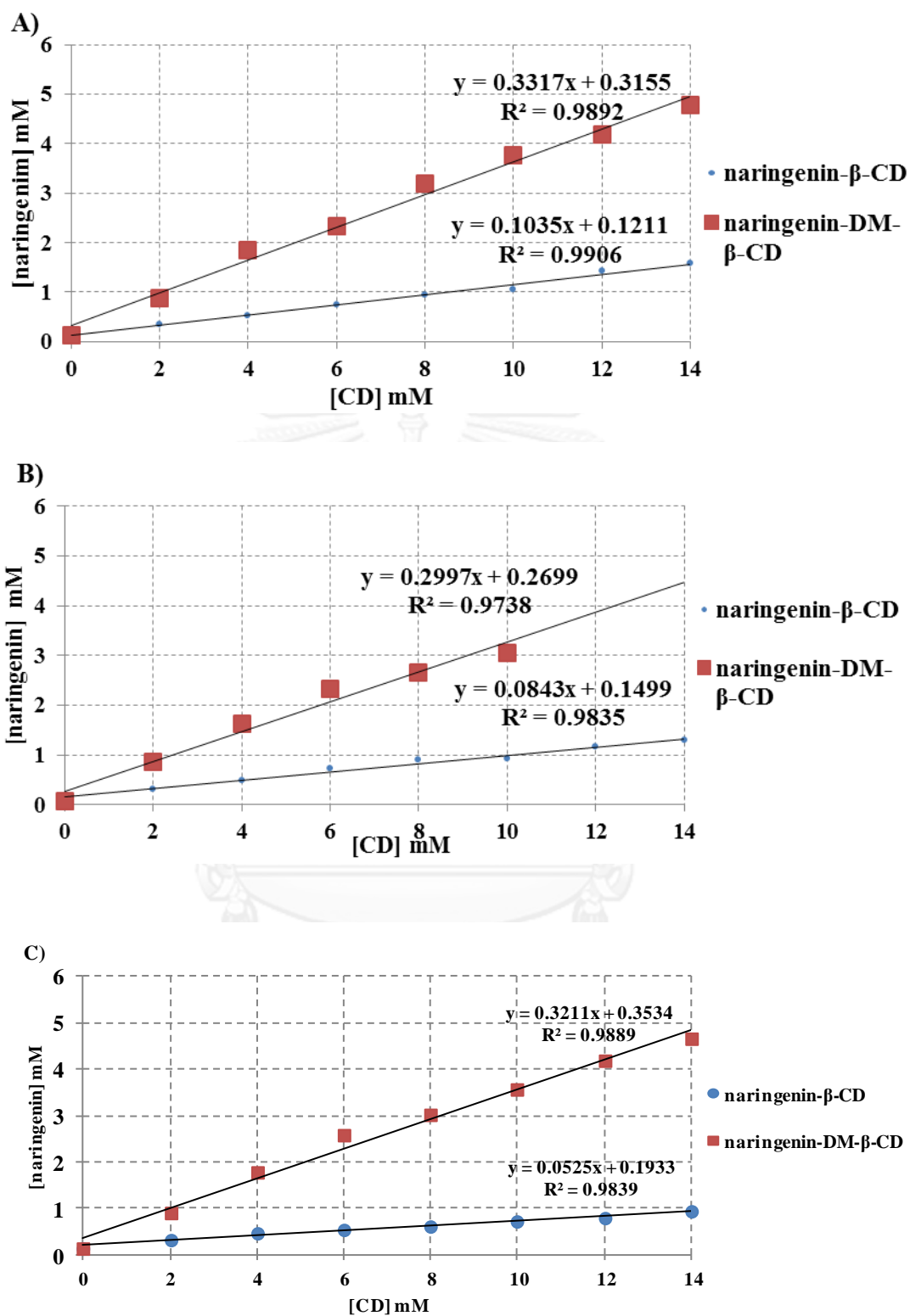


Figure 35. Phase solubility study of naringenin with β -CD (●) or DM- β -CD (■) in water at A) 30°C, B) 37°C and C) 45 °C

Table 7. Stability constants (K_c) of hesperetin-CD complex and naringenin-CD complex at different temperature

Temperature (°C)	K_c (M ⁻¹)			
	Hesperetin- β -CD	Hesperetin- DM- β -CD	Naringenin- β -CD	Naringenin- DM- β -CD
30	339.2	1289.3	425.0	1015.5
37	249.9	1030.5	367.8	999.9
45	195.6	1000.2	203.0	892.7

3.7 The Van't Hoff plot

The phase solubility data allow other information to be obtained, as the thermodynamic parameters involved in the complex formation. The Van't Hoff equation provides information about the temperature dependence of the equilibrium constant. The integrated form of Van't Hoff equation (Eq. 8) is used to calculate the values of enthalpy and entropy change. The phase solubility data allow other information to be obtained, as the thermodynamic parameters involved in the complex formation. The Van't Hoff equation provides information about the temperature dependence of the equilibrium constant. The integrated form of Van't Hoff equation (Eq. 8) is used to calculate the values of enthalpy and entropy change.

$$\ln K_c = -\frac{\Delta H^\ddagger}{RT} + \frac{\Delta S^\ddagger}{R}. \quad (11)$$

The CD-complexes of hesperetin and naringenin shown by Van't Hoff plot displayed a linear behavior. The negative values of enthalpy change and the slope is

positive, so the equilibrium constant decreased (Fig. 31 and 32) when the temperature increased which indicated that the interaction processes of all the four displayed a linear behavior. The negative values of enthalpy change and the slope is positive, so the equilibrium constant decreased (Fig. 29 and 30) when the temperature increased which indicated that the interaction processes of all the four systems were exothermic reactions [21] The relative thermodynamic parameters were calculated and shown in Table. 8. The free energy changes (ΔG_{30}) for the interactions involved in the complex formation were calculated using Gibbs equation (Eq. 9)

$$\Delta G_{25}^{\ddagger} = \Delta H - T\Delta S \quad (12)$$

The negative values of ΔG_{25} for hesperetin and naringenin (Table 8) showed that formation the four complexes was a spontaneous process. The free energy values of DM- β -CD complexed with hesperetin and naringenin were more negative than those of the β -CD complexes. From the calculation in terms of enthalpy and entropy, the entropic control was found in DM- β -CD complexes while both entropic and enthalpy control were observed in β -CD complexes.

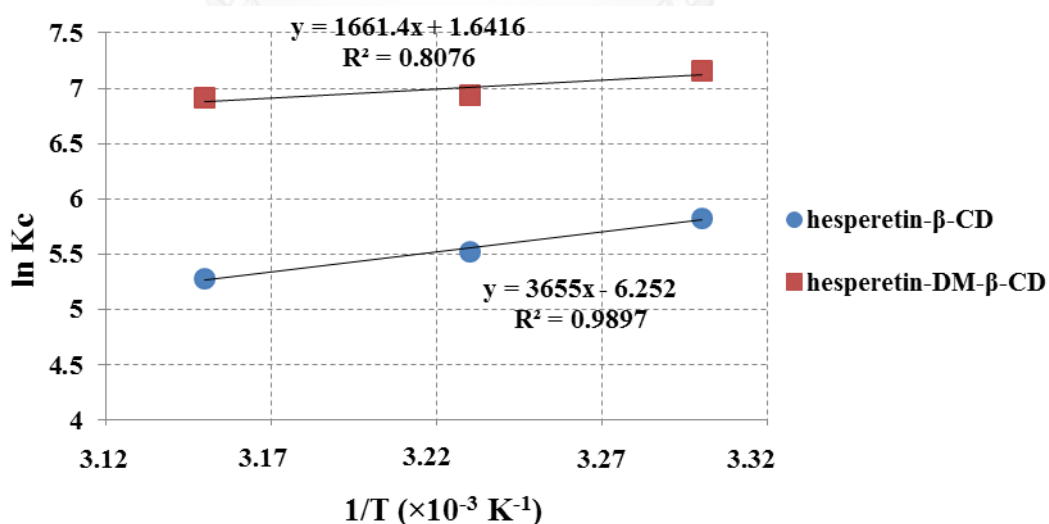


Figure 36. Van't Hoff plot of the formation of the complex between hesperetin and β -CD (●) or DM- β -CD (■)

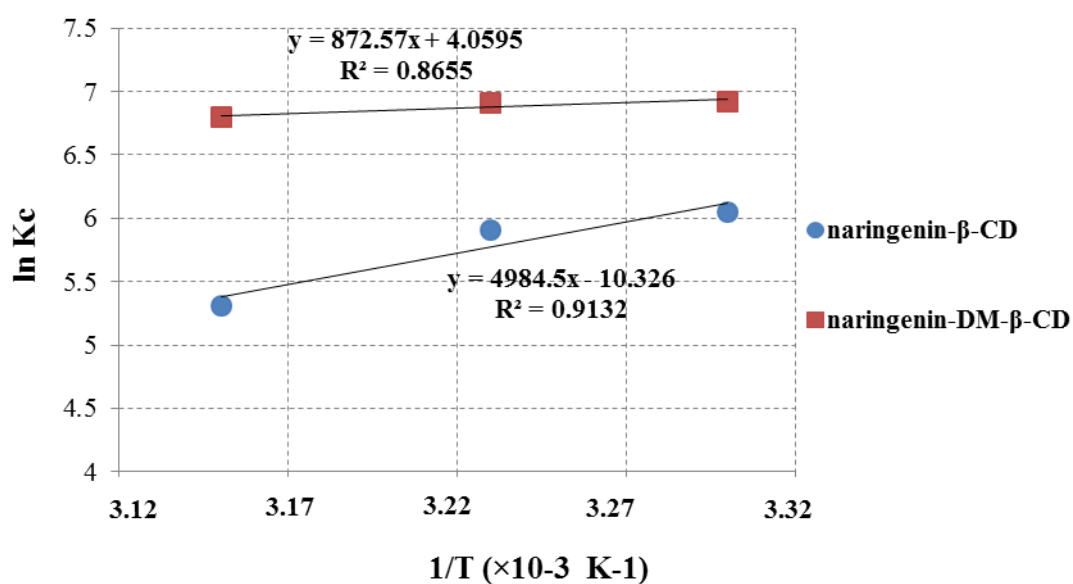


Figure 37. Van't Hoff plot of the formation of the complex between hesperetin and β-CD (●) or DM-β-CD (■)

Table 8. Thermodynamic values for complex formation of hesperetin and naringenin with β-CD and DM-β-CD

	$\Delta G(\text{kcal}\cdot\text{mol}^{-1})$	$\Delta H(\text{kcal}\cdot\text{mol}^{-1})$	$\Delta S(\text{kcal}\cdot\text{mol}^{-1})$
Hesperetin-β-CD	-3.56	-7.25	-0.012
Hesperetin-DM-β-CD	-4.27	-3.29	0.003
Naringenin-β-CD	-3.78	-9.89	-0.021
Naringenin-DM-β-CD	-4.14	-1.73	0.008

3.8 Preparation of flavanone: CD (β-CD and DM-β-CD) solid complexes

In the preparation of solid inclusion complex, kneading and freeze-drying method were used to form the flavanone: CD complexes. In kneading method, the kneaded mixture obtained were white homogeneous paste, liquid viscous. After the paste was oven-dried without sieve-screening, the product appeared as a white

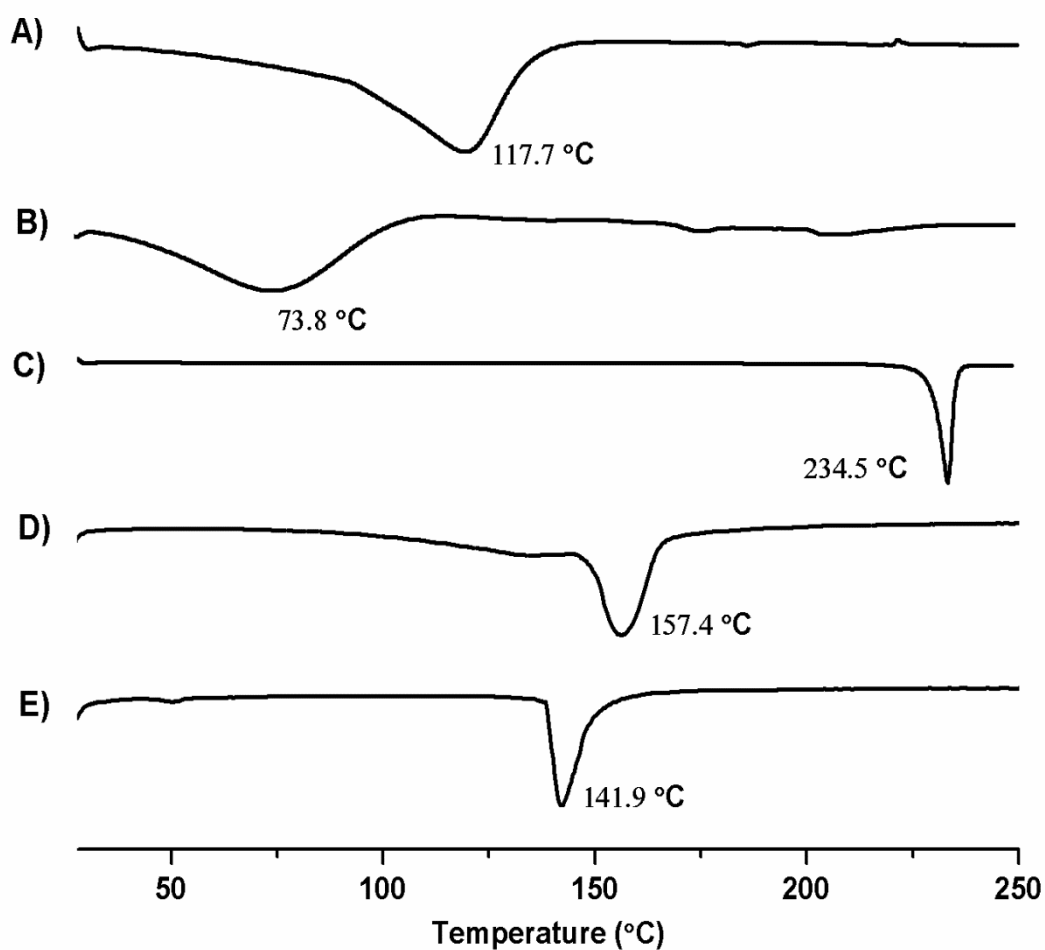
powder. For freeze-drying method, the mixture of flavanones and CDs in a mole ratio of 1:1 was prepared in distilled water. The solution was agitated for 24 hours until it turned into colloid. The solution was then filtered and freeze-dried. The solid complex obtained looks like fluffy cotton wool. The solid complexes were then determined whether they were real inclusion complexes by DSC and FTIR analyses.

3.9 Analysis of flavanone: CD (β -CD and DM- β -CD) solid complexes

3.9.1 Analysis by DSC

The differential scanning calorimetry (DSC) thermogram gave further information about the thermal properties of the starting free materials, (flavanones, β -CD and DM- β -CD) compared with those inclusion complexes obtained by freeze-drying method (Fig. 31 and 32) and kneading method (Fig. 33 and 34). The DSC confirms not only an interaction between the flavanones and CD, but also a real inclusion complex. The melting endothermic peaks characteristic of each of the free compounds: hesperetin at 234.5 °C (Fig. 31C), naringenin at 256.7 °C (Fig. 32C), β -CD at 117.7 °C (Fig. 31A and 32A), DM- β -CD at 73.8 °C (Fig. 31B and 32B) were determined. In case of the complexes obtained from freeze-drying, the endothermic peaks of free hesperetin and naringenin disappeared, corresponding with the appearance of a new peak at 157.4, 141.9, 145.5 and 150.5 °C for hesperetin- β -CD, hesperetin-DM- β -CD, naringenin- β -CD and naringenin-DM- β -CD system (Fig. 31D, 32E, 33D and 34E), respectively. The complete inclusion complexes were thus observed for the system obtained by freeze-drying. In contrast, kneading method resulted in a shift to lower temperatures of the flavanones, melting points in the thermogram of the complexes. In addition, there were peaks that could be ascribed to some

flavanones-CD interaction [65]. The result implied that kneading method yielded incomplete inclusion complexes.



CHULALONGKORN UNIVERSITY

Figure 38. DSC thermograms of A) β -CD, B) DM- β -CD, C) hesperetin, D) hesperetin- β -CD complex, and E) hesperetin-DM- β -CD complex prepared by freeze-drying method.

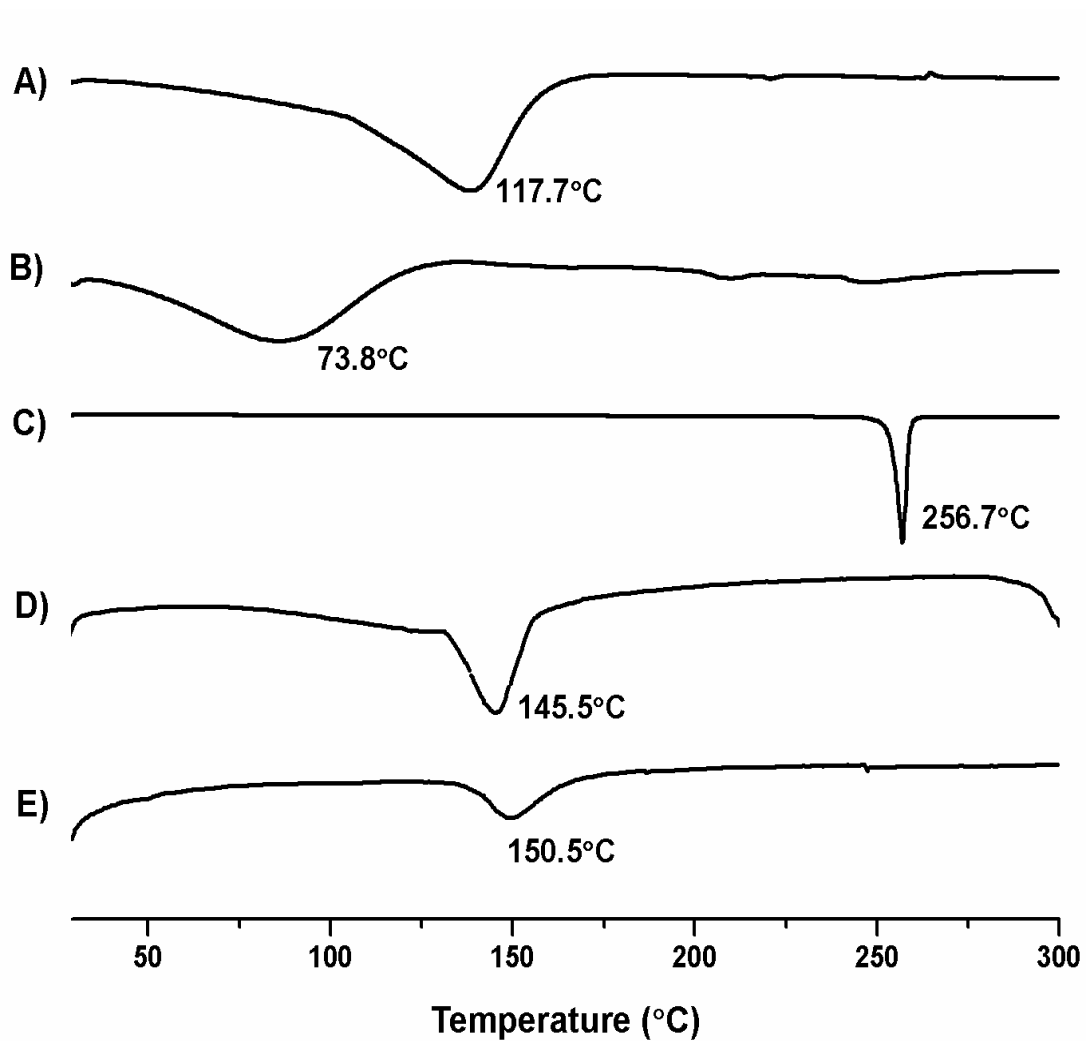


Figure 39. DSC thermograms of A) β -CD, B) DM- β -CD, C) Free naringenin, D) naringenin- β -CD complex, and E) naringenin-DM- β -CD complex prepared by freeze-drying method.

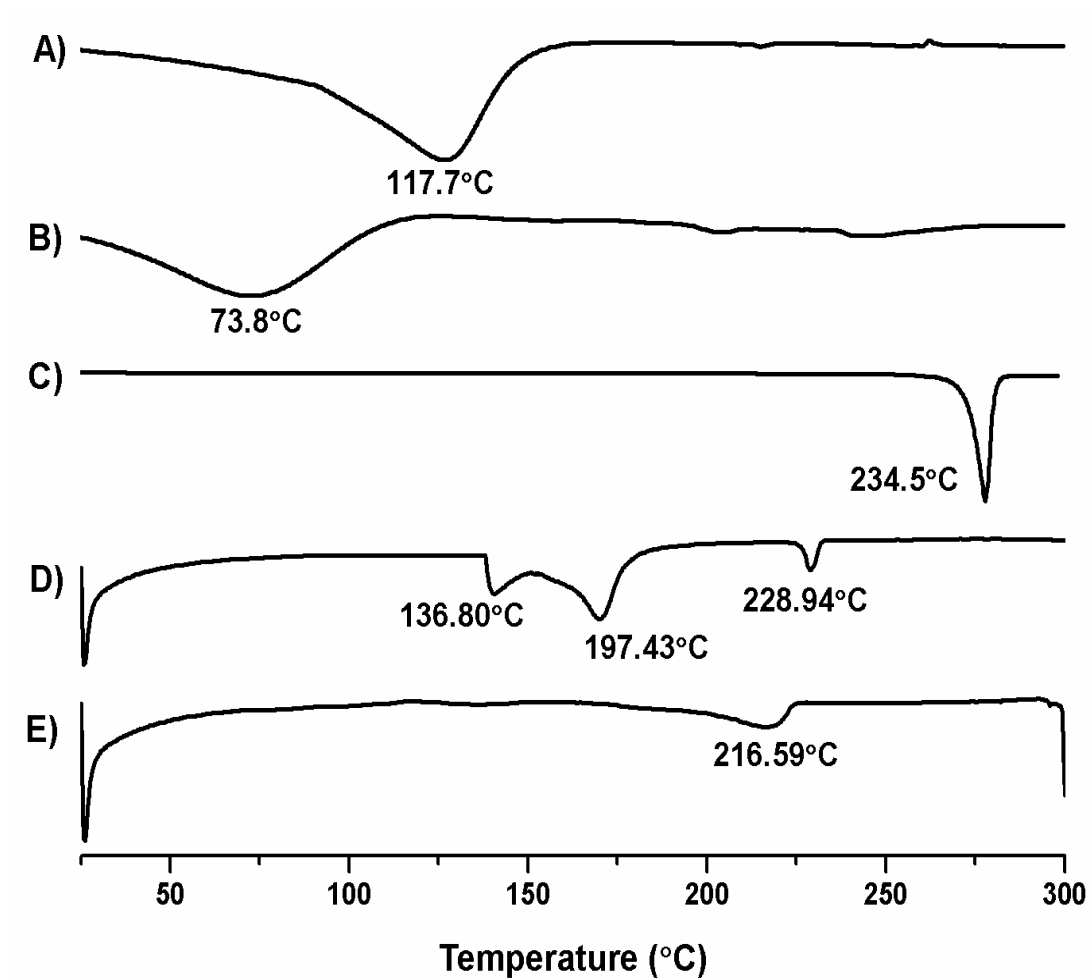


Figure 40. DSC thermograms of A) β -CD, B) DM- β -CD, C) Free hesperetin, D) hesperetin- β -CD complex, and E) hesperetin-DM- β -CD complex prepared by kneading method.

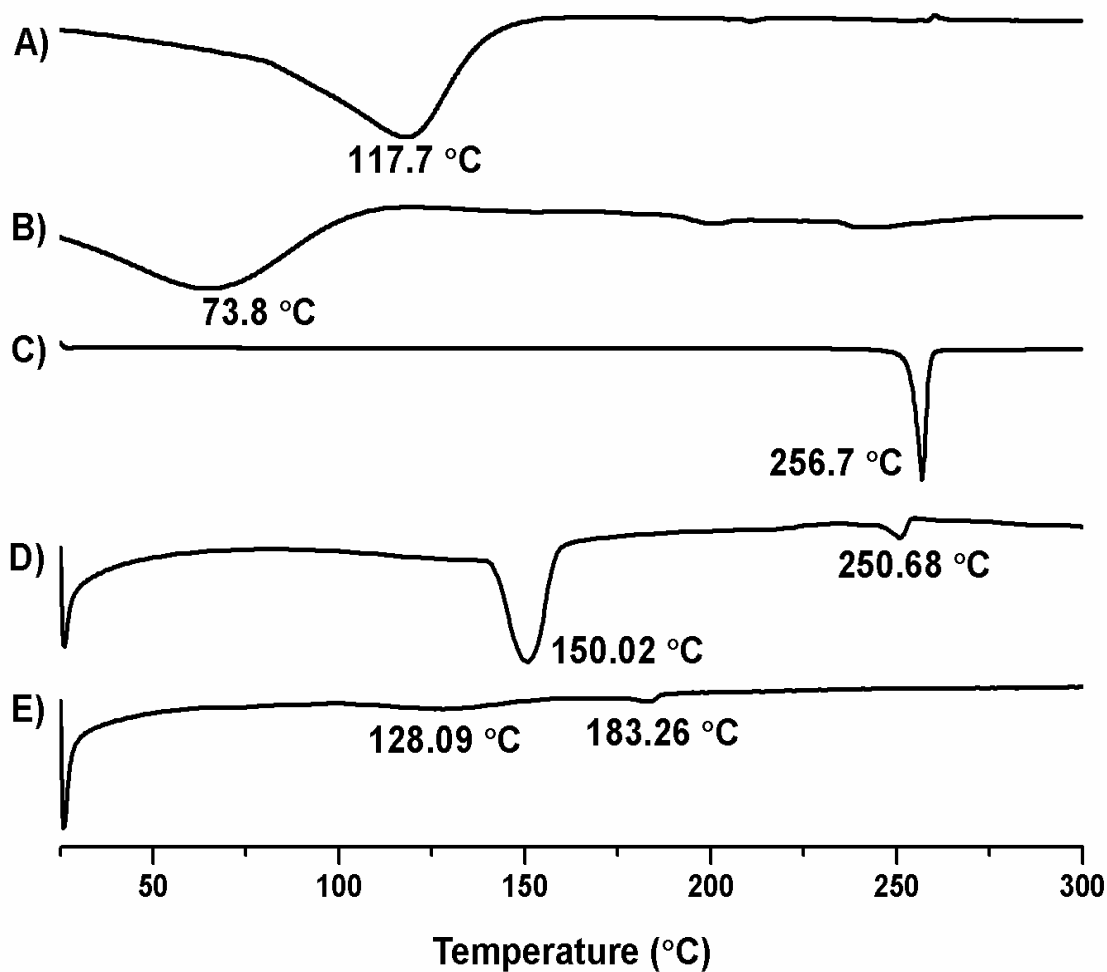


Figure 41. DSC thermograms of A) β -CD, B) DM- β -CD, C) Free naringenin, D) naringenin- β -CD complex, and E) naringenin-DM- β -CD complex prepared by kneading method.

3.9.2 Analysis by FTIR

Inclusion complexes were also analyzed by FTIR spectroscopy (Perkin Elmer, Spectrum One). The FTIR spectra of flavanones-CD complexes prepared by freeze-drying and kneading methods were compared with the free compounds in the wavelength range of 400 to 4000 cm^{-1} as shown in Fig. 35 and 37 (hesperetin) and Fig. 36 and 38 (naringenin). FT-IR spectra of the complex were analyzed for the changes in the characteristic bands of pure substance to confirm the formation of complex as a new compound with different spectroscopic bands. The IR spectrum of β -CD and DM- β -CD showed strong broad peak of OH stretching at about 3500-3300 cm^{-1} and C-C and C-O stretching vibration of β -CD and DM- β -CD at 1028 and 1046, respectively. Other characteristics were shown in Table 9-12. The IR spectrum of hesperetin showed the major peak at 1636 as C-C stretching (Aromatic ring), the -OH phenolic at 1200 cm^{-1} and methoxylic at 1250 cm^{-1} . For freeze-drying method, peaks of aromatic, -OH and methoxylic group of hesperetin disappeared which can be implied that hesperetin formed inclusion complex with CDs. In the same method, the inclusion complex of naringenin showed aromatic peak at 1630 cm^{-1} , the -OH phenolic at 1200 cm^{-1} ; a decrease in the intensity of the aromatic bands and the disappearance of the OH band were found. On the other hand, no change of peak in kneading method. This suggests that the real inclusion complexes were obtained by the freeze-drying preparation.

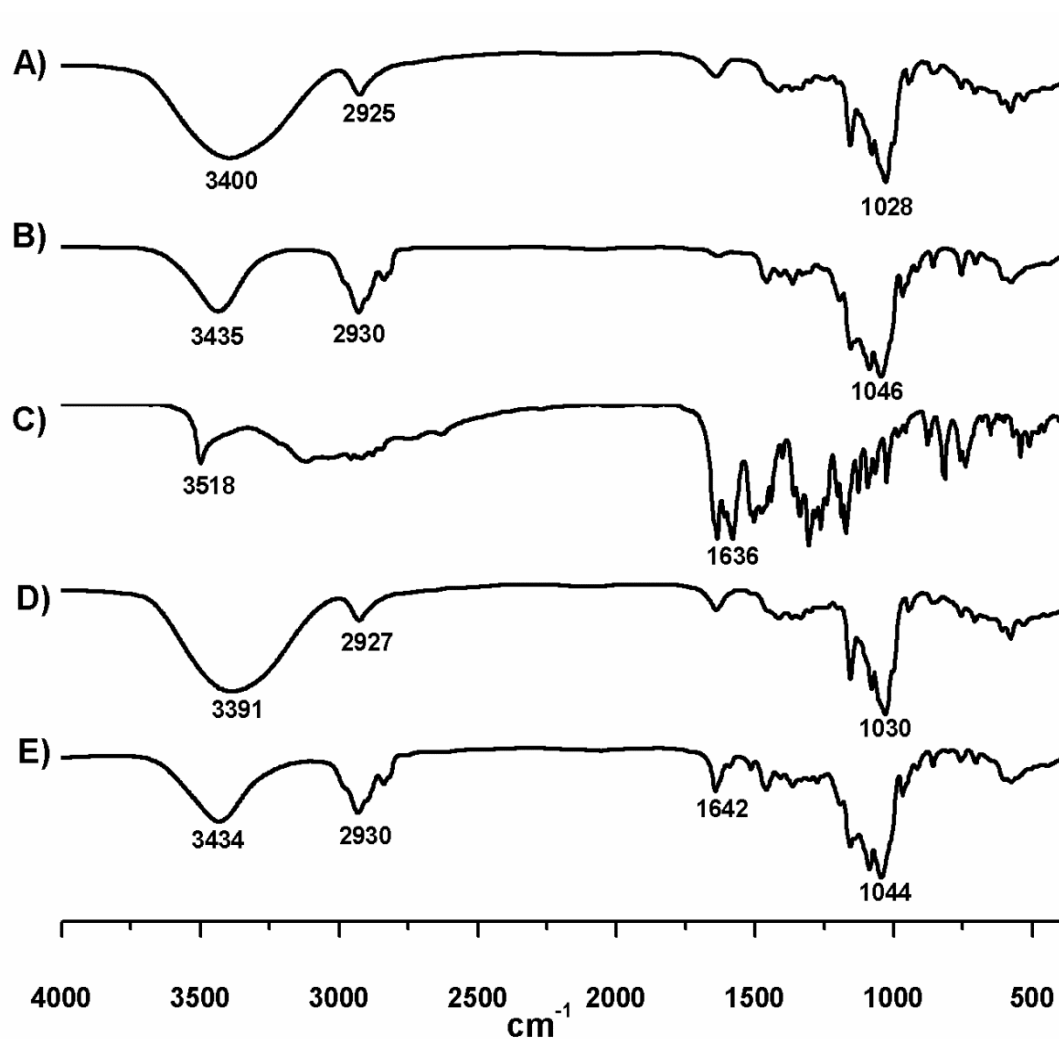


Figure 42. Infrared spectra of A) β -CD, B) DM- β -CD, C) free hesperetin, D) hesperetin- β -CD complex, and E) hesperetin-DM- β -CD complex. Complex formation was by freeze-drying method.

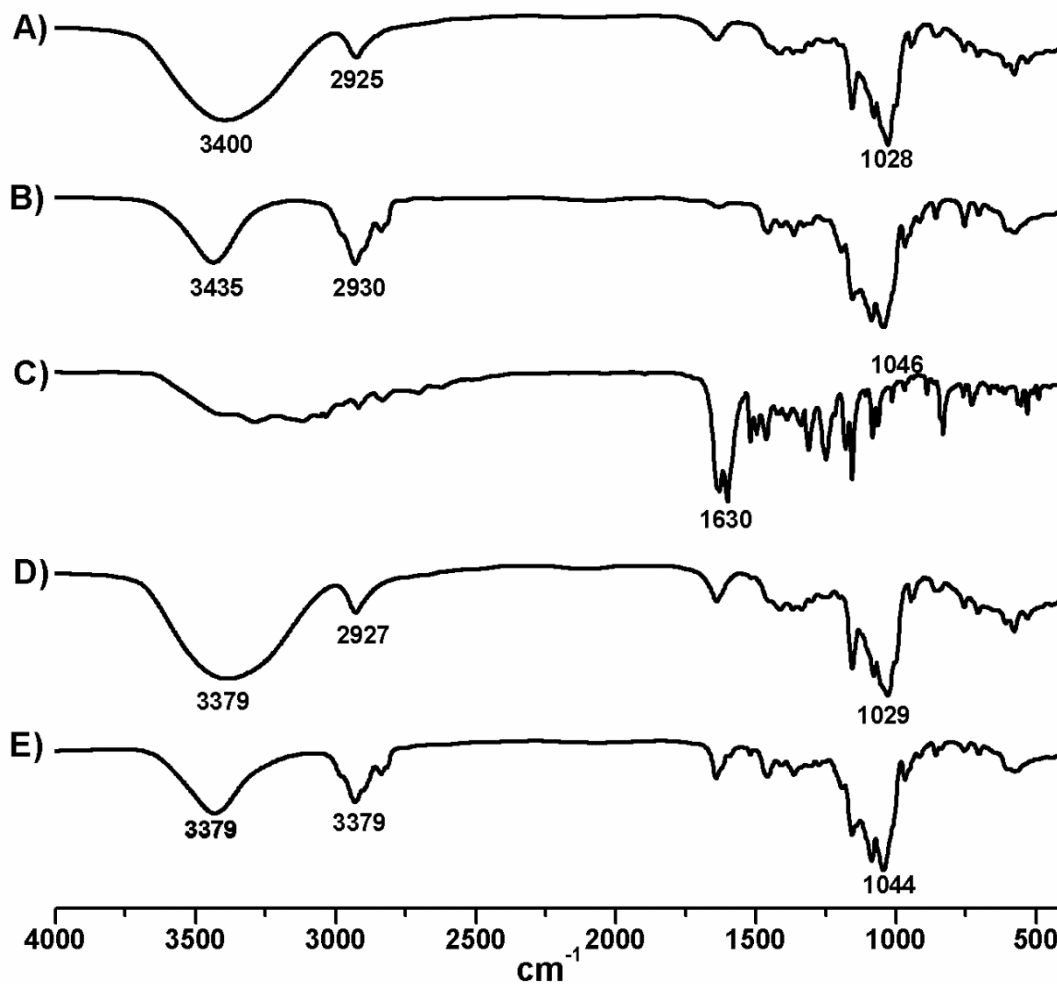


Figure 43. Infrared spectra of A) β -CD, B) DM- β -CD, C) free naringenin, D) naringenin- β -CD complex, and E) naringenin-DM- β -CD complex. Complex formation was by freeze-drying method.

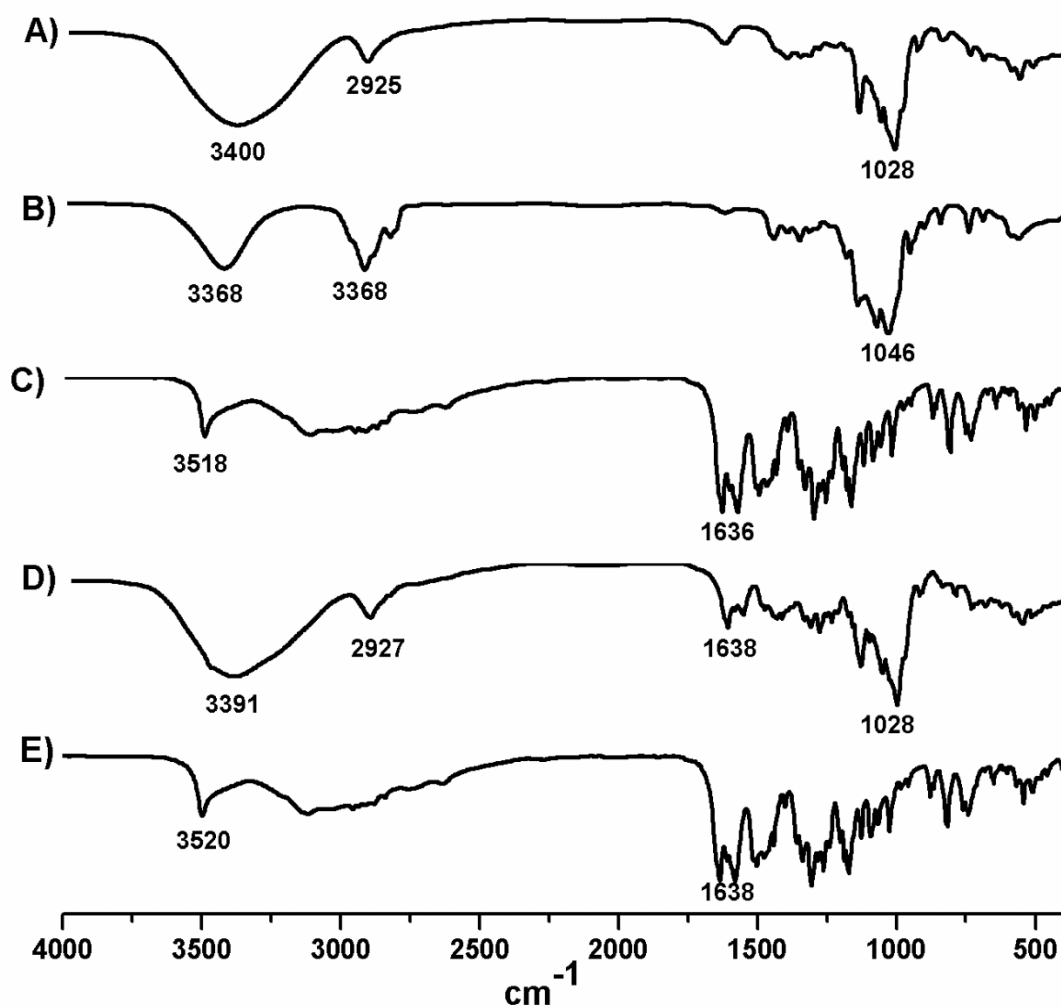


Figure 44. Infrared spectra of A) β -CD, B) DM- β -CD, C) free hesperetin, D) hesperetin- β -CD complex, and E) hesperetin-DM- β -CD complex. Complex formation was by kneading method.

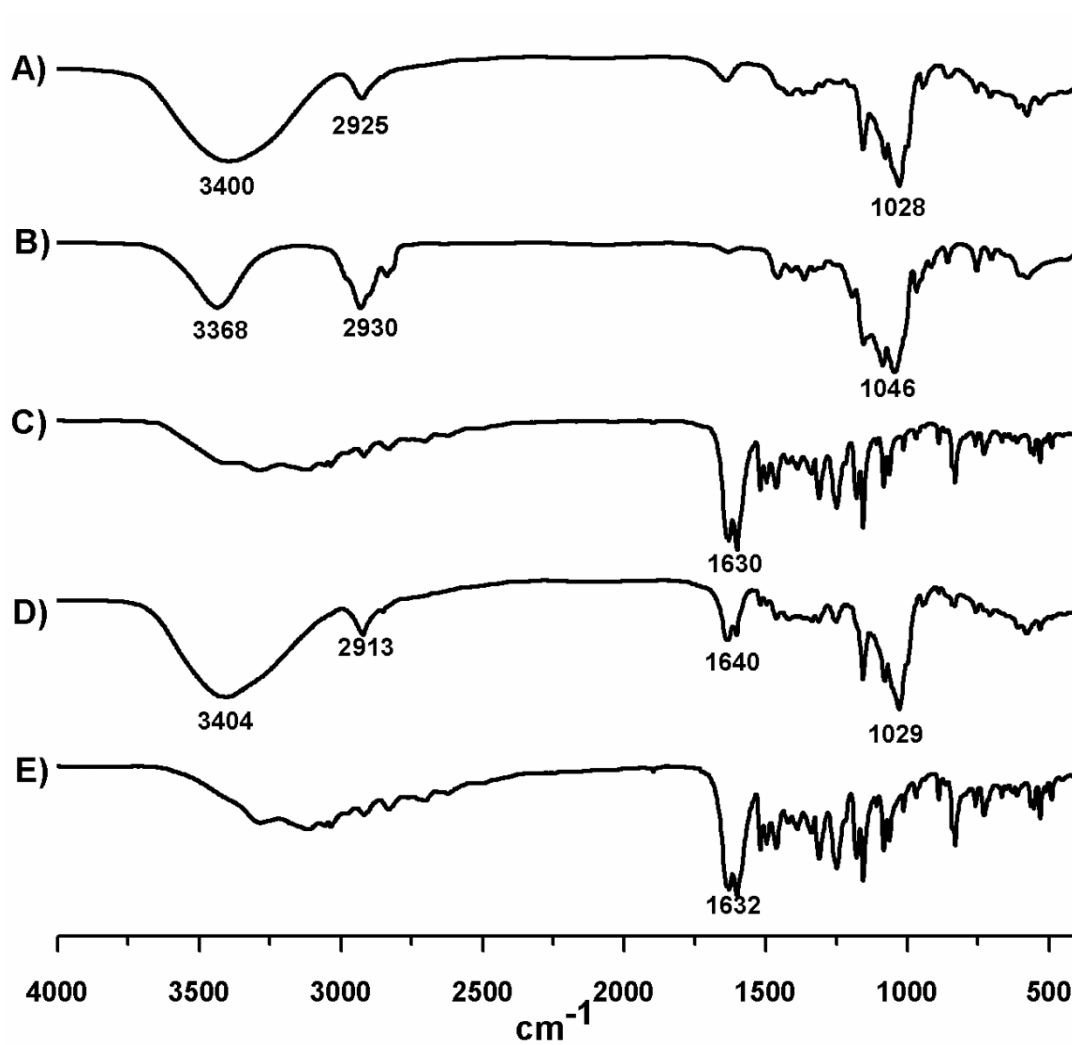


Figure 45. Infrared spectra of A) β -CD, B) DM- β -CD, C) Free naringenin, D) naringenin- β -CD complex, and E) naringenin-DM- β -CD complex. Complex formation was by kneading method.

Table 9. FTIR data of hesperetin, β -CD, and hesperetin- β -CD inclusion complex prepared by different method

Wavenumber (cm ⁻¹)				
Free compound		Complex		Assignment
Hesperetin	β -CD	Kneading	Freeze-drying	
	3500,3300	3500-3300	3391	Broad -OH stretching
	2926	2924	2927	-CH stretching
	1027	1026	1030	C-O stretching
1636, 1581		1612 and 1582 ↓	-	C-C stretching
1200, 1350		-	-	-OH phenolic
1250		-	-	methoxylic

Table 10. FTIR data of hesperetin, DM- β -CD, and hesperetin-DM- β -CD inclusion complex prepared by different method

Wavenumber (cm ⁻¹)				
Free compound		Complex		Assignment
Hesperetin	DM- β -CD	Kneading	Freeze-drying	
	3499	3500-3300	3434	Broad -OH stretching
	3119	3119	2930	-CH stretching
	1157	1027	1044	C-O stretching
1636, 1581		1610, 1581	1642	C-C stretching
1200, 1350			-	-OH phenolic
1250			-	methoxylic

Table 11. FTIR data of naringenin, β -CD, and naringenin- β -CD inclusion complex prepared by different method

Wavenumber (cm ⁻¹)				
Free compound		Complex		Assignment
Naringenin	β -CD	Kneading	Freeze-drying	
	3500-3300	3500-3300	3379	Broad -OH stretching
	2926	2923	2927	-CH stretching
	1027	1028	1029	C-O stretching
1638, 1602		1630 ↓	-	C-C stretching
1200		1157	1156	-OH phenolic

Table 12. FTIR data of naringenin, DM- β -CD and naringenin-DM- β -CD inclusion complex prepared by different method

Wavenumber (cm ⁻¹)				
Free compound		Complex		Assignment
Naringenin	DM- β -CD	Kneading	Freeze-drying	
	3499	3500-3300	3434	Broad -OH stretching
	3119	2913	2930	-CH stretching
	1157	1601 and 1628	1642	C-O stretching
1638, 1602		1157	1156	C-C stretching
1200		1200	-	-OH phenolic

3.10 Dissolution study

The dissolution diagram of hesperetin, naringenin and their inclusion complexes (1:1 molar ratio, formed by freeze-drying method) in water at 37 °C are shown in Fig 39 and 40. The dissolution of both hesperetin and naringenin were determined at different time, the amounts dissolved were determined by both spectrophotometric and HPLC methods (Table 13 and 14). The values obtained from the two methods were similar. The HPLC technique was used to determine the releasing of hesperetin or naringenin from their complexes with and β -CD at 30 minutes of dissolution time. A typical HPLC chromatogram of the hesperetin release from their complex (Fig. 41) and the naringenin release (Fig. 42) was shown here.

It can be observed that dissolution of the two flavanones was enhanced significantly when formed complexes with cyclodextrins while free flavanones exhibited poor dissolution. Both free and inclusion complexes of hesperetin and naringenin were dissolved with high rate for the first 10 min., then, gradually level off until plateau after one hour. When compared the dissolved amounts of free hesperetin, β -CD complex and DM- β -CD complex at 10 minutes, the amounts of hesperetin dissolved were 0.11, 0.33 and 0.63 mg/ml, respectively. For free naringenin, β -CD complex and DM- β -CD complex, the amounts dissolved were 0.13, 0.13 and 0.42 mg/ml. The results demonstrated that the inclusion complexes of both flavanones with DM- β -CD showed a higher dissolution rate than the inclusion complexes with β -CD.

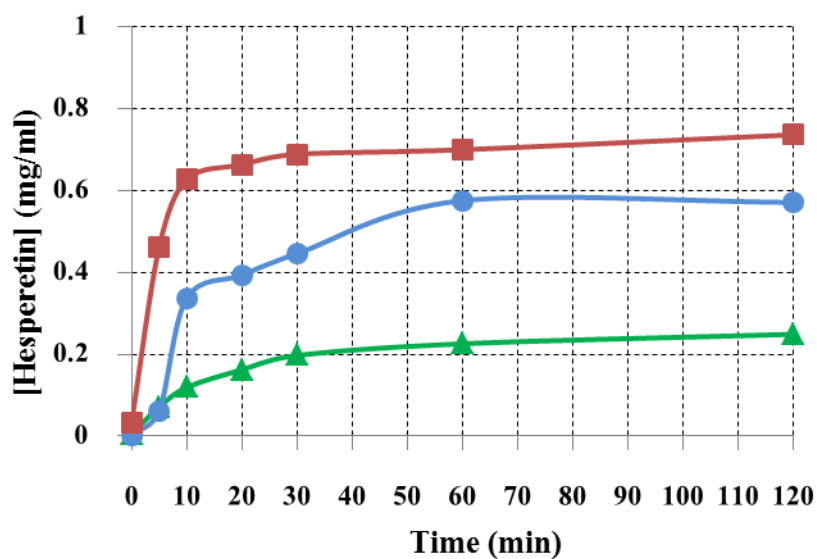


Figure 46. The dissolution diagram at 37 °C in water of hesperetin (▲), hesperetin-β-CD (●), and hesperetin-DM-β-CD (■). Complex formation was by freeze-drying.

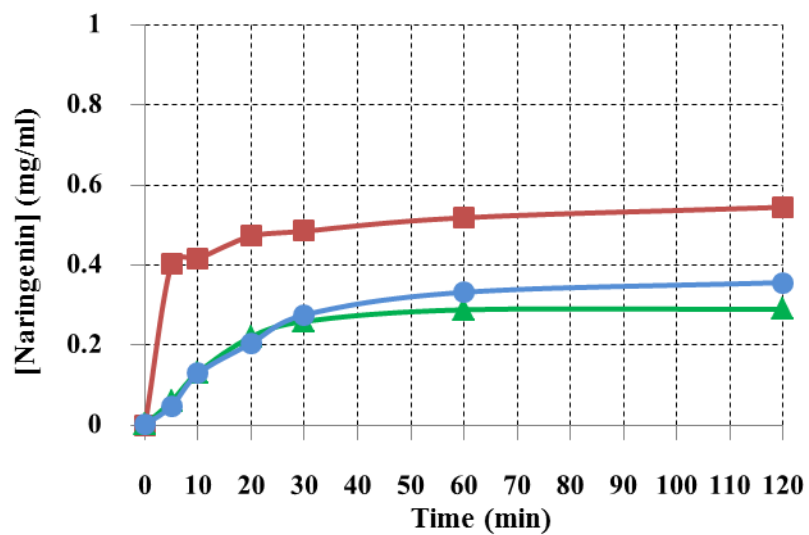


Figure 47. The dissolution diagram at 37 °C in water of naringenin (▲), naringenin-β-CD (●), and naringenin-DM-β-CD (■). Complex formation was by freeze-drying.

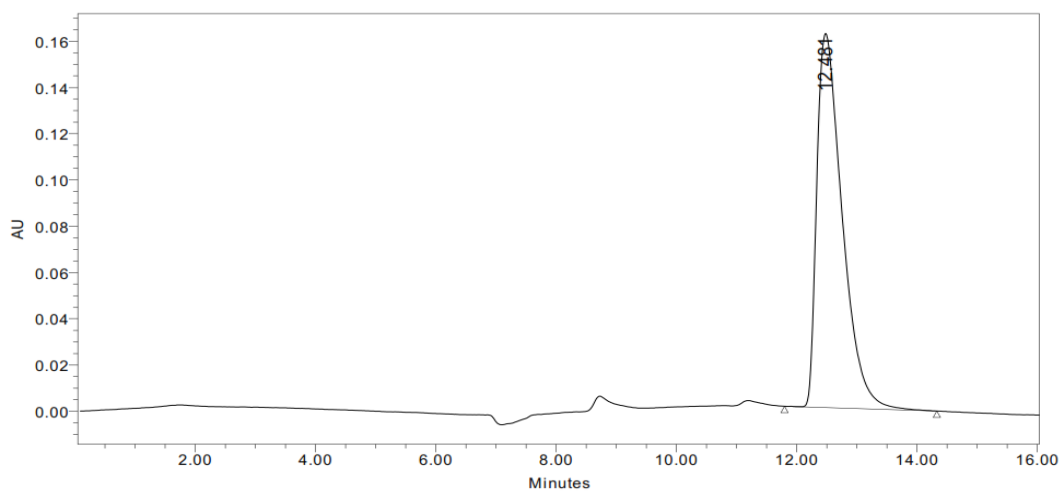


Figure 48. A typical HPLC chromatogram of hesperetin- β -CD complex when dissolution time was 30 minutes

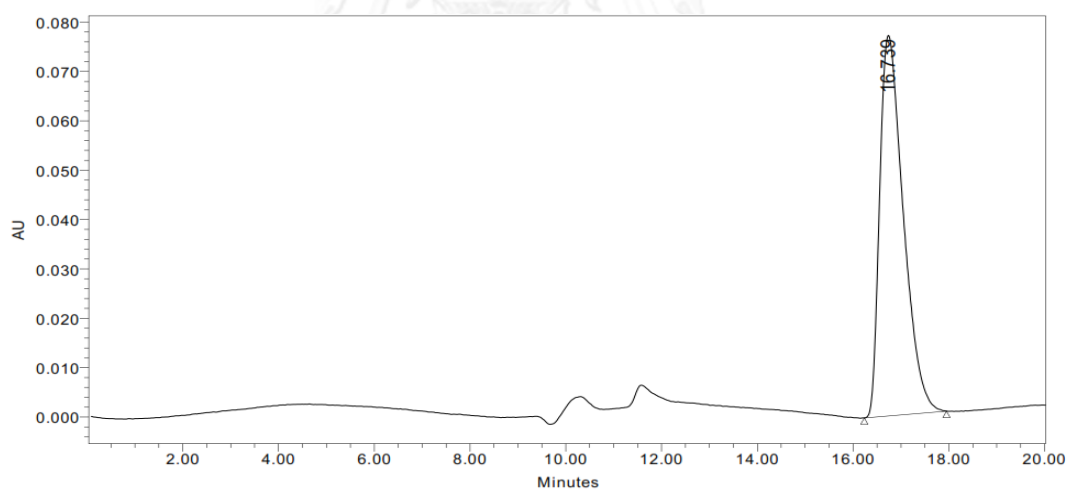


Figure 49. A typical HPLC chromatogram of naringenin- β -CD complex when dissolution time was 30 minutes

Table 13 Dissolution rate of hesperetin from free and complex form at different time by spectrophotometric and HPLC method

Compound	Time (min)	Dissolved amount (mg/ml) as analyzed by	
		Spectrophotometry	HPLC
[Free hesperetin]	10	0.1187	0.1248
	30	0.1969	0.1987
	60	0.2255	0.2189
	120	0.2487	0.2451
[Hesperetin- β -CD]	10	0.3366	0.3209
	20	0.4456	0.4301
	60	0.5751	0.5749
	120	0.5709	0.5884
[Hesperetin-DM- β -CD]	10	0.6269	0.6172
	20	0.6885	0.6852
	60	0.6997	0.7119
	120	0.7360	0.7374

Table 14 Dissolution rate of naringenin at different time compared method between by spectrophotometric and HPLC

Compound	Time (min)	Dissolved amount (mg/ml) as analyzed	
		by	
		Spectrophotometry	HPLC
[Free naringenin]	10	0.13221	0.1303
	20	0.2214	0.2196
	60	0.2886	0.2940
	120	0.2899	0.3027
[naringenin- β -CD]	10	0.1296	0.1983
	20	0.20511	0.2831
	60	0.3326	0.3393
	120	0.3568	0.3507
[naringenin-DM- β -CD]	10	0.4173	0.4119
	20	0.47276	0.4707
	60	0.5187	0.5066
	120	0.5449	0.5544

CHAPTER VI

DISCUSSION

4.1 Analysis of flavanones

For the fundamental analysis of flavanones, spectrophotometry was used because it is a convenient and low cost method. The maximum wavelength of absorption was observed at 286 nm for flavanones, hesperetin and naringenin, when solubilized in water. Zhang and coworker had reported that maximum wavelength of absorption of naringenin in the solution of binary system of ethanol and water was 288 nm [66]. It is known that solvent polarity has an effect on absorption spectra of a chromophore.

For CDs, no UV absorption peak was found since it contained no UV absorption functional group. From the scanning for UV spectra, no change in UV spectra of hesperetin was observed when it formed complex with CDs whereas the maximum wavelength of naringenin-CD complex was shifted from 286 to 288 nm which was the same as that reported in the previous study [67]. Analysis of both flavanones was also confirmed by using HPLC- C18 reverse phase column. The mobile phase used was 70% methanol as previously described [68]. The advantage of HPLC is due to its high sensitivity and small volume of samples needed.

4.2 Phase solubility study

The phase solubility diagram of flavanones-CDs system in aqueous solution at different temperature was shown in Fig 29 and 30. The linear relationship of the plot for all complexes, indicating that the phase solubility profiles were of the typical A_L -

type and the 1:1 molar ratio [26] of soluble guest and host, this finding agrees with previous study [21]. However, phase solubility depends on pH and polarity of the solvents used in the soluble complex formation which may cause unionized and charged forms. The phase solubility of many guest molecules with cyclodextrins has been reported in several studies [22, 69] e.g. hesperetin and its 7-rhamnoglucoside with (2-hydroxypropyl)- β -cyclodextrin, the phase solubility in both cases showed the A_L type diagrams illustrated the soluble 1:1 complexes. In addition, this work suggested that hesperetin may have higher hydrophobicity and a smaller size when compared to its 7-rhamnoglucoside, therefore exhibited a greater affinity and was better fitted into the cavity of the CD molecules.

The results showed that the water solubility of hesperetin and naringenin was remarkably increased approximately 10 and 40 times by the solubilizing effects of β -CD and DM- β -CD. Thus, the solubility of both flavanones in the presence of CDs followed the same rank of order of DM- β -CD > β -CD, reflecting an enhancement of binding and solubility of both flavanones. The methyl substitution plays an important role in balancing the CD water solubility and its complexing ability. It was previously reported that increasing the degree of substitution up to an optimum level improves the CD aqueous solubility and the binding of guests to CDs is increased by increasing the surface area of binding [70]. However, beyond the optimum level, the steric hindrances of the host molecule impair CD complexing (efficiency) capacity.

The stability constant (K_c) was calculated from the linear portion of the solubility diagram assuming a 1:1 complex in Eq. 9, where the solubility of flavanone in the absence of cyclodextrin can be estimated by interception of the graph that plot between the concentration of flavanone and cyclodextrin. In this case, the interception was used instead of the measured S_0 value in order to avoid the error

from human or instrumental error. The parameter demonstrates the strength of the interaction between the host and guest molecules that come together to form the complex. The host-guest size match may dominate the stability of the complexes formed between CDs and guests. Our result showed that the binding constants for the complexation of flavanones with β -CD and DM- β -CD were in the following order: DM- β -CD > β -CD. It implied that the DM- β -CD complex was more stable than β -CD system, the result which was well supported by the binding free energy obtained from the binding energy calculation using the computational method of study (Table 4 and 6 for hesperetin and naringenin, respectively). Moreover, we found that the van der Waals (vdW) energy was some six-fold greater than the electrostatic energy in both of the CDs complexes which implied that the vdW interaction played an important role in forming/stabilizing the inclusion complex. The obtained information was in good agreement with the previous studies in which the hydrophobic interaction was found to be the main driving force for flavanones-CD inclusion complexes [24, 71].

In addition, the temperature had an influence on the stability of the complexes. The K_c of the flavanones-CDs complexes obtained for temperature in the range of 30-45 °C, plotted in a Van't Hoff plot showed a linear function between K_c and the inverse of the temperature (1/T). From the calculation in terms of enthalpy and entropy, the entropic control was found in DM- β -CD complexes while both entropic and enthalpy controls were observed in β -CD complexes. The binding Gibbs free energy (ΔG) of complex can be determined by theoretical and experimental studies. The compared ΔG values were illustrated in Table 15. Hesperetin-DM- β -CD exhibited the lower ΔG than hesperetin- β -CD for 5.07 kcal•mol⁻¹. In the same way, naringenin-DM- β -CD also gave the lower theoretical ΔG than naringenin- β -CD for 2.50 kcal•mol⁻¹. From the theoretical data, it can suggest that the DM- β -CD complexes

were stable than that β -CD complexes. The theoretical data were supported by the experimental results which were calculated by Van't Hoff equation. Importantly, the experimental results showed the same trend binding free energy values to the values from theoretical results. All obtained results imply that the flavanone binds to and interacts with DM- β -CD stronger than that with β -CD. Moreover, experimental result also agreed well with the previous study of Tommasini *et al.* (2004).

Table 15. Comparison of ΔG values between the theoretical and experimental studies for hesperetin- β -CD, hesperetin-DM- β -CD, naringenin- β -CD, naringenin-DM- β -CD complexes

CDs	ΔG (kcal \cdot mol $^{-1}$)		
	Theoretical study* (QM/GBSA)	Experimental study*	Experiment**
hesperetin- β -CD	-2.20	-3.50	-3.39
naringenin- β -CD	-1.17	-3.64	-3.45
hesperetin-DM- β -CD	-7.27	-4.27	N/A
naringenin-DM- β -CD	-3.67	-4.14	N/A

* This study

** (Tommasini *et al.* 2004)

The stability constants decreased with increasing temperature, as expected for an exothermic process. The K_c value is a useful index to estimate the binding strength of the guest with the host: a small K_c value indicates a higher relative amount of free guest due to a weak interaction between flavanones and CDs. On the other hand, a large K_c indicates that the equilibrium is displaced towards the complex formation and a limited release of guest molecule. Similar temperature

effect on the stability constants were reported by other authors working on the solubility of naringenin and hesperetin or different compounds encapsulated in β -CD [21, 72, 73].

4.3 Preparation of the inclusion complex

The preparation of solid complex was carried out between hesperetin or naringenin and CDs (β -CD and DM- β -CD) using a 1:1 guest: host mole ratio. Kneading and freeze-drying were different method used in this study.

Kneading method, although this method is easy to do but it is usually not a good method to prepare complexes. We found that this method was unsuccessfully used for preparation of flavanones and CDs complexes in our study. Similar result was reported by Blanco *et al.*, (1991) that the influence of method of preparation on inclusion complexes of naproxen with different cyclodextrin was observed. Their complexes were prepared by freeze-drying, spray-drying and kneading method. The complex formed by kneading method did not provide complete encapsulation.

Freeze-drying method was successfully used in our study for preparation of inclusion complexes. This method was used in several studies, for example: Paramera *et al.*, (2011) worked with the microencapsulation of curcumin using three encapsulates: yeast cells, β -CD and modified starch. In the β -CD complex, the authors used freeze-drying, co-precipitation, co-evaporation and kneading methods for complex formation. The best result was from the freeze-drying method, followed by the method of co-precipitation. Kfoury *et al.*, (2014) reported the study of monoterpene complexation with HP- β -CD using freeze-drying method in the preparation of the true inclusion complex.

4.4 Detection of solid complex

4.4.1 Differential Scanning Calorimetry (DSC)

In the characterization of the solid complex for determining its thermodynamic properties, the use of DSC analysis was reported in many studies [74-77] to characterize CD complexes with different guests e.g. rutin, quercetin, carvediol and taxifolin.

The nature of the guests and cyclodextrins used and the method of preparation of the complex have been found to influence the inclusion complex formation. If the interaction between the guest molecules and the cyclodextrins is weak, the shift in the endothermic peak of the guest molecule is very small. That means the complex is not stable, leading to the inability to form the true inclusion complex [78].

In the present study, the formation of inclusion complexes of hesperetin and naringenin with cyclodextrins by kneading and freeze-drying methods was evaluated using DSC. The DSC endotherm of hesperetin at 234.5 °C was shifted to 228.9 °C and 216.5 °C in β -CD and DM- β -CD complex, respectively in the kneading method showing a weak interaction and incomplete inclusion complexes. But the freeze-dried complexes showed no endothermic peak of the guest around 210-235 °C indicating the formation of true inclusion complex. Formation of inclusion complex of naringenin with β -CD and DM- β -CD was also evaluated. The DSC curve of naringenin showed an endothermic peak with an onset temperature at about 256.7 °C. The DSC curve of the kneading method mainly showed the effects of naringenin and CDs, while the endothermic peak of naringenin disappeared in freeze-drying method. It was previously reported that naringenin was completely complexed in the CD molecules through interactions such as hydrogen bonds or van der Waals

force or their combination [79]. Our results agree well with those studies reported [20] in which the hesperetin and naringenin complexed with β -CD were prepared by co-precipitation method and the study in solution and solid state were performed by NMR, DSC and X-ray techniques.

4.4.2 Fourier Transform Infrared Spectroscopy (FTIR)

FTIR is also commonly used to estimate the interaction between cyclodextrins and the guest molecules in the solid state [80, 81]

Cyclodextrin bands often change only slightly upon complex formation. In the hesperetin spectrum, the major peak at 1636 cm^{-1} , which is C-C stretching (aromatic ring), the -OH phenolic at 1200 cm^{-1} and methoxylic at 1250 cm^{-1} were observed. For freeze-drying method, the peaks of these main functional groups of hesperetin disappeared which is a good evidence of complex formation. The same phenomenon occurred for naringenin system which showed aromatic peak at 1630 cm^{-1} , the -OH phenolic at 1200 cm^{-1} ; a decrease in the intensity of the aromatic bands and the disappearance of the OH band were found. Therefore, the FTIR technique confirms that the complete complexes were formed between the two flavanones and CDs using the freeze-drying method. The results of this study corresponded well with the previous report on complexes of hesperetin and naringenin with β -CD by the co-precipitation method, in which the relevant shift in the complex spectrum was found [20]. However, the technique is not generally suitable to detect all the inclusion complexes and may be less clarifying than other methods [82, 83]. This is because the application of the Infrared spectroscopy is limited to the guests having some characteristic bands, such as carbonyl or sulfonyl groups [84-86].

The true complex between CDs and flavanones which was prepared by the freeze-drying method was stable. The obtained information was in agreement with the binding energy in the computational results (Fig. 9, Table 4 for hesperetin and Table 6 for naringenin), of which the result showed vdW interaction and H-bond played the important role in forming the inclusion complex.

4.5 Dissolution study

The release of a guest molecule from CD-guest inclusion complex could be followed by dissolution study. Reports for release study of several guest/drug molecules e.g. ampelopsis, simvastatin, ketoconazole and famotidine have been found [84, 87-89].

From this work, free form of hesperetin or naringenin exhibited poor dissolution owing to its hydrophobicity. The insoluble complex was prepared by the freeze-drying method, existed in the solid state. It can be observed that dissolution of the two flavanones was enhanced significantly when formed complexes with cyclodextrins. For free naringenin, naringenin- β -CD and naringenin- DM- β -CD complex, the amounts of naringenin released and dissolved were 0.13, 0.13 and 0.42 mg/ml. As for the effect of the type of the carrier host, it was concluded that the DM- β -CD showed a dissolution rate higher than the inclusion complex with β -CD. The dissolved amount of both free and hesperetin complexes increased significantly within 30 minutes. The naringenin showed almost the same behavior, as the greatest solubilization occurs within 30 minutes as well. These results were in good agreement with previous report [21] in which the dissolution of hesperetin and naringenin complexed with β -CD in buffer solutions at different pH values were studied. It was found that pH had an influence on flavonoids release, high release

was observed at pH 8.0. Moreover, the improved dissolution rate may be due to the increase in solubility, as well as a decrease in the crystallinity of guest molecules, brought about by complexation with CDs [82].

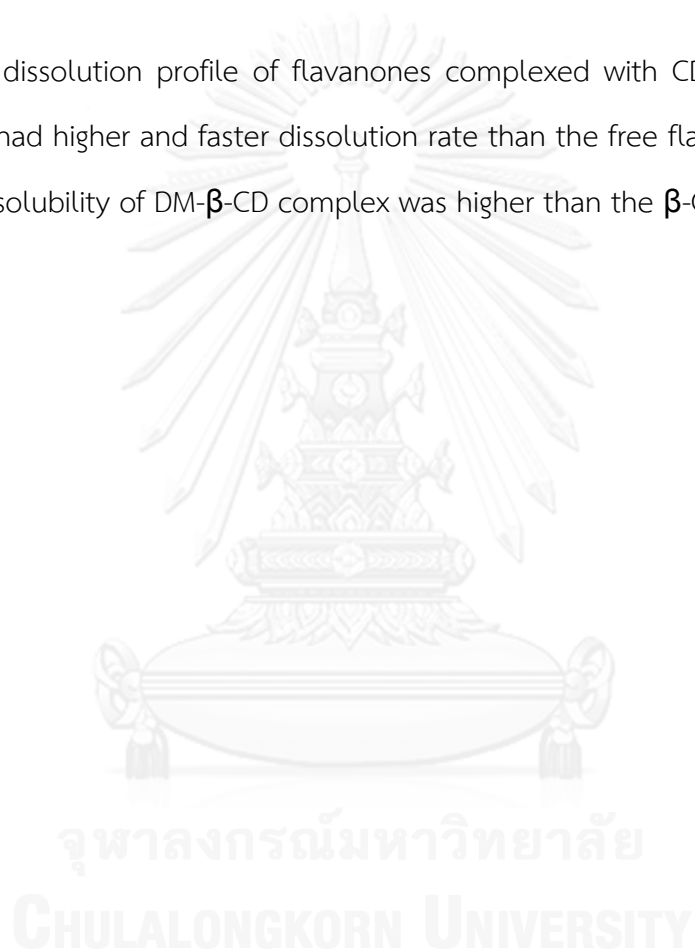
To support the experimental result, we studied potential mean force (PMF) on the binding process of CDs-guest molecules using umbrella sampling techniques. Many works have been devoted to studying the thermodynamics of cyclodextrin complexation using PMF calculations [90-92]. In recent year, Zhang and coworker had used PMF and entropy calculation to study the binding process between β -CD and four guest molecules (puerarin, daidzin, daidzein, nabumetone) using umbrella sampling techniques. On the basis of PMF calculations, the total enthalpy and entropy change are evaluated and further decomposed into individual items in order to quantify the energetics of binding in detail. The results assist in understanding thermodynamic properties of biological processes such as drug encapsulation and release from CDs [48].

CHAPTER V

CONCLUSIONS

1. In the present work, the stability of inclusion complexes of hesperetin and naringenin with β -CD and DM- β -CD was investigated by the theoretically approaches: molecular docking, multiple molecular dynamics simulations and four different free energy calculations. The obtained results revealed that the phenyl ring of the flavanones preferentially dipped into both CD molecules. Both chromone and phenyl rings of flavanones were well occupied inside the DM- β -CD's cavity, whilst the dramatically higher mobility of hesperetin and naringenin was observed in the complex with β -CD. A more stable complexation of DM- β -CD complexes was supported by MM-PBSA/GBSA and QM-PBSA/GBSA binding free energies. Importantly, the van der Waals was found to be the key host-guest interaction for flavanones binding inside the CDs.
2. The potential of mean force (PMF) for the host-guest complexation was studied by umbrella sampling technique. Lower energy consumption of flavanones releasing from the DM- β -CD cavity might suggest the dissolution rate of DM- β -CD complex higher than β -CD complex.
3. The solubility of both flavanones increased with increasing concentration of CDs, following the A_L type diagrams, indicating the 1:1 host-guest complexes. The stability constants of complexes of hesperetin or naringenin with DM- β -CD were significantly higher than those of β -CD complexes. The stability constant of the inclusion complexes decreased with an increase in temperature.

4. The 1:1 inclusion complexes were prepared by kneading and freeze-drying methods. DSC and FTIR spectrum confirm that the complete inclusion complexes were formed between hesperetin/naringenin and β -CD/DM- β -CD by the freeze-drying method.
5. The dissolution profile of flavanones complexed with CDs (β -CD and DM- β -CD) had higher and faster dissolution rate than the free flavanones. Moreover, the solubility of DM- β -CD complex was higher than the β -CD complex.



REFERENCES

1. Gattuso, G., et al., *Flavonoid composition of citrus juices*. *Molecules*, 2007. **12**(8): p. 1641-1673.
2. van Acker, F.A.A., et al., *Flavonoids can replace α -tocopherol as an antioxidant*. *FEBS Letters*, 2000. 473(2): p. 145-148.
3. Vinson, J.A., et al., *Polyphenol antioxidants in citrus juices: in vitro and in vivo studies relevant to heart disease, in Flavonoids in Cell Function*. 2002, Springer. p. 113-122.
4. So, F.V., et al., *Inhibition of human breast cancer cell proliferation and delay of mammary tumorigenesis by flavonoids and citrus juices*, 1996. 262: p. 167-81
5. Yang, M., et al., *Chemopreventive effects of diosmin and hesperidin on *N*-butyl-*N*-(4-hydroxybutyl)nitrosamine-induced urinary-bladder carcinogenesis in male ICR mice*. *International Journal of Cancer*, 1997. 73(5): p. 719-724.
6. Miyagi, Y., et al., *Inhibition of azoxymethane-induced colon cancer by orange juice*. *Nutrition and cancer*, 2000. 36(2): p. 224-229.
7. Tanaka, T., et al., *Chemoprevention of azoxymethane-induced rat colon carcinogenesis by the naturally occurring flavonoids, diosmin and hesperidin*. *Carcinogenesis*, 1997. 18(5): p. 957-965.
8. Borradaile, N.M., K.K. Carroll, and E.M. Kurowska, *Regulation of HepG2 cell apolipoprotein B metabolism by the citrus flavanones hesperetin and naringenin*. *Lipids*, 1999. 34(6): p. 591-598.
9. Lee, S., et al., *Cholesterol-lowering activity of naringenin via inhibition of 3-hydroxy-3-methylglutaryl coenzyme A reductase and acyl coenzyme A: cholesterol acyltransferase in rats*. *Annals of nutrition and metabolism*, 1999. 43(3): p. 173-180.
10. Santos, K.F.R., et al., *Hypolipidaemic effects of naringenin, rutin, nicotinic acid and their associations*. *Pharmacological Research*, 1999. 40(6): p. 493-496
11. Crespo, M., et al., *Anti-inflammatory activity of diosmin and hesperidin in rat colitis induced by TNBS*. *Planta medica*, 1999. 65(07): p. 651-653.

12. Manthey, J.A., *Biological properties of flavonoids pertaining to inflammation*. *Microcirculation*, 2000. 7(S1): p. S29-S34.
13. Middleton Jr, E. and C. Kandaswami, *Effects of flavonoids on immune and inflammatory cell functions*. *Biochemical Pharmacology*, 1992. 43(6): p. 1167-1179.
14. Ghosal, A., et al., *Inhibition and kinetics of cytochrome P4503A activity in microsomes from rat, human, and cdna-expressed human cytochrome P450*. *Drug Metabolism and Disposition*, 1996. 24(9): p. 940-947.
15. Kanaze, F.I., et al., *Simultaneous reversed-phase high-performance liquid chromatographic method for the determination of diosmin, hesperidin and naringin in different citrus fruit juices and pharmaceutical formulations*. *Journal of pharmaceutical and biomedical analysis*, 2003. 33(2): p. 243-249.
16. Bekers, O., et al., *Cyclodextrins in the Pharmaceutical Field*. *Drug development and industrial pharmacy*, 1991. 17(11): p. 1503-1549.
17. Chierotti, M.R. and R. Gobetto, *Solid-state NMR studies of weak interactions in supramolecular systems*. *Chemical Communications*, 2008(14): p. 1621-1634.
18. Brewster, M.E. and T. Loftsson, *Cyclodextrins as pharmaceutical solubilizers*. *Advanced drug delivery reviews*, 2007. 59(7): p. 645-666.
19. Qiu, Y., et al., *Developing solid oral dosage forms: pharmaceutical theory & practice*. 2009: Academic Press.
20. Ficarra, R., et al., *Study of flavonoids/ β -cyclodextrins inclusion complexes by NMR, FT-IR, DSC, X-ray investigation*. *Journal of pharmaceutical and biomedical analysis*, 2002. 29(6): p. 1005-1014.
21. Tommasini, S., et al., *Improvement in solubility and dissolution rate of flavonoids by complexation with β -cyclodextrin*. *Journal of pharmaceutical and biomedical analysis*, 2004. 35(2): p. 379-387.
22. Tommasini, S., et al., *The inclusion complexes of hesperetin and its 7-rhamnoglucoside with (2-hydroxypropyl)- β -cyclodextrin*. *Journal of pharmaceutical and biomedical analysis*, 2005. 39(3-4): p. 572-580.
23. Choi, Y., et al., *Binding Geometry of Inclusion Complex as a Determinant Factor for Aqueous Solubility of the Flavonoid/beta-Cyclodextrin Complexes*

- Based on Molecular Dynamics Simulations.* bulletin-korean chemical society, 2005. 26(8): p. 1203.
24. Liu, B., et al., *Empirical, thermodynamic and quantum-chemical investigations of inclusion complexation between flavanones and (2-hydroxypropyl)-cyclodextrins.* Food chemistry, 2012. 134(2): p. 926-932.
 25. Yang, L.-J., et al., *Preparation and characterization of inclusion complexes of naringenin with β -cyclodextrin or its derivative.* Carbohydrate Polymers, 2013. 98(1): p. 861-869.
 26. Higuchi, T. and K.A. Connors, *Advances in Analytical Chemistry and Instrumentation*, Chapter 4. Phase Solubility Studies, 1965: p. 117-212.
 27. Duchêne, D., *Cyclodextrins and Their Industrial Uses.* 1987: Editions de Santé.
 28. Loftsson, T. and M.E. Brewster, *Pharmaceutical applications of cyclodextrins. 1. Drug solubilization and stabilization.* Journal of pharmaceutical sciences, 1996. 85(10): p. 1017-1025.
 29. Sigurðóardóttir, A.M. and T. Loftsson, *The effect of polyvinylpyrrolidone on cyclodextrin complexation of hydrocortisone and its diffusion through hairless mouse skin.* International Journal of Pharmaceutics, 1995. 126(1-2): p. 73-78.
 30. Hussain, M.A., R.C. Diluccio, and M.B. Maurin, *Complexation of moricizine with nicotinamide and evaluation of the complexation constants by various methods.* Journal of pharmaceutical sciences, 1993. 82(1): p. 77-79.
 31. Másson, M., et al., *Stabilisation of ionic drugs through complexation with non-ionic and ionic cyclodextrins.* International Journal of Pharmaceutics, 1998. 164(1-2): p. 45-55.
 32. JS, P., et al., *Inclusion complex system; A novel technique to improve the solubility and bioavailability of poorly soluble drugs: A review,* 2010. 2(2).
 33. Loftsson, T., et al., *Cyclodextrin complexation of NSAIDs: physicochemical characteristics.* European journal of pharmaceutical sciences, 1993. 1(2): p. 95-101.

34. Pitha, J. and T. Hoshino, *Effects of ethanol on formation of inclusion complexes of hydroxypropylcyclodextrins with testosterone or with methyl orange*. International Journal of Pharmaceutics, 1992. 80(1-3): p. 243-251.
35. Broadhead, J., S. Edmond Rouan, and C. Rhodes, *The spray drying of pharmaceuticals*. Drug development and industrial pharmacy, 1992. 18(11-12): p. 1169-1206.
36. Mujumdar, A.S., Handbook of industrial drying. 2006: CRC Press.
37. Holzgrabe, U., B.W.K. Diehl, and I. Wawer, *NMR spectroscopy in pharmacy*. Journal of pharmaceutical and biomedical analysis, 1998. 17(4-5): p. 557-616.
38. Gowthamarajan, K. and S.K. Singh, *Dissolution testing for poorly soluble drugs: a continuing perspective*. Dissolution Technologies, 2010. 17(3): p. 24-32.
39. Ahmadi, P. and J.B. Ghasemi, *3D-QSAR and docking studies of the stability constants of different guest molecules with beta-cyclodextrin*. Journal of Inclusion Phenomena and Macrocyclic Chemistry, 2013: p. 1-13.
40. Ghasemi, J.B., et al., *Docking and 3D-QSAR study of stability constants of benzene derivatives as environmental pollutants with α -cyclodextrin*. Journal of Inclusion Phenomena and Macrocyclic Chemistry, 2012. 73(1-4): p. 405-413.
41. Raut, V.P., et al., *Molecular dynamics simulations of peptide-surface interactions*. Langmuir, 2005. 21(4): p. 1629-1639.
42. Zhang, H., et al., *Investigation of the inclusions of puerarin and daidzin with β -cyclodextrin by molecular dynamics simulation*. The Journal of Physical Chemistry B, 2010. 114(14): p. 4876-4883.
43. Fernandes, A., et al., *Structural characterization of inclusion complexes between cyanidin-3-O-glucoside and β -cyclodextrin*. Carbohydrate Polymers, 2014. 102(0): p. 269-277.
44. Kästner, J., *Umbrella sampling*. Wiley Interdisciplinary Reviews: Computational Molecular Science, 2011. 1(6): p. 932-942.
45. Rosta, E., et al., *Artificial reaction coordinate "tunneling" in free-energy calculations: The catalytic reaction of RNase H*. Journal of computational chemistry, 2009. 30(11): p. 1634-1641.

46. Yu, Y., et al., *Molecular Dynamics Study of the Inclusion of Cholesterol into Cyclodextrins*. The Journal of Physical Chemistry B, 2006. 110(12): p. 6372-6378.
47. El-Barghouthi, M.I., K.I. Assaf, and A.M.M. Rawashdeh, *Molecular dynamics of methyl viologen-cucurbit [n] uril complexes in aqueous solution*. Journal of Chemical Theory and Computation, 2010. 6(4): p. 984-992.
48. Zhang, H., et al., *Quantification of Solvent Contribution to the Stability of Noncovalent Complexes*. Journal of Chemical Theory and Computation, 2013. 9(10): p. 4542-4551.
49. Alecu, I., et al., *Computational thermochemistry: scale factor databases and scale factors for vibrational frequencies obtained from electronic model chemistries*. Journal of Chemical Theory and Computation, 2010. 6(9): p. 2872-2887.
50. Walker, R.C., M.F. Crowley, and D.A. Case, *The implementation of a fast and accurate QM/MM potential method in Amber*. Journal of computational chemistry, 2008. 29(7): p. 1019-1031.
51. Kirschner, K.N., et al., *GLYCAM06: a generalizable biomolecular force field. Carbohydrates*. Journal of computational chemistry, 2008. 29(4): p. 622-655.
52. Arsawang, U., et al., *How do carbon nanotubes serve as carriers for gemcitabine transport in a drug delivery system?* Journal of Molecular Graphics and Modelling, 2011. 29(5): p. 591-596.
53. Kaiyawet, N., T. Rungrotmongkol, and S. Hannongbua, *Effect of halogen substitutions on dUMP to stability of thymidylate synthase/dUMP/mTHF ternary complex using molecular dynamics simulation*. Journal of chemical information and modeling, 2013.
54. Khuntawee, W., T. Rungrotmongkol, and S. Hannongbua, *Molecular dynamic behavior and binding affinity of flavonoid analogues to the cyclin dependent kinase 6/cyclin D complex*. Journal of chemical information and modeling, 2011. 52(1): p. 76-83.

55. Luty, B.A. and W.F. van Gunsteren, *Calculating electrostatic interactions using the particle-particle particle-mesh method with nonperiodic long-range interactions*. The Journal of Physical Chemistry, 1996. 100(7): p. 2581-2587.
56. Rastelli, G., et al., *Fast and accurate predictions of binding free energies using MM-PBSA and MM-GBSA*. Journal of computational chemistry, 2010. 31(4): p. 797-810.
57. Duchêne, D., *Cyclodextrins and Their Inclusion Complexes, in Cyclodextrins in Pharmaceutics, Cosmetics, and Biomedicine*. 2011, John Wiley & Sons, Inc. p. 1-18.
58. Malaisree, M., et al., *Source of oseltamivir resistance in avian influenza H5N1 virus with the H274Y mutation*. Amino Acids, 2009. 37(4): p. 725-732.
59. Rungrotmongkol, T., et al., *Molecular insight into the specific binding of ADP-ribose to the nsP3 macro domains of chikungunya and venezuelan equine encephalitis viruses: Molecular dynamics simulations and free energy calculations*. Journal of Molecular Graphics and Modelling, 2010. 29(3): p. 347-353.
60. Bjornsson, R. and I. Arnason, *Conformational properties of six-membered heterocycles: accurate relative energy differences with DFT, the importance of dispersion interactions and silicon substitution effects*. Physical Chemistry Chemical Physics, 2009. 11(39): p. 8689-8697.
61. Wu, G., et al., *Detailed analysis of grid-based molecular docking: A case study of CDOCKER—A CHARMM-based MD docking algorithm*. Journal of computational chemistry, 2003. 24(13): p. 1549-1562.
62. Kano, K., et al., *Static and dynamic behavior of 2: 1 inclusion complexes of cyclodextrins and charged porphyrins in aqueous organic media*. Journal of the American Chemical Society, 2002. 124(33): p. 9937-9944.
63. Ayala-Zavala, J., et al., *High Relative Humidity In-Package of Fresh-Cut Fruits and Vegetables: Advantage or Disadvantage Considering Microbiological Problems and Antimicrobial Delivering Systems?* Journal of food science, 2008. 73(4): p. R41-R47.

64. Szejtli, J., *Introduction and general overview of cyclodextrin chemistry*. Chemical Reviews, 1998. 98(5): p. 1743-1754.
65. Zingone, G. and F. Rubessa, *Preformulation study of the inclusion complex warfarin- β -cyclodextrin*. International Journal of Pharmaceutics, 2005. 291(1-2): p. 3-10.
66. Wen, J., et al., *Preparation and physicochemical properties of the complex of naringenin with hydroxypropyl- β -cyclodextrin*. Molecules, 2010. 15(6): p. 4401-4407.
67. Zhang, P., et al., *Solubility of Naringenin in Ethanol and Water Mixtures*. Journal of Chemical & Engineering Data, 2013. 58(9): p. 2402-2404.
68. Shulman, M., et al., *Enhancement of Naringenin Bioavailability by Complexation with Hydroxypropoyl- β -Cyclodextrin*. PLoS ONE, 2011. 6(4): p. 1-8.
69. Fang, T., et al., *A rapid LC/MS/MS quantitation assay for naringin and its two metabolites in rats plasma*. Journal of pharmaceutical and biomedical analysis, 2006. 40(2): p. 454-459.
70. Jullian, C., et al., *Complexation of quercetin with three kinds of cyclodextrins: an antioxidant study*. Spectrochimica Acta Part A: Molecular and Biomolecular Spectroscopy, 2007. 67(1): p. 230-234.
71. Challa, R., et al., *Cyclodextrins in drug delivery: an updated review*. Aaps Pharmscitech, 2005. 6(2): p. E329-E357.
72. Del Valle, E., *Cyclodextrins and their uses: a review*. Process Biochemistry, 2004. 39(9): p. 1033-1046.
73. Rekharsky, M.V. and Y. Inoue, *Complexation thermodynamics of cyclodextrins*. Chemical Reviews, 1998. 98(5): p. 1875-1918.
74. Karathanos, V.T., et al., *Study of the solubility, antioxidant activity and structure of inclusion complex of vanillin with β -cyclodextrin*. Food chemistry, 2007. 101(2): p. 652-658.
75. Haiyun, D., et al., *Preparation and spectral investigation on inclusion complex of β -cyclodextrin with rutin*. Spectrochimica Acta Part A: Molecular and Biomolecular Spectroscopy, 2003. 59(14): p. 3421-3429.

76. Pralhad, T. and K. Rajendrakumar, *Study of freeze-dried quercetin–cyclodextrin binary systems by DSC, FT-IR, X-ray diffraction and SEM analysis*. Journal of pharmaceutical and biomedical analysis, 2004. 34(2): p. 333-339.
77. Wen, X., et al., *Preparation and study the 1: 2 inclusion complex of carvedilol with β -cyclodextrin*. Journal of pharmaceutical and biomedical analysis, 2004. 34(3): p. 517-523.
78. Yang, L.-J., et al., *Host–guest system of taxifolin and native cyclodextrin or its derivative: Preparation, characterization, inclusion mode, and solubilization*. Carbohydrate Polymers, 2011. 85(3): p. 629-637.
79. Singh, R., et al., *Characterization of cyclodextrin inclusion complexes-a review*. J. Pharm. Sci. Technol, 2010. 2(3): p. 171-183.
80. Tayade, P. and P. Vavia, *Inclusion complexes of Ketoprofen with β -cyclodextrins: Oral pharmacokinetics of Ketoprofen in human*. Indian Journal of Pharmaceutical Sciences, 2006. 68(2): p. 164.
81. Jadhav, G. and P. Vavia, *Physicochemical, in silico and in vivo evaluation of a danazol– β -cyclodextrin complex*. International Journal of Pharmaceutics, 2008. 352(1): p. 5-16.
82. Erden, N. and N. Çelebi, *A study of the inclusion complex of naproxen with β -cyclodextrin*. International Journal of Pharmaceutics, 1988. 48(1–3): p. 83-89.
83. Lee, P.S., et al., *Physicochemical characteristics and bioavailability of a novel intestinal metabolite of ginseng saponin (IH901) complexed with β -cyclodextrin*. International Journal of Pharmaceutics, 2006. 316(1): p. 29-36.
84. Hassan, M.A., M.S. Suleiman, and N.M. Najib, *Improvement of the in vitro dissolution characteristics of famotidine by inclusion in β -cyclodextrin*. International Journal of Pharmaceutics, 1990. 58(1): p. 19-24.
85. Chun, I.K. and D.S. Yun, *Inclusion complexation of hydrocortisone butyrate with cyclodextrins and dimethyl- β -cyclodextrin in aqueous solution and in solid state*. International Journal of Pharmaceutics, 1993. 96(1): p. 91-103.
86. Ammar, H., et al., *Formulation and biological evaluation of glimepiride–cyclodextrin–polymer systems*. International Journal of Pharmaceutics, 2006. 309(1): p. 129-138.

87. Esclusa-Diaz, M.T., et al., *Characterization and in vitro dissolution behaviour of ketoconazole/ β -cyclodextrin and 2-hydroxypropyl- β -cyclodextrin inclusion compounds*. International Journal of Pharmaceutics, 1996. 143(2): p. 203-210.
88. Ruan, L.-P., et al., *Improving the solubility of ampelopsin by solid dispersions and inclusion complexes*. Journal of pharmaceutical and biomedical analysis, 2005. 38(3): p. 457-464.
89. Jun, S.W., et al., *Preparation and characterization of simvastatin/hydroxypropyl- β -cyclodextrin inclusion complex using supercritical antisolvent (SAS) process*. European Journal of Pharmaceutics and Biopharmaceutics, 2007. 66(3): p. 413-421.
90. Zhang, H., et al., *Molecular Recognition in Different Environments: β -Cyclodextrin Dimer Formation in Organic Solvents*. The Journal of Physical Chemistry B, 2012. 116(42): p. 12684-12693.
91. He, J., et al., *Cyclodextrin-Mediated Recruitment and Delivery of Amphotericin B*. The Journal of Physical Chemistry C, 2013. 117(22): p. 11750-11756.
92. López, C.A., A.H. de Vries, and S.J. Marrink, *Computational microscopy of cyclodextrin mediated cholesterol extraction from lipid model membranes*. Scientific reports, 2013. 3.

VITA

Name: Miss Waratchada Sangpheak

Date of Birth: June 15, 1990

Nationality: Thai

University Education:

2008-2011 Bachelor Degree of Science (Food Technology), Faculty of Engineering and Industrial Technology, Silpakorn University, Nakhon Pathom, Thailand

Work Experience:

2010	Position	Student Internship
	Company	Prantalay Company

Pubilcation:

1. W. Sangpheak, W. Khuntawee, P. Wolschann, P. Pongsawasdi, T. Rungrotmongkol (2014) Enhanced stability of a naringenin/2,6-dimethyl β -cyclodextrin inclusion complex: Molecular dynamics and free energy calculation based on MM- and QM-PBSA/GBSA. *Journal of Molecular Graphics and Modelling* 50:10-15.

Proceeding:

1. W. Sangpheak, W. Khuntawee, P. Wolschann, P. Pongsawasdi, T. Rungrotmongkol (2014) Binding mode of flavanones inside cyclodextrins: Molecular dynamics simulation, Pure and Applied Chemistry International Conference 2014 (PACCON2014), 8-10th January 2014, Faculty of Science, Khon Kaen University, Khon Kaen, PHY P035, 171 (poster presentation)

International Conference:

1. W. Sangpheak, W. Khuntawee, P. Wolschann, P. Pongsawasdi, T. Rungrotmongkol. Enhancement of water solubility of hesperetin and naringenin by complexation with beta-cyclodextrin and its dimethyl derivative, 7th Asian Cyclodextrin Conference, 27-29th November 2013, Faculty of Science, Chulalongkorn University, Bangkok, Thailand, PA-05, 43 (poster presentation)

2. W. Sangpheak, W. Khuntawee, P. Wolschann, P. Pongsawasdi, T. Rungrotmongkol. Investigation of the inclusion complex of flavanones/cyclodextrin based on molecular dynamics simulation, 18th Biological Sciences Graduate Congress, 6–8th January 2014, Faculty of Science, University of Malaya, Kuala Lumpur, Malaysia, PT2-07, 138 (poster presentation)

3. W. Sangpheak, W. Khuntawee, P. Wolschann, P. Pongsawasdi, T. Rungrotmongkol. 18th International Annual Symposium on Computational Science and Engineering (ANSCSE 18), 18-19th March 2014, Faculty of Science at Si Racha and Ambassador city, Jomtien, Thailand (oral presentation)

National Conference:

1. W. Sangpheak, W. Khuntawee, P. Wolschann, P. Pongsawasdi, T. Rungrotmongkol. The 10th Thai Summer School of Computational Chemistry Workshop “Computational modeling of protein-ligand interactions”, 14-17 October 2013, Kasetsart University, Molecular dynamics simulation of flavanones-cyclodextrin inclusion complexes, P01 (poster presentation)